Simplified t-channel models for Dark Matter searches

Relatore:
Prof. Roberto Soldati

Presentata da:
Luca Mantani

Correlatore:
Prof. Fabio Maltoni

A Deborah,
che mi accompagna ogni giorno

Sommario

Una enorme quantità di evidenze sperimentali sulla esistenza di una forma di materia non luminosa nell'Universo, si sono accumulate nel corso di circa un secolo. Chiarire la sua natura è diventata una delle sfide più eccitanti ed urgenti negli sforzi per capire il nostro Universo.

In questo lavoro presento uno studio su un approccio per scoprire la Materia Oscura interpretata come particella elementare e sulla possibilità di produrla e rilevarla negli acceleratori.

Nella parte introduttiva presento una breve storia delle evidenze astrofisiche e astronomiche che hanno portato alla ipotesi della esistenza di Materia Oscura. Assumendo che la Materia Oscura sia costituita da una particella elementare ulteriore a quelle predette dal Modello Standard, delineo poi i tre principali metodi di rilevazione utilizzati attualmente per identificarla.

Nella seconda parte discuto come si possono costruire teorie nelle quali sia possibile interpretare le ricerche attuali ed i risultati corrispondenti. Eseguo un confronto tra approcci diversi, partendo da modelli completi fino a quelli che utilizzano teorie di campo effettive. In particolare, discuto i loro lati positivi e negativi, motivando l'utilizzo di uno schema intermedio, il cosiddetto approccio con modelli semplificati, caratterizzati da un numero limitato di nuovi stati e parametri e che supera le limitazioni intrinseche delle teorie effettive nel contesto delle ricerche negli acceleratori.

Nell'ultima parte fornisco una esaustiva classificazione dei modelli semplificati nel canale t, che non sono ancora stati analizzati sistematicamente nella letteratura. Per ciascuno di essi presento un possibile completamento UV e i segnali più promettenti ad LHC. Per questa ragione tutti i modelli considerati sono stati implementati in strumenti Monte Carlo, validati nel confronto con risultati analitici, studiati in dettaglio e resi pronti per un rilascio pubblico per la comunità fenomenologica e sperimentale di LHC.

Abstract

An overwhelming observational evidence of the existence of a form of non-luminous matter in the Universe has mounted over almost a century. Elucidating its nature has now become one of the most exciting and urgent challenges in the current efforts to understand our Universe.

In this work I present a study on an approach to discover Dark Matter that focuses on the elementary particle interpretation and on the possibility of producing and detecting it at colliders.

In the introductory part I give a brief history of the astrophysical and astronomical evidence that has led to the Dark Matter hypothesis in order to explain a large set of observations at different scales. Assuming that Dark Matter is an elementary particle beyond those predicted by the Standard Model, I then outline the three main detection methods currently employed to identify it and shed light on its nature.

In the second part I discuss how theoretical frameworks can be built where current searches and corresponding results can be interpreted. I compare approaches starting from UV complete models to those employing effective field theories. In particular, I critically discuss their virtues and drawbacks, motivating the use of an intermediate setup, the so-called simplified model approach, which features a limited number of new states and parameters and overcomes the intrinsic limitations of the EFT's in the context of collider searches.

In the last part I provide an exhaustive classification and study of simplified t-channel models, which have not been systematically analysed in the literature so far. For each of them I present possible UV completions as well as the most promising signatures at the LHC. To this aim, all considered models have been implemented in cutting-edge Monte Carlo tools, validated against analytic computations, studied in detail, and made ready for a public release to the LHC phenomenology and experimental communities.

Contents

I

Bibliography   **113**

Introduction

The existence of Dark Matter is by now firmly established because of indirect cosmological and astrophysical observations of gravitational effects. Notwithstanding, we have not directly detected it yet. In order to explain the observed Universe, we need a relic abundance of Dark Matter of $\Omega_{DM}h^2 = 0.12$, that is almost a quarter of the total energy density of the Universe. We also have evidence for the existence of DM from velocity dispersion of galaxy clusters, the flattening of galaxy rotation curves and the measurement of the Cosmic Microwave Background, since all of them need a significant presence of Dark Matter in order to be explained. Nevertheless, assuming it is made of unknown particles, we have no other evidence that can lead us to determine its nature and its interaction with the Standard Model particles.

From a particle physics perspective, the effort to detect it is carried out with different approaches, which can be grouped into three categories:

- Direct detection: experiments that aim at measuring the recoil of heavy nuclei or electrons hit by Dark Matter particles passing by our planet;

- Indirect detection: searches for Standard Model products of Dark Matter annihilation from the center of the galaxy, from the sun or elsewhere;

- Collider searches: direct production of Dark Matter in association with Standard Model particles at colliders.

The most studied incarnation for DM particles is the WIMP (Weakly Interacting Massive Particle), characterized by weak scale SM-DM interaction and mass in the range of the GeV-TeV. This is motivated by the so-called WIMP miracle, the fact that such candidate can explain very well the relic density, no matter the details of the specific model.

So far no experiment has been able to give clear indication that DM particles interact with the SM particles other that through gravity.

In order to exploit the interplay of the various detection methods, we first need a framework that allow us to obtain results in a model independent way, particularly so from the collider perspective. One common approach is to use the Effective Field Theory

method, describing the unknown DM-SM interaction as a contact interaction, where heavy partners have been integrated out. Although this is the approach that guarantees a full model independence, its validity in collider experiments is questionable, since at the LHC energies we might be able to produce the other degrees of freedom that are neglected in the EFT framework.

On the other hand, the employment of complete models, such as Supersymmetry, has also some important drawbacks. Despite their theoretical appeal, they in general introduce several new particles and many parameters and only some of them are related to the Dark Matter scenario. Therefore we have to deal with a parameter space with many dimensions and we face the so-called inverse problem, i.e. the presence of degeneracies in the map that links measurements and the theory space. In other words we are unable to unequivocally determine which is the correct model.

The in-between way is to employ simplified models, i.e. to maintain model independence expanding the interaction of the EFT method adding a mediator particle which connects the Dark sector and the Standard Model. Despite their intrinsic limitations they are characterized by a small number of parameters and can be easily connected to the complete UV model behind them.

In recent years, particularly motivated by collider searches, the simplified model approach has gained the attention because of their convenient features. They are commonly characterized by a single Dark Matter candidate interacting with the Standard Model through an s-channel or a t-channel mediator, whose quantum number are fixed by global and gauge symmetries. In this work we focus on t-channel models, studying them both from a theoretical point of view and from a phenomenological one thanks to a combination of simulation tools, including FeynRules, MadGraph and FeynCalc.

In Chapter 1 we present a brief history of the Dark Matter problem and then we describe the various Dark Matter detection approaches from a particle physics perspective and the historically relevant Dark Matter candidate that have been considered over the years. In Chapter 2 we focus on the different theoretical frameworks, highlighting their virtues and their drawbacks. In the final Chapter we present a complete list of t-channel models, focusing on those with color triplet mediators. We studied their theoretical structure, discussing from which complete model they come from and their collider phenomenology.

Chapter 1

Dark Matter from a particle physics perspective

The study of Dark Matter has gained interest in the last decades, engaging various fields of physics in the attempt to understand its nature. In this work we will focus on the particle physics aspects. We will describe Dark Matter in terms of a Quantum Field Theory and not consider effects connected to astrophysics, nuclear physics, cosmology or general relativity. The main purpose of our approach is to build a model that can in principle describe and account for Dark Matter and costrain its parameter space through several independent set of data. To begin with, we briefly report the historical observations that have led to the formulation of the hypothesis of the existence of Dark Matter. We then continue by discussing the three detection methods that physicists employ in order to find it and some of the most famous candidates.

1.1 A brief history of Dark Matter

Throughout history, philosophers and scientists have discussed about the nature of matter and wondered if there could be some form of matter that is imperceptible, either because too dim or truly invisible. Galileo's discovery of four satellites of Jupiter encapsulates two concepts that remain relevant to research of Dark Matter today: the Universe may contain objects that are not observable in ordinary ways and we may need the introduction of new or improved technology to reveal them.

The concept of Dark Matter evolved through time [1]. At first, whenever dealing with an astrophysical observation that did not fit in the theoretical gravitational paradigm, astronomers were usually looking for unseen planets or stars that could explain the deviation from the theoretical prediction. A famous example is the discovery of the planet

Neptune, which presence was first predicted mathematically in order to explain anomalies in the motion of Uranus and then observed directly. In the 19th century and in the early 20th century, the search for "Dark Matter" was basically focused on Dark Stars, Dark Planets and Dark Clouds. Today, when we think of Dark Matter in the Universe, we think of a different kind of matter made of Beyond Standard Model particles.

1.1.1 Galaxy clusters

One of pioneer in the field of Dark Matter is the Swiss-American astronomer Fritz Zwicky. In 1933, studying the redshifts of the Coma Cluster (a large cluster of galaxies that contains over 1000 identified galaxies) he noticed a large scatter in the apparent velocities of eight galaxies, with differences that exceeded 2000 km/s. The fact that these galaxies exhibited a large velocity dispersion compared to other galaxies was already known but Zwicky tried to understand deeply the phenomenon applying the virial theorem to the cluster in order to estimate its mass. He estimated the total mass of the cluster, calculating it as the product of the number of observed galaxies, 800, and the average mass of a galaxy, 10^9 solar masses. He then estimated the dimension of the cluster in order to obtain the potential energy of the system. Having that he was able to compute the kinetic energy and then the velocity dispersion. From the data in his possession he estimated a velocity dispersion of 80 km/s, well below the observed one. From this observation, he concluded:

> *If this would be confirmed, we would get the surprising result that dark matter is present in much greater amount than luminous matter.*

This sentence has an historic meaning, usually (but inaccurately) considered the first time the phrase "Dark Matter" appeared in the literature. Zwicky however when talking about Dark Matter was thinking of cool and cold stars, gases and solid bodies incorporated in nebulae. In the following years the scientific discussion about this observation went on and by the late 1950s, a number of other articles had been published regarding the mass-to-light ratio in galaxy clusters (Fig. 1.1.1).

The Dark Matter hypothesis, however, was neither commonly accepted nor it was disregarded. In particular, some astronomers started to wonder what such Dark Matter might be made of. Studying the relaxation process of galaxy clusters it was clear that the mass must to be found within the intergalactic space and not in the galaxies themselves. Also the idea that this missing matter was made of gas was ruled out observing the emission of X-Rays.

Objects	Distance (in kpc)	Luminosity (in sol. lum.)	Mass (in sol. mass)	Mass/Lum. f
Solar Neighborhood	—	—	—	4
Triangulum Nebula, M33	480	1.4×10^9	5×10^9	4
Large Magellanic Cloud	44	1.2×10^9	2×10^9	2
Andromeda Nebula	460	9×10^9	1.4×10^{11}	16
Globular Cluster, M92	11	1.7×10^5	$<8 \times 10^5$	<5
Elliptical Galaxy, NGC 3115	2100	9×10^8	9×10^{10}	100
Elliptical Galaxy, M32	460	1.1×10^8	2.5×10^{10}	200
Average S in Double Gal.	—	1.3×10^9	7×10^{10}	50
Average E in Double Gal.	—	8×10^8	2.6×10^{11}	300
Average in Coma Cluster	25000	5×10^8	4×10^{11}	800

Figure 1.1.1: A summary of the Dark Matter problem in the 1950s: a table produced by M. Schwarzschild in 1954 [2] showing mass to light ratio for numerous clusters.

1.1.2 Galactic rotation curves

The rotation curves of galaxies, i.e. the angular velocity profile of stars as a function of the distance from the center of the galaxy, had a really important role in the formulation of the Dark Matter hypothesis. In particular, it was the observation of a flat rotation curve in the outer part of the galaxies that led astronomers to the idea that a large amount of unseen matter was present.

In 1914 astronomers noticed that the spectral lines from Andromeda were inclined when the slit of the spectrogram was aligned with the major axis of the galaxy, while they were straight when aligned with the minor axis, concluding that the galaxy is rotating. In 1917 Francis Pease measured the rotation of the central region of Andromeda, finding an approximately constant angular velocity. In the following years, this kind of measurements were used to calculate the mass to light ratio of various galaxies, but at the end of the 1950s there were not enough evidence nor consensus that the observed rotation curves were in conflict with the understanding of galaxies.

Things began to change a decade later, when the quality and precision of measurements improved. In 1970 Ken Freeman, after comparing the radius at which the rotation curve was observed to peak to the theoretically predicted radius obtained with an exponential distribution of matter (the distribution that basically match the observed luminous matter), stated:

> if [the data] are correct, then there must be in these galaxies additional matter which is undetected, either optically or at 21 cm. Its mass must be at least as large as the mass of the detected galaxy, and its distribution must be quite different from the exponential distribution which holds for the optical galaxy.
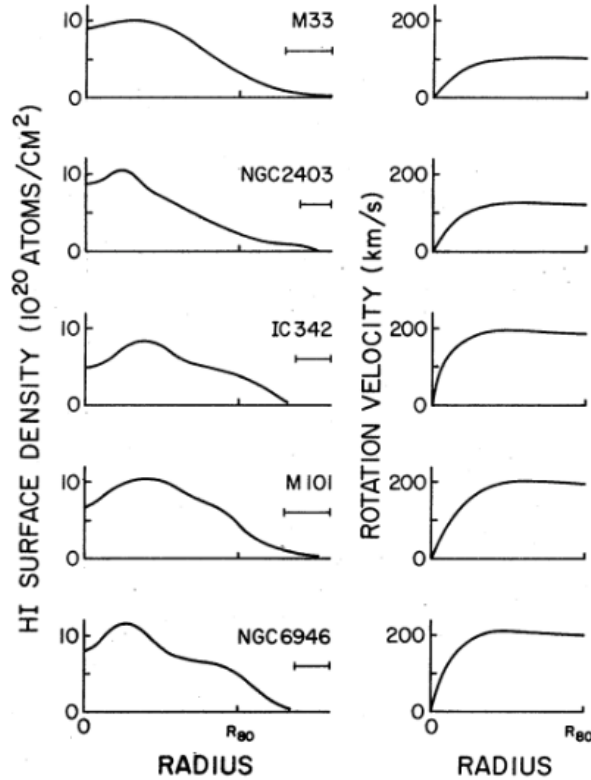
Figure 1.1.2: Here it is shown the hydrogen surface density profile on the left and the corresponding rotation curves on the right [3]. The bars under the galaxy names indicate the average radial beam diameter, i.e. the effective spatial resolution.

This statement provide the first example where it was explicitly argued that additional mass was needed to explain the rotation curves profile. A few years later Rogstad and Shostak analysed the rotation curves of five more galaxies and noticed the same pattern (see fig. 1.1.2), the rotation curves remain flat out to the largest radii observed. Given that, they also argued that additional mass is needed in the outer area of those galaxies to account for these experimental data. In particular it started to become evident that the last measured radius cannot be the edge of the galaxies. In the following years the astrophysical community widely accepted this conclusion, since more and more studies confirming this property for several galaxies were published. It was not clear at all at the time what the additional mass was made of (neither it is in present days) but there already was the sense that it could not be made of "dark stars", that is was probably matter in the form of gas.
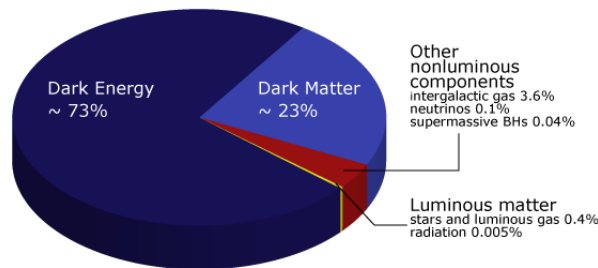
Figure 1.1.3: A pie chart showing the composition of our Universe in today understanding.

1.1.3 Cosmological evidence

As astronomers were studying and gathering information about the presence of additional matter in the Universe structures, cosmologists began to wonder if this unknown matter could have a significant relevance in the formation and evolution of our Universe. At the beginning of the 1970s the common opinion was that the estimated matter in the Universe was not enough to account for a density that is close to the critical density of the Universe, the luminous matter was less than a tenth of what was needed. This conclusion, however, was in stark contrast with cosmological observations that all pointed towards a flat Universe, i.e. the density of matter is precisely the critical value. To solve this problem, cosmologists began to consider the hypothesis of the presence of Dark Matter and its influence in the large-scale geometrical structure of the Universe. Unfortunately, not even Dark Matter could solve the enigma, being the total amount of ordinary matter and dark matter insufficient. Only a few decades later, with the discovery of the accelerating expansion rate of the Universe, the puzzle has been solved. Taking also into account the contribution of the Dark Energy, responsible for this phenomenon, to the total energy density, the observation of a flat Universe was finally justified. In fig. 1.1.3 is shown the current estimates of the composition of our Universe.

Meanwhile, Jim Pebbles had noticed that the absence of fluctuations in the Cosmic Microwave Background at a level of 10^{-4} was incompatible with a Universe dominated by baryonic matter and that if it was otherwise dominated by massive weakly interacting particles (a candidate of Dark Matter), this problem could be relieved. This problem and subsequent works related to the solution of it rapidly led the community to think that cold dark matter, i.e. massive particles weakly interacting, was the leading paradigm to describe the evolution of the observed Universe.
The comprehension of the evolution of Dark Matter in the universe and the formation of astrophysical structure is highly influenced by computer simulations. In particular the results of these simulations are not particularly dependent on what the Dark Matter consists of, they are almost insensitive to the electro-weak and non-gravitational interac-

tions. In other words, for the purpose of structure formation, the Dark Matter particles con be effectively considered collisionless. From a dynamical point of view, however, it is really important the initial velocity distribution of the particles. This gives cosmologists a way to discriminate between various candidates of Dark Matter. For Example, Standard Model neutrinos decouple from the thermal equilibrium in the early Universe at a temperature much higher than their mass and so they are relativistic in the epoch of structure formation. This kind of candidate is therefore called hot Dark Matter. On the other hand, if the candidate has a not too small mass, the particles decouple from equilibrium at a temperature below their mass and so they are non-relativistic throughout cosmic history. This kind of candidate is then called cold Dark Matter. While at large scale, i.e. at the level of galaxy clusters, the simulations are largely insensitive to the initial velocity, at smaller scales the formation of structures is predicted to be suppressed if the Dark Matter is relativistic or hot. Conversely, the cold Dark Matter could explain pretty well the pattern of formation of galaxies and therefore is now considered the best fit to the observed Universe.

1.2 Dark Matter detection

Over the past decades the meaning of Dark Matter has changed considerably. At the beginning it was a way to refer to objects of which we could see the effects but not signals coming from them. In this sense, dark was merely an adjective to stress the fact that we couldn't see it. Today instead, when we talk about Dark Matter, we think of Beyond Standard Model particles that can help us explain the observations. This idea that Dark Matter is made of unknown particles has gained support since the late 1980s and nowadays it is the leading paradigm. First we discuss the main experimental constraints that come into play to test the validity of a Dark Matter model from particle physics point of view. Then we discuss some of the candidates that have been studied, their features and their weaknesses.

1.2.1 Relic density

One of the constraint that we have to deal with when talking about a Dark Matter candidate is the relic density, i.e. the content of Dark Matter in the Universe. When studying the history of the Universe focusing on the matter content, we need to define some parameters that will come in handy later.

- The Hubble constant H_0 is a parameter that gives information on the expansion of the Universe. The Hubble law states that the velocity of expansion between two objects increases linearly with the distance. The value of the constant nowadays is

$$H_0 = \frac{\dot{r}}{r} \approx 70 \frac{Km}{s \, Mpc} \,. \tag{1.2.1}$$

  In order to make it a dimensionless quantity, we define

$$h = \frac{H_0}{100 \frac{Km}{s \, Mpc}} \approx 0.7 \,. \tag{1.2.2}$$

- The cosmological constant Λ which accounts for most of the energy density in the Universe (see fig. 1.1.3) and is defined through the gravitational Einstein-Hilbert action:

$$S = \frac{M_{pl}^2}{2} \int d^4x \, \sqrt{-g} \, (R - 2\Lambda) \,, \tag{1.2.3}$$

  with $M_{pl}^2 = 1/8\pi G_N$. It is useful to define a dimensionless parameter:

$$\Omega_\Lambda \equiv \frac{\Lambda}{3H_0^2} \, . \tag{1.2.4}$$

- One key parameter is the matter content of the Universe that can be divided into three contributions: baryonic matter, radiation and Dark Matter. These quantities change with time and the actual composition of the Universe was different in the past as compared to today. We define the dimensionless quantities

$$\begin{aligned}
\Omega_B &\equiv \frac{\rho_B}{\rho_c} \\
\Omega_R &\equiv \frac{\rho_R}{\rho_c} \\
\Omega_\chi &\equiv \frac{\rho_\chi}{\rho_c} \, ,
\end{aligned} \tag{1.2.5}$$

where ρ_B is the density of baryonic matter, ρ_R the density of radiation and ρ_χ is the density of Dark Matter. The parameter ρ_c is the critical density, i.e. the value of the density of the Universe that correspond to a flat geometry, separating the case of a closed universe from a open universe.[1]

To understand how these parameters affect the evolution of the Universe we observe, we need to understand some basic properties derived from cosmology. In particular we can briefly study the simplest model of expanding Universe, known as the Friedmann-Lemaitre-Robertson-Walker model. We assume that the universe is spatially homogeneous and isotropic, while we do not make assumptions about the time evolution. The most general line element satisfying the aforementioned conditions is

$$ds^2 = dt^2 - a^2(t) \left(\frac{dr^2}{1 - kr^2} + r^2(d\theta^2 + \sin^2\theta \, d\phi^2) \right) , \tag{1.2.6}$$

where the only function left to fix is $a(t)$, i.e. the cosmic scale factor. The parameter k is the curvature constant and it is an input parameter of the model, taking the possible values $-1, 0, +1$ corresponding to the case of open universe (the 3-D space is an hyperboloid), flat universe (the 3-D space is $\mathbb{R}^3$) and closed universe (the 3-D space is a 3-Sphere) respectively. The Hubble law can be defined in function of $a(t)$ in the following way:

---

[1]These definitions come from the solutions of the Friedmann-Lemaitre-Robertson-Walker model, describing a homogeneous and isotropic universe in expansion or contraction. We will talk about it a little bit later, but for a complete study see Ray D'Inverno, Introducing Einstein's Relativity (Ch 22).

$$H(t) = \frac{\dot{a}(t)}{a(t)} \, . \tag{1.2.7}$$

It is clear from the definition that in general the Hubble constant is not a constant at all but depends on time and can vary during the evolution of the Universe. When we refer to it as a constant, we are in fact talking about the value that this function has today. If one assumes that the Universe is filled with a perfect fluid, then the energy-momentum tensor takes the form

$$T^{\mu}_{\nu} = diag(-\rho, p, p, p) \, , \tag{1.2.8}$$

with ρ and p being the energy density and the pression, both functions of time. The energy-momentum tensor satisfies the continuity equation $\nabla_{\mu} T^{\mu}_{\nu} = 0$ and in particular, the zero component of this equation leads to the energy conservation that in this simplified case is

$$-\frac{\partial \rho}{\partial t} - 3\frac{\dot{a}}{a}(p + \rho) = 0 \, . \tag{1.2.9}$$

The relation between ρ and p specifies the kind of fluid we are dealing with. In general we can assume the equation of state for the fluid to be

$$p = \omega \rho \, , \tag{1.2.10}$$

where ω is a constant. Up to the choiche of this parameter that characterise what the fluid is made of, we can compute the functional dependence of the energy density from the cosmic scale factor. Taking into account equation (1.2.9), we have

$$\frac{\dot{\rho}}{\rho} = -3(1 + \omega)\frac{\dot{a}}{a} \quad \Rightarrow \quad \rho \propto a^{-3(1+\omega)} \, . \tag{1.2.11}$$

For a long time it was commonly thought that the early Universe was dominated by radiation ($\omega = 1/3$), while the present day Universe is dominated by matter in the form of dust, i.e. the only relevant interaction between astrophysical object is the gravitational force, corresponding to $\omega = 0$. Now we know however that the expansion of the Universe is accelerated and this is incompatible with a dust-dominated Universe. The simplest way to take into account such behavior is assuming the presence of the so called Dark Energy corresponding to $\omega = -1$. In this case, the energy density of the Universe is constant and it is related to the celebrated cosmological constant Λ.

Given the specific form of the metric in equation (1.2.6), one can solve for the cosmic scale factor a. Defining the critical density as

$$\rho_c = \frac{3H^2}{8\pi G_N} , \tag{1.2.12}$$

one can write the so called Friedman equation derived from Einstein equation in the form

$$\frac{\rho}{\rho_c} = 1 + \frac{k}{H^2 a^2} . \tag{1.2.13}$$

This equation leads to the following conclusions:

- $\rho < \rho_c \quad \Leftrightarrow \quad k = -1 \quad \Leftrightarrow \quad$ Open Universe

- $\rho = \rho_c \quad \Leftrightarrow \quad k = 0 \quad \Leftrightarrow \quad$ Flat Universe

- $\rho > \rho_c \quad \Leftrightarrow \quad k = 1 \quad \Leftrightarrow \quad$ Closed Universe

It can be easily seen that the spatial curvature determines the evolution of the scale factor. Since observations point to a flat Universe, we can finally solve and determine the time dependence of $a(t)$. In particular in the three cases considered, setting $k = 0$ in equation (1.2.13), we find

$$a(t) \propto \begin{cases} t^{2/3} & \text{non-relativistic matter} \\ t^{1/2} & \text{radiation} \\ e^{H_0 t} & \text{dark energy} \end{cases} \tag{1.2.14}$$

Notice that the dark energy case is characterised by an exponential law for the scale factor, leading to an inflationary expansion.

To describe the evolution of the Universe we know, we need to take into account all of these constituents. In particular following equation (1.2.11), we can understand naively which component dominates in the evolution of the Universe. As can be seen in figure 1.2.1, as the scale factor increases, the radiation density (including both photons and neutrinos) drops as $1/a^4$, while the matter density which accounts for both baryonic and Dark Matter decrease as $1/a^3$. On the other hand the vacuum energy density is constant through time evolution, which means that it will surely come the time for it to dominate and this is happening around now. We can then distinguish three main eras: the radiation era in the early Universe, the matter era and the dark energy era. Each of these period is characterised by a different rate of expansion, according to equation
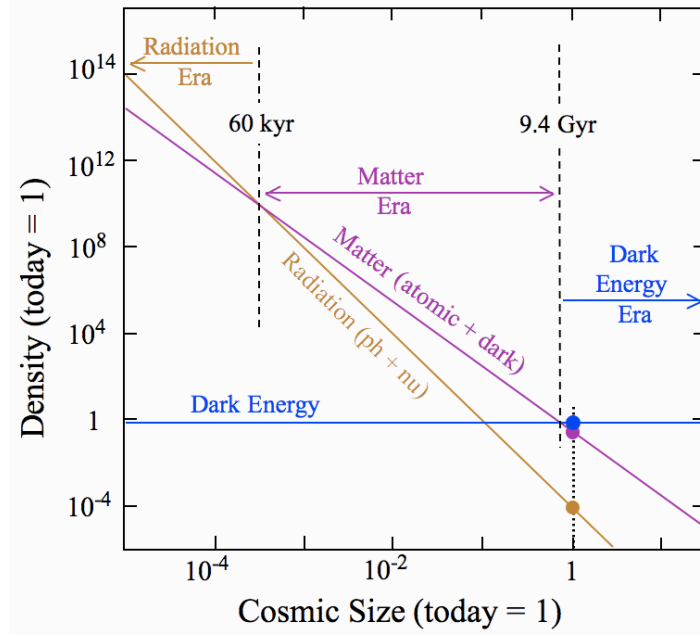
Figure 1.2.1: Evolution of the energy density of the three kind of constituent in function of the cosmic scale factor [4].

(1.2.14).

We know from experimental measurements that most of the matter content in the Universe is Dark Matter and not baryonic. In order to understand its production and explain its relic density, we need to apply some statistical mechanics. Among the candidates of Dark Matter, it is important to distinguish whether they were created thermally or not. Thermal and non-thermal relics have different behavior and give rise to different relic density Ω. We will focus on analysing the thermal scenario. As can be seen in figure 1.2.1, in the early Universe the vacuum energy Ω_Λ does not play a role and can be neglected. In the assumption of a Flat Universe, the Friedman equation (1.2.13) becomes:

$$\Omega_M + \Omega_R = 1 \,, \tag{1.2.15}$$

where $\Omega_M = \Omega_B + \Omega_\chi$ is the density of matter.

In thermal creation one supposes that at high temperatures in the early Universe, everything was at thermal equilibrium and because of that the number density of radiation such as photons and the number density of particles of Dark Matter was the same. Following the expansion of the Universe and the ensuing cooling down, the number density of both was decreasing until the temperature remained higher than the mass of

Dark Matter (natural units are understood). After that, the average energy of collisions would not be enough to produce Dark Matter particles and they decoupled from the thermal bath. Since the Dark Matter particle has to be stable, the number density will "freeze-out" and substantially remain the same until today. To give a more quantitative analysis, we can compute the number density of relativistic and non relativistic particles in thermal equilibrium, assuming an ideal gas description:

$$
n_{eq}(T) = g \int \frac{d^3p}{(2\pi)^3} \frac{1}{e^{E/T} \pm 1}
$$

$$
= \begin{cases} g \left(\frac{mT}{2\pi}\right)^{3/2} e^{-m/T} & \text{non-relativistic case} \\[2ex] \frac{\zeta_3}{\pi^2} g T^3 & \text{relativistic bosons} \\[2ex] \frac{3\zeta_3}{4\pi^2} g T^3 & \text{relativistic fermions} \end{cases} \tag{1.2.16}
$$

where g is the number of degrees of freedom of each particle, accounting for the anti-particle, spin and color states, while ζ_3 is the Riemann zeta function.

In the early Universe the number of Dark Matter particles per unit volume was proportional to T^3, being relativistic and in thermal equilibrium with radiation. As the Universe expanded, the temperature dropped and when it became comparable to the Dark Matter mass, the number density became proportional to $e^{-m/T}$. Basically, the density of Dark Matter dropped with an exponential factor because while it was still possible for them to collide and annihilate in ordinary particles, the inverse process was inhibited by the fact that the average energy of collision was not enough anymore. As the particles were annihilating, it became more and more difficult for them to find each other and collide, so it was not possible for their density to continue to exponentially decrease. This mechanism indeed stops being efficient when the interaction rate become comparable to the value of the Hubble constant, that gives the rate of expansion of the Universe.

In order to compute the decoupling temperature, we first need to find the relation between the Hubble constant and the temperature of the Universe. To do so, let's compute also the energy density of non-relativistic and relativistic particles in thermal equilibrium. We have

$$\rho_{eq}(T) = g \int \frac{d^3p}{(2\pi)^3} \frac{E}{e^{E/T} \pm 1}$$

$$= \begin{cases} mg \left(\frac{mT}{2\pi}\right)^{3/2} e^{-m/T} & \text{non-relativistic case} \\[3mm] \frac{\pi^2}{30} g T^4 & \text{relativistic bosons} \\[3mm] \frac{7\pi^2}{240} g T^4 & \text{relativistic fermions} \end{cases} \tag{1.2.17}$$

where we can recognise in the relativistic case the Stephan-Boltzmann law. We now can insert this result in equation (1.2.15) assuming the relativistic regime, i.e. both ρ_R and ρ_M are proportional to T^4, and we can find

$$H^2(t) \propto \frac{1}{t^2} \propto \rho_r \propto T^4 \,. \tag{1.2.18}$$

This relation allows us to find, at least in the radiation dominated era, a link between time, temperature and the Hubble constant. We can define the interaction rate $\Gamma = \sigma v n$, with σ being the cross-section of the annihilation, v the relative velocity of collision and n the number density of Dark Matter. At this point it is important to understand whether the particle decouples from the thermal bath in the relativistic or in the non relativistic regime using the appropriate number density. Assuming it to be massive enough to decouple in the non relativistic scenario in the radiation era, we can solve the implicit equation

$$\Gamma(T) = H(T) \tag{1.2.19}$$

and find T_{dec}. After it decouples, Dark Matter energy density drops like $\rho \propto 1/a^3$ in the non-relativistic regime and we can compute its energy density today:

$$\rho_\chi(T_0) = m_\chi n_\chi(T_0) = m_\chi n_\chi(T_{dec}) \left(\frac{a(T_{dec})}{a(T_0)}\right)^3 =$$

$$m_\chi n_\chi(T_{dec}) \left(\frac{a(T_{dec})T_{dec}}{a(T_0)T_0}\right)^3 \frac{T_0^3}{T_{dec}^3} = m_\chi n_\chi(T_{dec}) \left(\frac{g(T_0)}{g(T_{dec})}\right) \frac{T_0^3}{T_{dec}^3} \,. \tag{1.2.20}$$

The value of $g(T)$ depends on the temperature, taking into account only the degrees of freedom of the particles that compose the thermal bath at that given T. Thanks to this result, we can then evaluate the relic density

$$\Omega_\chi h^2 = \frac{\rho_\chi(T_0)h^2}{3M_{pl}^2 H_0^2} \, , \tag{1.2.21}$$

asking it to be consistent with the value we measure today, namely $\Omega_\chi h^2 \approx 0.12$. It is clear from the treatment that an important role is played by the cross-section of the annihilation process and so it is the type of interaction that is highly influenced by the constraints on the parameter space (masses and couplings) of the model. Whenever building a new model that aims at describing Dark Matter, it is always necessary to check which regions of the parameter space are allowed by the observed relic abundance.

1.2.2 Indirect detection

We start now to discuss the ways of searching for Dark Matter under the assumption that the new particles interact with Standard Model particles not only gravitationally. This is motivated by the fact that the relic density is compatible with the existence of a stronger interaction between the Dark sector and the Standard Model.

In this section we discuss the possibility of detecting Dark Matter particles through indirect searches. After the freeze-out from the thermal bath of the Universe, the number density of Dark Matter has roughly remained the same, but the spatial distribution of it has changed considerably in the era of galaxies and clusters formation. The idea behind indirect searches is the fact that, since Dark Matter is concentrated in regions of space where there is a huge amount of gravitational matter, the number density is enhanced locally despite being very low globally. For this reason, the same annihilation process that was happening in the thermal bath before the decoupling can still happen in these regions and we should be able to measure the products coming from there. In particular we can expect a significant flux of photons, neutrinos and even pairs of particles and anti-particles. When considering this scenario, one have to keep in mind that Dark Matter particles move very slowly in these regions, i.e. they are non-relativistic, and therefore they collide with each other almost at rest. For this reason we should expect the produced particles to have a well defined energy of approximately the mass of the annihilating particles. Typically we expect them to have a mass in the order of few hundred GeV. Apart from photons or neutrinos directly produced by Dark Matter annihilation that can travel long distances, the other products might interact with galaxies halos or decay in stable leptons or protons that can propagate and reach us. For example, positrons can eventually annihilate with electrons in the interstellar plasma and produce a photon emission in a specific range of the spectra [5]. We can list some examples of processes that can take place and that we can effectively measure:

$$\chi\chi \to l^+l^-$$
$$\chi\chi \to q\bar{q} \to p\bar{p} + X\,.$$

Unlike leptons and photons that come from many sources, the anti-particles are much rarer and therefore can in principle give a distinctive signal.

Let's consider now the scenario of a possible γ-ray signal. While DM particles are not charged and so they cannot interact directly to photons, the process can still happen through loops of charged particles such as quarks. The signal can come from different kinematic patterns. If they are produced by direct annihilation they will be detected as a mono-energetic line in the spectrum

$$\chi\chi \to \gamma\gamma \quad \Rightarrow \quad E_\gamma \approx m_\chi \tag{1.2.22}$$

because of the fact that Dark Matter particles are almost at rest when colliding. However they could also be produced as secondary particles from decay or interactions with the interstellar halos

$$\chi\chi \to \tau^+\tau^-, b\bar{b}, W^+W^- \to \gamma + ...\,, \tag{1.2.23}$$

giving rise to a fragmentation pattern in the photon spectrum.

The measurement of such signal requires to be aware of astrophysical backgrounds photons that are produced from known objects and the capability of identify an excess in the spectrum. In the past there were some observations of these kind of excess but nowadays they seem to find an explanation with common and known processes. Examples of these signals are the TeV-band γ-ray emission [6] and the INTEGRAL 511-KeV line [7] measured from the galactic center. Also the Fermi-Large-Area-Telescope detector has measured an excess in photon emission (see Fig. 1.2.2) coming from the inner Milky Way and while part of it can be interpreted with astrophysical explanations, a γ-ray excess on smaller scales could be caused by Dark Matter annihilation. If Dark Matter is responsible for this signal, we would expect a mass in the range of 10-50 GeV. However, astrophysical explanations cannot be excluded a priori but we can at least use these data to place an upper bound and constrain the cross-section of DM annihilation. The Fermi-LAT has produced upper limits on the cross-section for the production of final states such as $e^+e^-, \mu^+\mu^-, \tau^+\tau^-, u\bar{u}, b\bar{b}$ and so on.

Dark Matter annihilation takes place on many scales, from cosmological to processes within the solar system. An example is the search for DM captured by the Sun. Passing through the galactic halo, particles of Dark Matter will scatter with the Sun and
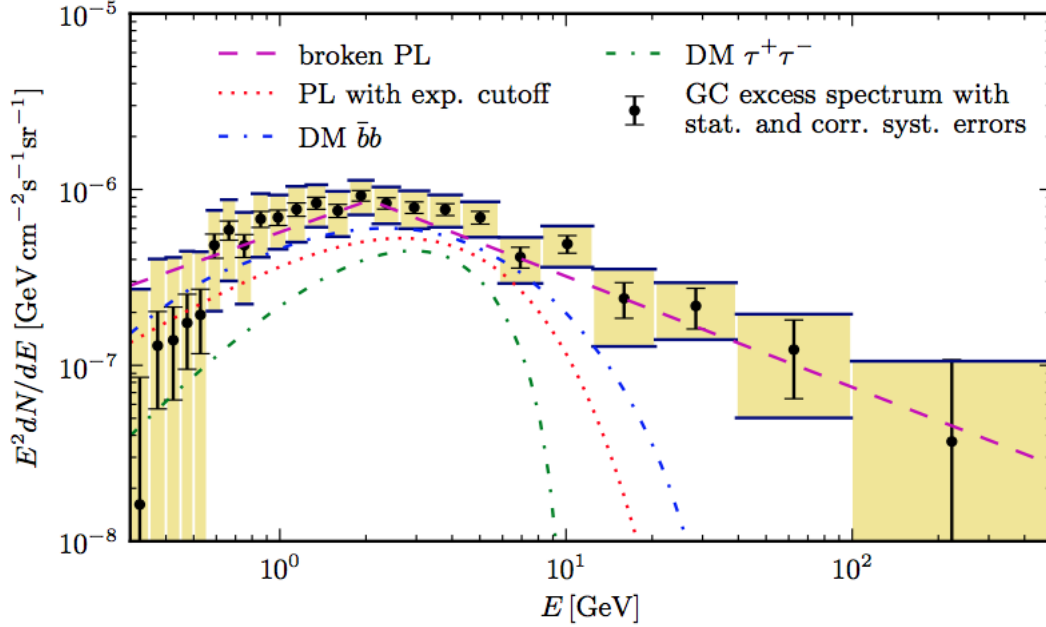
Figure 1.2.2: The Fermi-LAT GeV excess. This plot shows the residual γ-ray spectrum after the subtraction of astrophysical known background. The prediction of some hypothetical annihilation channels are also displayed [8].

get gravitationally bound. We know that the annihilation rate is proportional to the number density and therefore, after a sufficient time, the Sun will have captured enough Dark Matter to start the annihilation process. The time will come when the rate of collision will be high enough to balance the capture rate and the amount of Dark Matter in the Sun will reach equilibrium. At this point the Sun will become a storage of DM, with the quantity of it depending on the scattering rate. The number of DM particles captured over the age by the solar system should be already enough to have a significant effect. The only possible measurable product from this phenomenon are neutrinos and so experiments such as IceCube in Antarctica and other neutrino observatories, should be able to place constraints on scattering cross sections of Dark Matter.

A nice feature of this kind of searches is the fact that when studying the energy dependence of the particles flux produced by annihilating Dark Matter, we are able to separate a contribution relative to astrophysics and a contribution coming from particle physics. In particular the flux inside a solid angle $\Delta\Omega$ can be written as

$$\frac{d\Phi_i}{dE} = \frac{\langle\sigma v\rangle}{8\pi m_\chi^2}\frac{dN_i}{dE}\int_{\Delta\Omega} d\Omega \int_{l.o.s.} dz\, \rho_\chi^2(z)\,, \tag{1.2.24}$$

where E and N_i are the energy and the number of the produced particle, the integral of the energy density is performed along the line of sight and $\langle\sigma v\rangle$ is the thermal averaged cross section defined as

$$\langle\sigma v\rangle = \frac{\int d^3p_{\chi,1}d^3p_{\chi,2}\, e^{-(E_{\chi,1}+E_{\chi,2})T}\sigma_{\chi\chi\to ff}(s)v}{\int d^3p_{\chi,1}d^3p_{\chi,2}\, e^{-(E_{\chi,1}+E_{\chi,2})T}}\,. \tag{1.2.25}$$

The main problem is the fact that we do not know precisely the distribution of Dark Matter ρ_χ and we have to rely on numerical simulations of the profile. So we can define a quantity

$$J \propto \int_{\Delta\Omega} d\Omega \int_{l.o.s.} dz\, \rho_\chi^2(z) \tag{1.2.26}$$

that can be produced numerically and depends only on the astrophysical aspect of the problem. We can then recognise in the formula the part that comes directly from particle physics property and observations can therefore put constraints on the thermal averaged cross section, up to the knowledge of J and the spectrum per annihilation dN/dE.

1.2.3   Direct detection

Experiments in direct detection aim at measuring the recoil of nuclei in underground detectors on Earth caused by scattering with Dark Matter particles coming from the halo of the galaxy. The most important background for this kind of measurement are cosmic rays and natural rocks radioactivity. Because of this the detectors have to be shielded appropriately. In particular the measurements rely on three possible type of signals: energy deposition in calorimeters (phonons), scintillation light (photons) and ionisation (electrons).

Let us now evaluate the range of recoil energy we are dealing with. The relative velocity between Dark Matter particles in the halo and the Earth is in the order $v = 10^{-3}$ ($c = 1$) and therefore we are in the non relativistic regime. Denoting with m_A the mass of the

nucleus and m_χ the mass of Dark Matter, we have in the center of mass frame

$$v = \left| \frac{p_A}{m_A} - \frac{p_\chi}{m_\chi} \right| = |p_A| \left(\frac{m_a + m_\chi}{m_A m_\chi} \right), \tag{1.2.27a}$$

$$|p_A|^2 = 2 m_A E_A \approx \left(\frac{m_A + m_\chi}{m_A m_\chi} \right)^2 v^2. \tag{1.2.27b}$$

We can now compute the maximum recoil energy by taking the derivative in m_A of the former expression to get

$$\frac{dE_A}{dm_A} \approx \left(\frac{1}{(m_A + m_\chi)^2} - \frac{2 m_A}{(m_A + m_\chi)^3} \right) m_\chi^2 \frac{v^2}{2} = 0 \quad \Leftrightarrow \quad m_A = m_\chi. \tag{1.2.28}$$

In order to get the max recoil we need then to find a nucleus that has a similar mass to the particle of DM. Assuming the mass in the TeV range, we have a maximum recoil energy

$$E_A \approx \frac{m_\chi^2}{4} \frac{1}{2 m_\chi} v^2 \approx 10^4 \text{ eV}. \tag{1.2.29}$$

This tells us that the momentum transfer for direct detection are well below the electroweak scale. Thanks to the above relation we can translate the lowest measurable recoil in an experiment in a lower limit of Dark Matter masses that we can probe. Particles with masses below 1 GeV are usually below the detection threshold for nuclei recoil but they can interact with electrons and then can be detected through ionization or excitation.

The velocity of Dark Matter in this kind of experiments is a combination of the thermal velocity which has not a preferred direction and the velocity of the Earth moving around the Sun. For this reason we can estimate an annual modulation of it and if we were able to measure it, we would be able to confirm that the recoil are due to Dark Matter scattering. The approximate behavior of the velocity of the Earth around the Sun can be written as

$$v_e \approx \frac{v}{15} \cos \left(2\pi \frac{t - 152.5 d}{365.25 d} \right). \tag{1.2.30}$$

If we assume the velocity distribution of Dark Matter to follow a Gaussian distribution, it can be shown that it can be written as
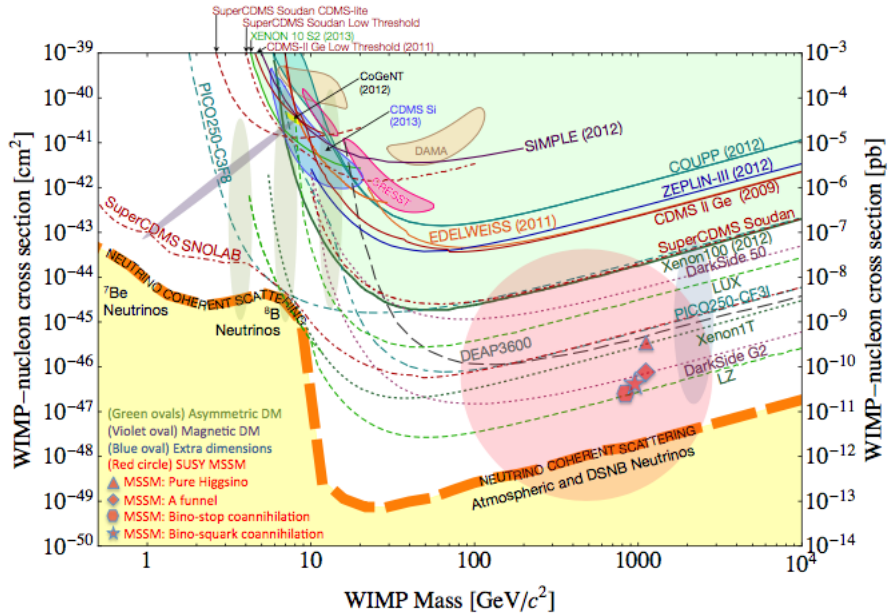
Figure 1.2.3: This plot shows spin indipendent limits for the nucleon-DM cross section in direct detection experiments. The yellow region indicate a parameter space area that is dominated background consisting of neutrinous [9].

$$f(v)dv = \frac{vdv}{v_e v_0 \sqrt{\pi}} \left(\exp\left[-\frac{(v - v_e)^2}{v_0^2} \right] - \exp\left[-\frac{(v + v_e)^2}{v_0^2} \right] \right), \tag{1.2.31}$$

where $v_0 = 220$ km/s is the velocity of the Sun around the galactic center and the distribution is not defined for velocities higher than $v_{esc} \approx 500$ km/s, the escape velocity of the galaxy. The direct detection rate is also related to the local Dark Matter density that is approximately $\rho \approx 0.39$ GeV/cm^3. The Dark Matter flux passing through Earth can then be significant, $nv = \rho v/m_\chi \approx 10^5$ cm^{-2} s^{-1} for m_χ in the order of 100 GeV.

If we consider a detector that has different kind of nuclei, the total recoil energy spectrum can be obtained by summing over all of them. The differential rate is

$$\frac{dR}{dE_R} = \sum N_N \frac{\rho}{m_\chi} \int_{v_{min}}^{v_{esc}} \frac{d\sigma_N}{dE_R} v f(\boldsymbol{v}) d^3 v \tag{1.2.32}$$

with N_N the number per unit mass of the nucleus. This rate is usually small, in the order of 1 event/100 kg day.
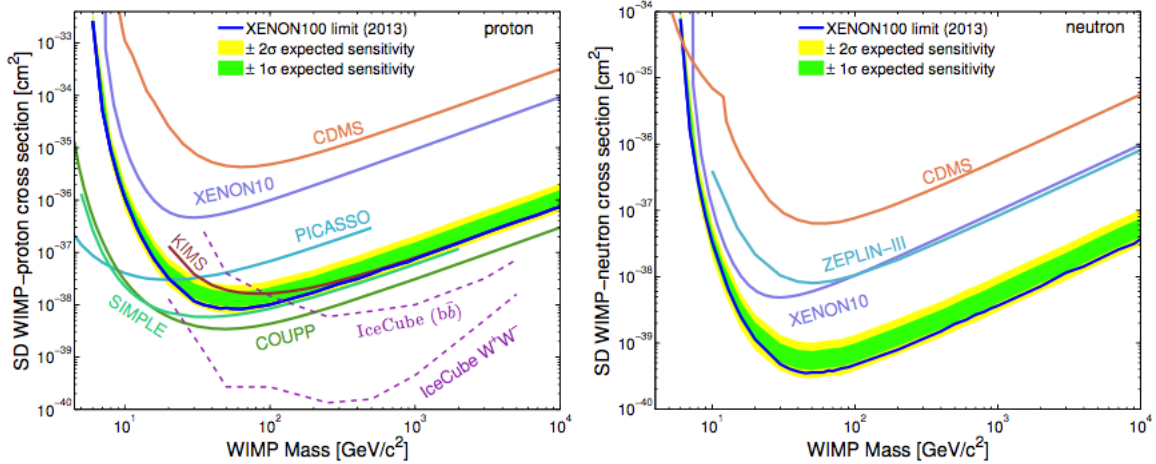
21

Figure 1.2.4: Spin dependent cross sections limits. The left plot shows constraints for protons while the right plot for neutrons [10].

There are two types of interactions that we are dealing with when talking about nuclear scattering: spin independent and spin dependent. We are in the first case when the interaction is through a scalar or a vector mediator with no axial coupling. The spin independent cross section has the form

$$\sigma^{SI}(E_R) = \left[Z + (A - Z)\left(\frac{f_n}{f_p}\right) \right]^2 \frac{\mu^2}{\mu_p^2} \sigma_p F_{SI}^2(E_R), \qquad (1.2.33)$$

where Z and A are the number of protons and nucleons in the nucleus, $f_{p/n}$ is the dark matter coupling to protons and neutrons, μ and μ_p are the reduced mass with respect to the nucleus and the proton and σ_p is the cross section for protons. $F_{SI}(E_R)$ is the spin independent nuclear form factor, namely the Fourier transform of the nucleon density in the nucleus and is usually considered similar for protons and neutrons. If the couplings of neutrons and protons are the same, the nucleus interact coherently with Dark Matter, as an elementary particle. On the other hand if the couplings are different and opposite to each other, for some nuclei with an abundance of neutrons the cross section can be significantly reduced and therefore avoid experimental constraints (see Fig. 1.2.3).

Spin dependent interactions are characterized by an axial vector coupling and the cross section has the form

$$\sigma^{SD}(E_R) = 32\mu^2 G_F^2 [(J_N + 1)/J_N][< S_p > a_p + < S_n > a_n]^2 F_{SD}^2(E_R), \qquad (1.2.34)$$

22

with J_N nuclear spin, $a_{p/n}$ Dark Matter coupling to protons and neutrons, $F^2_{SD}(E_R)$ nuclear form factor and $< S_{p/n} >$ expectation value of the proton and neutron spin. Since these are in the order of unity, the spin dependent cross sections are smaller than the independent ones by a factor A^2 and the constraints on SD cross sections are therefore weaker (see Fig. 1.2.4).

While some Dark Matter candidates are still to be tested, direct detection experiments have already excluded a wide range of them.

1.2.4   Colliders searches

Colliders searches for Dark Matter have both advantages and disadvantages. First of all, in order to effectively detecting it, it is necessary that Standard Model particles and particles of the Dark sector talk to each other either through a direct coupling (for example to leptons or quarks) or through a new mediator. We also need to consider that we are looking for particles that are weakly interacting and so we might need high precision measurements to distinguish the signal from the background. Dark Matter has to be a stable and neutral particle and therefore it is not easy to detect. At the same time we have to be aware of the fact that even if the particle does not decay before passing through the detector, that does not mean that it is stable on cosmological time scales, which is the property we need to explain the relic density.

On the other hand, colliders experiments have the advantage of producing a huge amount of data, since the high luminosity characteristic of these machines is translated in a great number of events. Therefore we expect to produce a significant amount of Dark Matter particles to analyse. Also colliders are provided with many different detectors which can measure different observables and once studied in detail all the background processes, we should be able to spot a signal and if it passes all the requirements to be considered a discovery, we will be able to tell a lot of properties of the particle.

The most important observable that we can theoretically predict and verify is the expected number of events for a specific process in a given time interval. The rate of events is defined as

$$R_e = \sigma \mathcal{L} \epsilon \, , \tag{1.2.35}$$

where σ is the total cross section of the process, $\mathcal{L}$ is the luminosity of the collider and ϵ is the detection efficiency, including phase-space cuts and trigger requirements deciding which events are going to be kept and analysed. The luminosity is one of the most important parameter for a colliding beam, giving a measure of the number of scattering events produced. The luminosity of LHC in Run 1 for example was $\mathcal{L} \sim 10^{34}$ cm^{-2}s^{-1}. The actual rate of events however is also related to the cross section and if the interactions

are weak, despite a huge luminosity, we produce a small number of events.

There are two main categories of colliders: electron colliders and hadron colliders.

Electron colliders

In electron colliders we collide electrons and positrons. The energy reach of these kind of machines is lower than the energy in hadron colliders, but there are also advantages in using them. If we want to detect Dark Matter particles we have to consider that we can not measure an event that produces only them because they are invisible for our detectors. We then need to produce at least a standard model particle that we can detect and then look for missing energy. Lepton colliders have a big advantage with respect to hadron colliders because we know precisely the kinematics of the initial state. Assuming that the Dark Sector has a quantum number of its own, we can only produce an even number of DM particles in each collision and so to produce at least a pair we need $\sqrt{s} > 2m_\chi$. Suppose that we produce a pair of Dark Matter particles and a photon, that we measure.

$$e^+e^- \to \chi\chi\gamma \tag{1.2.36}$$

Since we know the initial state and the four-momenta of the photon, we are now able to reconstruct the four-momenta of the pair of DM particles. Experimentally this kind of signature is called γ plus missing momentum. The problem with this kind of collider is that despite the relatively clean environment, we have not so much energy in the center of mass and to detect Dark Matter we also need to produce a hard photon, lowering the rate of significant events.

Hadron colliders

Hadron colliders can reach higher energies in the center of mass but they also have other complications. Historically, many massive particles have been discovered thanks to collisions of protons and anti-protons, since they are much heavier than electrons and therefore they store more energy to release in collisions. On the other hand the environment is much more problematic, there is always a huge background for every process and the analyses are less precise.

At LHC we have to consider two kind of processes: backgrounds and signal. We are interested in the signals, i.e. evidence of new particles, but we cannot get rid of QCD background processes that, characterised by a strong coupling, dominate the scene. Signals are very rare, but we are able to predict background and so we should be able to detect a deviation from it. Another problem is that we cannot store all the data we
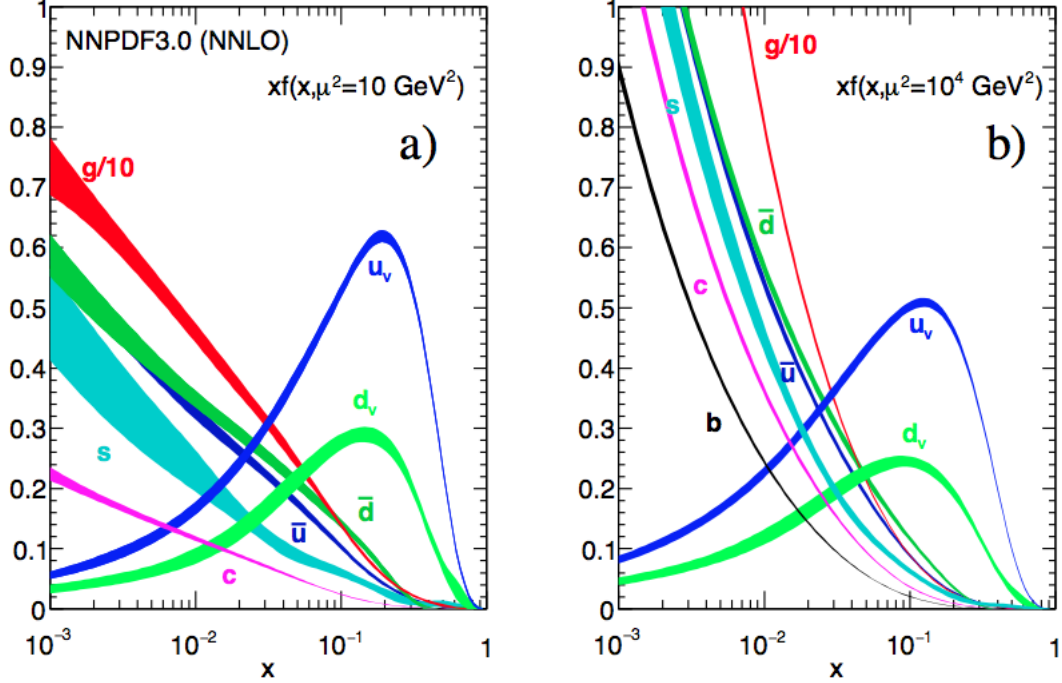
Figure 1.2.5: These plots show the parton distribution at two different scales of the transferred momentum Q, with $\alpha_s(M_Z^2) = 0.118$ [12].

produce, we have to set up a trigger that has to evaluate whether an event is physically interesting for Dark Matter searches or not, in order to decide whether to keep it or not. While in hadron colliders we are able to reach higher energies, we are not able to know precisely the initial state, since we are able to resolve the proton constituents. This means that we have to describe collisions not in terms of protons but in terms of quarks and gluons that carry a fraction of the proton momentum. For this reason, despite the energy of the protons being 13 TeV at LHC, the actual collisions between elementary particles happen at the TeV scale [11]. The problem is that we are not able to predict the distribution of energy of the partons, i.e. the Parton Distribution Functions, since it is not an observable unless we integrate it together with the partonic cross section. Therefore we have to rely on experiments to determine it (see Fig. 1.2.5).

Unlike in electron colliders, we then cannot reconstruct the momentum of the pair of Dark Matter particles from the measurement of the momentum of the other particles produced, but we can do it with the transverse 3-momentum since it is supposed to be zero either in the initial and in the final state. The transverse momentum is defined as

$$\vec{p}_T = \vec{p}\sin\theta\,, \tag{1.2.37}$$

where θ is the angle between the outgoing particle and the collision beam. The missing momentum of the Dark Matter particles is then defined

$$\not{\vec{p}}_T = -\sum\vec{p}_T\,. \tag{1.2.38}$$

The most common way to look for Dark Matter in hadron colliders is to search for Mono-Jet and missing energy $\not{E}_T$, corresponding to processes like

$$q\bar{q}\to\chi\chi + g\,, qg\to\chi\chi + q\,, gg\to\chi\chi + g\,. \tag{1.2.39}$$

The missing energy is defined as $\not{E}_T = |\not{\vec{p}}_T|$. We might also consider processes in which instead of jets, we produce mono-photon, mono-W/Z or Higgs. The main background processes that we have to deal with to detect this signal are

$$pp\to j + Z\,, Z\to\nu\bar{\nu} \tag{1.2.40a}$$

$$pp\to j + W\,, W\to l\nu\,. \tag{1.2.40b}$$

While the first one is inevitable and related to the difficult measurement of neutrinos, the second can be reduced since it is due to the fact that, because of detectors or reconstruction inefficiencies, we could miss the charged lepton.

1.2.5 Dark Matter particle candidates

Until now we have analysed various ways to detect Dark Matter from a particle physics perspective, the different approaches can be summarised in figure 1.2.6. We are now interested in listing some of the most famous Dark Matter candidates, focusing on the characteristic features of each one of them.

Most of the evidence we previously talked about is based on gravitational effects of Dark Matter. Since we know about gravitational interactions, we can only speculate about its nature. Both particle physics and astrophysics could provide information on how to identify it [13].
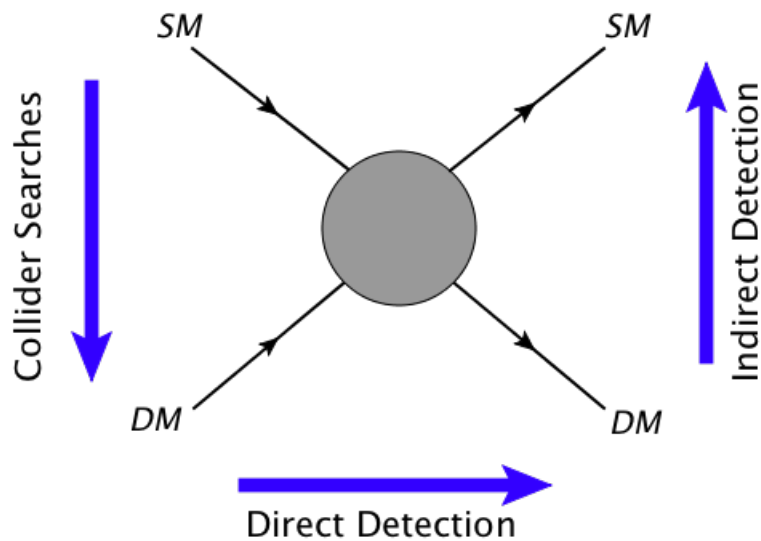
Figure 1.2.6: A diagram summarising the Dark Matter searches formerly described.

Neutrinos

The first thing that comes to mind when trying to solve the Dark Matter problem is to look for a solution in the framework we already know. In the Standard Model the neutrinos stand out immediately: they are stable and do not have electromagnetic or strong interactions, characteristics that are mandatory for a Dark Matter candidate. Unfortunately, they cannot explain the large scale structure formation of our Universe, since being very light thermal relics, they are predicted to decouple from the thermal bath of the Universe with a highly relativistic velocity distribution. They are a classic example of hot Dark Matter. However, computer simulations have shown that hot Dark Matter would tend to form large structures before of the formation of galaxies and only later, because of fragmentation, they would form smaller structures. This is incompatible with the Universe we observe and therefore hot Dark Matter and in particular neutrinos cannot account for most of the Dark Matter we observe.

However, the simplest extension of the Standard Model, the Neutrino Minimal SM proposed by Shaposhnikov, takes also into account the three right-handed neutrinos which have not been observed yet and could also address the problem. They are also called sterile neutrinos since they only interact with the other SM particles through gravitational interaction and are characterized by Majorana mass terms in the Lagrangian. In this model their mass is assumed to be smaller than the electroweak scale (see [14] for further details).

Supersymmetry

The inability to find a solution within the Standard Model has led physicists to study Beyond Standard Model scenarios. One of the most famous BSM approach is the one related to Supersymmetry. In the early 1970s many physicists started to study models with a new space-time symmetry that relates bosons and fermions. Supersymmetry requires for every boson of the Standard Model to have a fermionic partner with the same quantum numbers and viceversa. One of the most notable prediction of this theory is the fact that the vacuum energy of the model should be exactly zero, since for every boson contribution there is an opposite one from the superpartner. Supersymmetry therefore predicts many particles that could be stable and electrically neutral such as the partner of the neutrino, of the photon, of the Z boson, of the Higgs boson and of the graviton. Some examples of the most studied supersymmetric candidates are the gravitino and the neutralino, a mix of photino, Zino and two Higgs bosons, which is probably the most popular. Supersymmetry is not a theory brought to life to explain the Dark Matter problem and possible solutions comes out from it as a bonus. Many physicists formulated Beyond Standard Model theories in recent decades, motivating their proposal with the fact that their model account for a possible Dark Matter candidate. It can be argued that if a new theory has no viable candidate for Dark Matter, despite other attractive feature, it would be seen as incomplete.

Axions

As successfully as it is, Quantum Chromo Dynamics suffers from one issue, called the strong CP problem. Indeed we can write in the QCD Lagrangian the term

$$\mathcal{L}_{QCD} \supset \theta \frac{g_s^2}{32\pi^2} G^{a\mu\nu} \tilde{G}_{a\mu\nu} \,, \tag{1.2.41}$$

where g_s is the strong coupling, θ is a quantity related to the vacuum phase and $\tilde{G}_{a\mu\nu}$ is the dual of the gluon field strength. This term introduces a charge-parity violation, causing the electric dipole moment of the neutron to be much higher than expected. For this reason, observations constrain the value of θ to be of order 10^{-9}. The unnaturalness of this parameter has led physicists to find a reason why θ is so small. In 1977 Peccei and Quinn proposed a model with an additional spontaneously broken $U(1)$ symmetry that can dynamically drive the value of θ to zero. The axion a is the pseudoscalar Goldstone boson of this broken symmetry and its interaction with the Standard Model is

$$\mathcal{L}_a = -\frac{g_s^2}{32\pi^2} \frac{a}{f_a} \epsilon^{\mu\nu\rho\sigma} G_{\mu\nu}^a G_{\rho\sigma}^a \,, \tag{1.2.42}$$
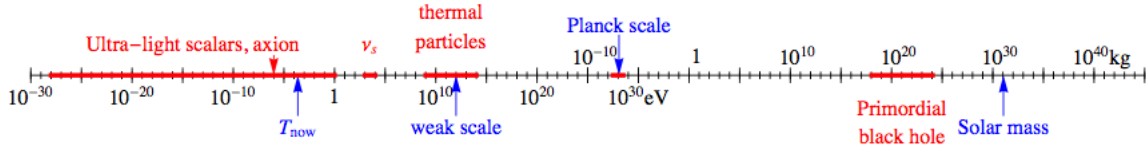
Figure 1.2.7: A Summary of Dark Matter candidates and their mass scale [11].

with f_a being the scale at which the symmetry is broken. The axion acquire also a small mass, proportional to f_a^{-1}, in the process. This particle has to be light and weakly interacting to avoid constraints from particle physics observations and therefore it can be stable on cosmological time scales and could account for Dark Matter.

WIMPs

In recent years, the idea that Dark Matter is made of cold and non-baryonic particles has become widely accepted among particle physicists and astrophysicists. In particular, the most studied Dark Matter candidate at the moment is the Weakly Interacting Massive Particle or WIMP. These are particles whose masses lie in the $10 - 10^3$ GeV scale and interact through the weak force. For a particle of this kind to be consistent with the thermal relic abundance, the self-annihilation cross-section has to be $\sigma v \sim 10^{-26}$ cm^3/s, in the weak force scale. This feature is called the WIMP Miracle, since a particle with the mass and interaction in the weak scale naturally accounts for the observed relic density. This is the main reason, combined with the fact that there are also other theoretical arguments in favor of new physics in the weak scale, that made WIMP candidates so popular and the leading candidate for Dark Matter. They are predicted in many theories, such as Supersymmetry, and they may be detected in many ways. The improvements of astrophysical experiments and the advent of LHC, should allow us to explore this possibility in great detail and either we will discover them or we will have to start to think at other viable solutions. This is the Dark Matter candidate that we will consider in this work.

Primordial Black Holes

As of now we cited the most common DM candidates related to particle physics, but astrophysicists in particular have suggested other kind of structures to describe the effects of Dark Matter, called MACHO (Massive Compact Halo Objects). They have to be compact astronomical objects, much less luminous than ordinary stars, like planets and

neutron stars. A particularly suggestive option is the theory that Dark Matter is made of primordial black holes, i.e. small black holes that formed in the epoch of nucleosyntesis and that can therefore escape the constraints coming from the low rate of gravitational microlensing in our galaxy. We can also place a lower limit on their masses since we do not observe Hawking radiation coming from them (a black hole should emit a black body radiation at a temperature that is proportional to the inverse of their mass). Primordial black holes with masses in the range 10^{-13} - 10^{-7} $M_\odot$ are stable on cosmological scales and are almost collisionless, making them a possible candidate to explain the observed gravitational anomalies.

Chapter 2

Theoretical approach in Dark Matter searches

After studying the various detection methods physicists are employing in order to detect Dark Matter, we would like to focus on the theoretical perspective. To interpret the constraints coming from experiments is needed a theoretical model predicting Dark Matter. There are many possible models with different features and they all together constitute the theory space of models. We can identify three main categories: ultraviolet complete models, Dark Matter effective field theory models and the simplified models (see fig. 2.0.1). We will quickly describe the limitations of complete models and then focus on the comparison between the effective field theory and the simplified models approach, enlightening the pros and the cons of each one of them.

2.1 UV complete models and the inverse problem

Ultraviolet complete models are not meant to describe only Dark Matter, but they usually introduce many new particles and parameters to the Standard Model. The idea behind them is usually to complete the Standard Model in order to solve some of its problems, such as the hierarchy problem and the mass generation of neutrinos, or to build a Grand Unified Theory in which at high energies, the three gauge forces of Standard Model, i.e. electromagnetic, weak and strong interaction, are merged into one single gauge group. While these models can be extremely satisfying because they answer a lot more questions than just "what is Dark Matter?", several of the new particles have nothing to do with it. An example is the Minimal Supersymmetric SM, in which every particle of the Standard Model gets a superpartner and Dark Matter is described by the LSP (Lightest Supersymmetric Particle), a weakly interacting massive particle. Complete
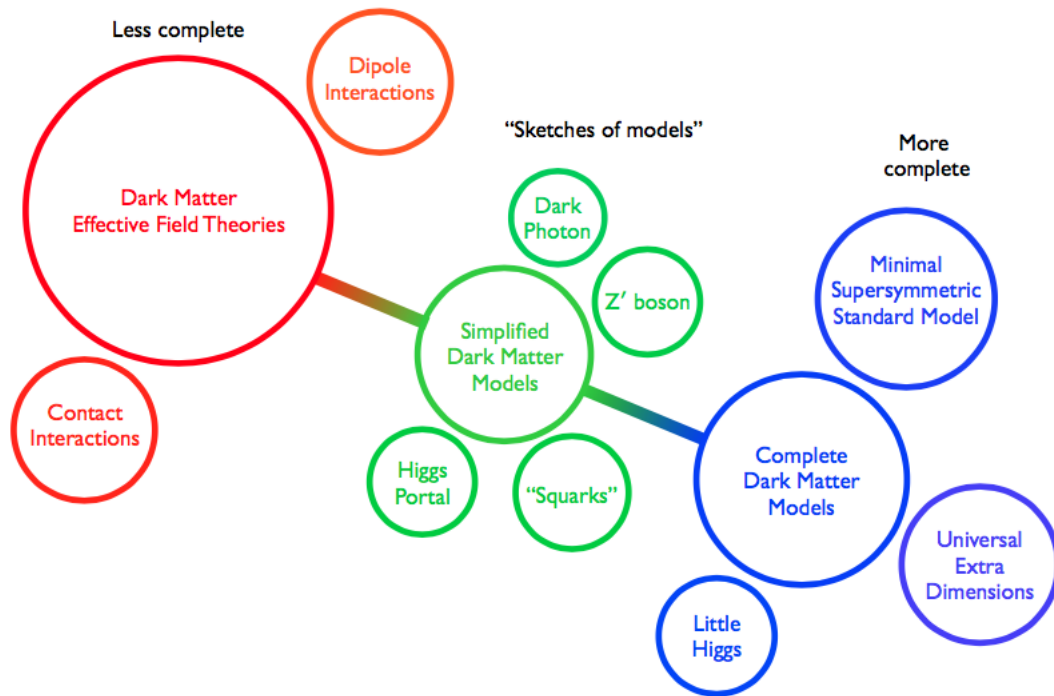
Figure 2.0.1: A diagram showing the three main categories of Dark Matter models [15].

models add many new parameters to the description of Nature, some of them not at all related to the Dark Matter problem. It is true that these models can show relations between couplings that in other approaches can look like accidents, but their structure is so rich that it might be very difficult to unambiguously determine the model parameters from experiments. This problem is called the "inverse problem".

Suppose we build a new model accounting for a Dark Matter particle. We can then study the phenomenology and make a prediction on what signals should be there if we do an experiment, for a particular choice of the parameters. Let's consider now the inverse operation. Suppose we do an experiment at LHC and we find a signal, how do we understand the underlying new physics? While spotting a signal incompatible with the Standard Model could be easy, determining the properties of the underlying model can be challenging. Can we be able to distinguish if we found SUSY or another model? Hopefully if we have enough models and we study them in the forward direction, we can have a sufficient understanding of the differences between each model and we might be able to distinguish them, but that is not always the case.

Any signal at LHC is likely to receive contribution from several channels and so the observables we can rely on are not that many. A given set of observations identify
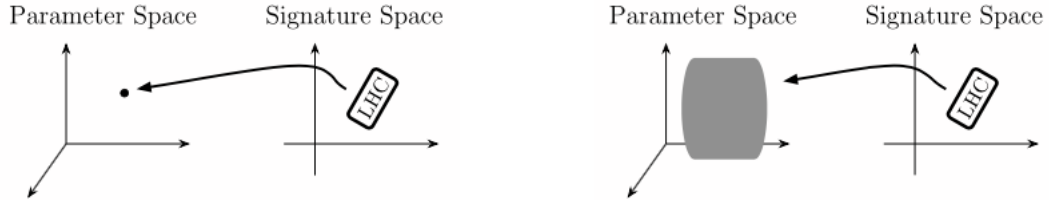
Figure 2.1.1: These diagrams shows the best and the worst case scenario. Ideally the map would be one-to-one, identifying a very small region in the parameter space. In the most pessimistic scenario the region is too wide and we do not have a clue of what model we found.

a small region in the signature space, with the dimension of it related to the intrinsic quantum fluctuations and the experimental errors. What does the map to the parameter space of the theory look like? (see Fig. 2.1.1)

In the best case scenario, we will have a one-to-one map and at a small region in the signature space will correspond a small region in the parameter space, allowing us to identify a model. In this case with better measurements we would restrict the region and better determine the underlying model. In the worst case scenario, the inverse map will associate to the small region in the signature space a huge one in the parameter space, preventing us to even have a clue at what is the structure of the theory. Another possible situation is to have some sort of degeneracies in different small regions of the parameter space, with all of them corresponding qualitatively to the same region in the signature space.

This problem can arise because the degrees of freedom of the complete model, i.e. the free parameters, are too many and at different sets of them could correspond the same observables at LHC. This is why despite the appeal, UV complete models can be too rich and some other approaches might be more efficient in tackling the Dark Matter problem.[1]

---

[1]For a more complete analysis of this problem see [16]

2.2 Effective Field Theory description

Suppose we would like to study the dynamic of a billiard ball on a table, scattering with other balls. We know that the ball is a very complicated object made out of atoms, which are made of electrons, protons and neutrons that are made of quarks. From this perspective, studying the dynamic of a ball colliding with other balls looks like an impossible job, since every elementary particle interacts with particles in the same ball and in the other balls, making the computation extremely difficult to carry out. Fortunately, however, we do not have to do that to solve this problem. If we look at this system from very far away, we see no internal elementary particles, we only see pointlike mass objects scattering through each other under the laws of newtonian mechanics. Basically, we see a contact interaction. This example is obviously trivial, nobody would ever even think about tackling this problem with a quantum field theory approach, but it contains the basic premise that leads to the idea of effective field theory: one does not need to know the short distance (high energy) physics if he only wants to describe the long distance (low energy) physics. This is a very important property of the world we observe, since without it we could not have been able to make any advance in physics because to describe a human scale phenomenon we would need to know the small scale behavior of Nature. Thanks to this principle we can think of describing a very complicated quantum field theory using an effective Lagrangian that contains only the degrees of freedom and the symmetries important at the specific scale of energy we are interested in. This is exactly the reason why effective field theory is so powerful. The other side of the coin is that is very difficult to obtain information on high energy physics from low energy experiments [17] [18].

The way to build an effective field theory is very similar to the way to build a quantum field theory. We need to decide which are the degrees of freedom, represented by spacetime fields, and which groups of symmetries (such as Lorentz transformations, gauge symmetries and so on) we want the dynamics to be constrained by. Then we will be able to write the most general Lagrangian containing terms that are invariant under the group transformations. We have to write all the possible terms compatible with the symmetries, not because we want to be general, but because of the Gell-Mann's totalitarian principle, i.e. in quantum field theory everything that is not forbidden is compulsory. This is because if a certain process is not forbidden, then there will be a probability for it to happen thanks to short distance fluctuations. The only difference with respect to usual quantum field theory is that we do not require the renormalizability of the theory. The purpose of having a renormalizable theory is indeed to have a model that can describe physics at all scales, but now we do not want to be that ambitious, we only want to describe Nature up to some scale. Also it can be argued from a philosophical point of view, that we do not have experiments that probe our models up to arbitrary scales, so the request to have a theory that have this ambition is beyond our aims.

When we study a renormalizable theory, we know that the maximum engineering dimensions of the operators we can write is four. Given this constraint, the number of terms we can write is finite and therefore we have a finite amount of parameters to fix with experiments. Once we have done that, we can start to make prediction for results of other observables with our theory. A problem we have is that, when we do computation at next to leading order, we have to compute loop diagrams that are divergent. Since we want the model to be predictive at every scale, we have to deal with ultraviolet divergences and we need to renormalize the theory absorbing the infinities in the parameters. The starting point of an effective field theory is to accept that we are not going to be predictive at arbitrary short distance and that we have an energy cut-off Λ beyond which our theory is not valid anymore. If we do this, we will also solve the problem of ultraviolet divergences since we will not integrate over all the phase space in loops but we will restrain ourselves in the energy regime below the cut-off Λ. Of course nothing comes for free and we have to deal with a totally different problem. Since we are not requesting renormalizability, we can write an infinite amount of terms in the Lagrangian and with them an infinite amount of parameters, making our theory totally unusable and not predictive.

However, as long as we are willing to renounce at exact predictions and stick with approximate solutions the theory is predictive. Since we are interested at the low energy behavior, we can understand which operators are more important than others in a specific energy range. It turns out that this operation is quite straightforward since it is related to the naive dimension of the operators. Let's consider a scalar field theory in D dimensions. Since the action S has to be dimensionless (in natural units),the kinetic term $(\partial\phi)^2$ has dimension D. The derivative has dimension 1 and therefore the field ϕ has dimension $D/2 - 1$. Therefore an operator $O_{p,q}$ with p fields and q derivatives has dimension $p(D/2 - 1) + q$ and in the action can be written as

$$S \supset \int d^D x \frac{g_{p,q}}{\Lambda^{p(D/2-1)+q-D}} O_{p,q} \, , \qquad (2.2.1)$$

where $g_{p,q}$ is the dimensionless coupling and we have explicitly written the cut-off scale Λ in order to make the dimensions right.

When we do computation for processes at energy E, for dimensional reasons we expect each operator to contribute to the action with

$$S \supset g_{p,q} \left(\frac{E}{\Lambda}\right)^{p(D/2-1)+q-D} \, . \qquad (2.2.2)$$

Thanks to this expression we can classify each operator in three categories:

- Relevant operators: if $p(D/2-1)+q-D < 0$ then for $E < \Lambda$ the operator becomes more and more important as the energy is small compared to the cut-off. The mass term falls in this category.

- Marginal operators: if $p(D/2-1)+q-D = 0$ then the operator is equally important at every scale. The kinetic term falls in this category.

- Irrelevant operators: if $p(D/2-1)+q-D > 0$ then for $E < \Lambda$ the operator becomes less and less important as the energy decrease.

In an effective field theory we have to decide at which precision $(E/\Lambda)^n$ we want to do the calculation, then we take into account every contribution coming from operators with dimension smaller than $n+D$. Provided we are able to deal with a large amount of contributions (the number of possible operators increase exponentially with the dimension), we can obtain predictions at an arbitrary precision. The only thing we have to do is to write the most general Lagrangian up to dimension $n+D$. This model will have a finite amount of coefficients and therefore we will be able to fix them with an appropriate number of experiments. We notice that the precision of our prediction becomes better and better as the energy of the experiment $E \to 0$, since the neglected contributions become less and less important. Also, if the energy approach the cut-off value Λ the theory fails by construction, since we cannot neglect any term, ending up with an infinite amount of contributions. The cut-off value, however, is not arbitrary, we cannot choose it. We have to determine it through measurements for each given theory.

In order to understand how to build an effective field theory out of a complete theory, let us briefly mention an example, the Fermi Theory. Historically it happened the other way around, Fermi built the effective theory ad hoc to describe the decay of the neutron without being aware of the underlying SU(2) structure. In the Standard Model, the weak interactions are mediated by the W bosons and the interaction term between quarks is

$$\mathcal{L}_{EW} \supset -\frac{ig}{\sqrt{2}}V_{ij}\bar{q}_i\gamma^\mu P_L q_j W_\mu \,, \tag{2.2.3}$$

where V_{ij} is the Cabibbo-Kobayashi-Maskawa matrix and P_L is the left-handed projector. At the lowest order, the matrix element of a scattering amplitude between a up quark and a down quark arising because of a W exchange is

$$\mathcal{M} = \left(\frac{ig}{\sqrt{2}}\right)^2 |V_{ud}|^2 (\bar{u}\gamma^\mu P_L d)(\bar{d}\gamma^\nu P_L u)\left(\frac{-ig_{\mu\nu}}{p^2 - M_W^2}\right) \,, \tag{2.2.4}$$

where p is the momentum transferred by the W boson and u and d are the quarks spinors.

The amplitude is characterized by a non-local interaction, but if the momentum of the W boson is small compared to its mass

$$\frac{1}{p^2 - M_W^2} = -\frac{1}{M_W^2}\left(1 + \frac{p^2}{M_W^2} + O\left(\frac{p^4}{M_W^4}\right)\right) . \tag{2.2.5}$$

If we only consider the first order of this expansion, we can write the amplitude as

$$\mathcal{M} = \frac{i}{M_W^2}\left(\frac{ig}{\sqrt{2}}\right)^2 |V_{ud}|^2 (\bar{u}\gamma^\mu P_L d)(\bar{d}\gamma_\mu P_L u) + O\left(\frac{1}{M_W^4}\right) . \tag{2.2.6}$$

The same amplitude could be obtained with an effective Lagrangian, that was the one Fermi wrote from the start

$$\mathcal{L} \supset -\frac{4G_F}{\sqrt{2}}|V_{ud}|^2 (\bar{u}\gamma^\mu P_L d)(\bar{d}\gamma_\mu P_L u) , \tag{2.2.7}$$

where G_F is the Fermi constant that from the complete theory we understand is defined as

$$\frac{G_F}{\sqrt{2}} \equiv \frac{g^2}{8M_W^2} . \tag{2.2.8}$$

As long as we do not probe the weak interactions in the weak energy range $M_W \approx 80$ GeV, the Fermi Theory gives a good enough description and we do not need to know the full details of the underlying small scale theory to make predictions. The interaction between quarks become a contact interaction, just like billiard balls when you watch them from the daily life distance scale.

When we are computing something in effective field theory, we always have to keep in mind the precision of the calculation we want. Let's suppose that we want to do calculation up to dimension four operators. At tree level, the cut-off Λ always comes at the denominator and therefore we can neglect all the operators with dimension higher than four. However, we have to be sure that when we start to include loops to get more precise predictions, they do not modify the power counting, i.e. operators with dimension higher than four do not give unsuppressed contributions. Unfortunately, this is exactly the case if we use the cut-off regularization, since we get Λ at the numerator by cutting off the loop momenta at Λ. It is easy to see this phenomenon explicitly in the scalar field theory
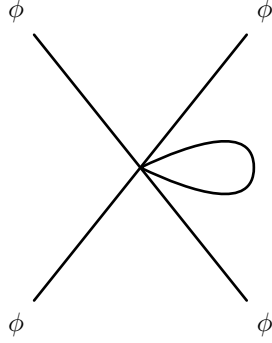
Figure 2.2.1: The Feynman diagram of the contributions coming from higher order operators.

$$\mathcal{L} = \frac{1}{2}\partial_\mu\phi\partial^\mu\phi - \frac{1}{2}m^2\phi^2 - \frac{1}{4!}\lambda\phi^4 - \frac{1}{6!}\frac{c_6}{\Lambda^2}\phi^6 - \frac{1}{2\cdot 4!}\frac{c_8}{\Lambda^4}\phi^4(\partial\phi)^2 \,. \qquad (2.2.9)$$

If we look for contributions at the four-vertex operator coming from higher order operators (Fig.2.2.1), we get

$$\Gamma_6 \approx \frac{c_6}{\Lambda^2}\int^\Lambda \frac{d^4k}{(2\pi)^4}\frac{1}{k^2-m^2} \sim \frac{c_6}{\Lambda^2}\frac{\Lambda^2}{16\pi^2} \sim O(1) \qquad (2.2.10a)$$

$$\Gamma_8 \approx \frac{c_8}{\Lambda^4}\int^\Lambda \frac{d^4k}{(2\pi)^4}\frac{k^2}{k^2-m^2} \sim \frac{c_6}{\Lambda^4}\frac{\Lambda^4}{16\pi^2} \sim O(1) \,. \qquad (2.2.10b)$$

The power counting is lost and we see that higher order operators give contributions that does not scale with E/Λ. This is a problem because it means that if we want to make a prediction we have to take into account every operator, but there are an infinite number of them and the model becomes then useless. Fortunately there is a solution, we need to choose a mass independent renormalization scheme, such us dimensional regularization and the minimal subtraction scheme, in which the renormalization scale μ appears only in logarithms. If we estimate the previous contributions with this approach we have

$$\Gamma_6 \approx \frac{c_6\mu^{2\epsilon}}{\Lambda^2}\int \frac{d^{4-\epsilon}k}{(2\pi)^{4-\epsilon}}\frac{1}{k^2-m^2} \sim \frac{c_6}{\Lambda^2}\frac{m^2}{16\pi^2}\frac{1}{\epsilon} - \frac{c_6}{\Lambda^2}\frac{m^2}{16\pi^2}\log\frac{m^2}{\mu^2} \qquad (2.2.11a)$$

$$\Gamma_8 \approx \frac{c_8\mu^{2\epsilon}}{\Lambda^4}\int \frac{d^{4-\epsilon}k}{(2\pi)^{4-\epsilon}}\frac{k^2}{k^2-m^2} \sim \frac{c_8}{\Lambda^4}\frac{m^4}{16\pi^2}\frac{1}{\epsilon} - \frac{c_8}{\Lambda^4}\frac{m^4}{16\pi^2}\log\frac{m^2}{\mu^2} \,. \qquad (2.2.11b)$$
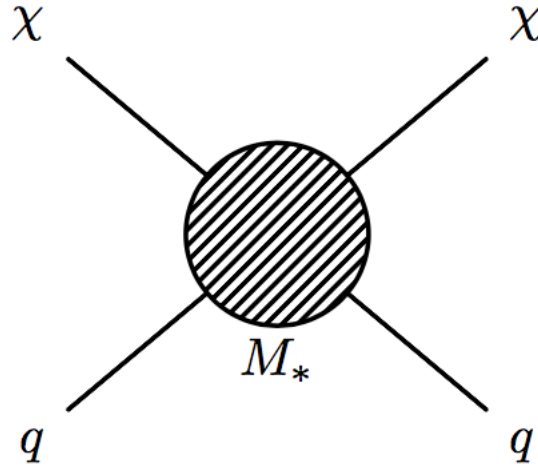
Figure 2.2.2: The picture shows a generic interaction between Dark Matter and quarks from the Standard Model from the EFT perspective [19].

Therefore we see that a mass independent scheme preserves the power counting and we are then able to neglect the higher operators contributions in loops. The only mass scale that appears is m, the mass of a particle that we observe in the low energy regime, so that $m \ll \Lambda$. At fixed order the effective field theory behaves exactly like a renormalizable theory, since there are only a finite number of terms in the Lagrangian and every higher order operator can be safely neglected.

However there is an important drawback in a mass independent scheme, heavy particles do not decouple. This happens because the β function that gives us information on the running of the coupling constants does not depend on the mass of the particles, i.e. every particle gives a contribution at the same order. If we use a "top-down" approach, i.e. we know the high energy theory and we want a simpler theory to describe the low energy behavior, we need to be careful when we integrate out the heavy particles. Usually one employs an approach called "matching", using the theory with the heavy particle for $\mu > M$ and one without it for $\mu < M$. Then to be consistent, the matching condition requires that the matrix elements for the theory without the particle and the theory with the particle have to be equal at $\mu = M$. The two theories will agree in the infrared regime but differ in the ultraviolet.

However sometimes we do not know the underlying high energy theory and we employ a "bottom-up" approach, directly writing the low energy theory. The parameters of this model will be fixed by experiments and therefore we will not have this problem.

Virtues and drawbacks of EFT in Dark Matter searches

We now want to discuss the application of effective field theory to the study of the Dark Matter problem. Since Dark Matter and its interaction with the Standard Model particles is unknown, the EFT looks like a perfect paradigm to study in a general and model independent way, the interaction between the Dark sector and the particle physics we know. The fact that predictions will not be related to a specific model is maybe the greatest virtue of the EFT approach because it allows us to easily compare results and constrain the parameters of the model from the various experiments in a general way.

When building our model we also have to bear in mind that since effective field theory does not have the objective of describing UV physics, we are not bound to enforce gauge symmetries. As already mentioned, we can have a model in which the interaction term between quarks and Dark Matter is a contact interaction. For example, the leading term, if Dark Matter is represented by a fermion and the interaction is supposedly mediated by a scalar field, might be the dimension-6 operator

$$\mathcal{L} \supset \frac{1}{M_*^2}(\bar{q}q)(\bar{\chi}\chi)\,. \tag{2.2.12}$$

Even without knowing what happens at small scales (see fig. 2.2.2), we can study the low energy behavior of such interaction. The mass scale M_* is the cut-off energy scale and it is strictly related to the mass of the mediator. It is clear then, that this kind of approach makes sense only if the energy we are dealing with is small compared to the mass of the mediator and it gets more and more effective when there is a clear separation between the energy of the experiment and the mass scale M_*. As we previously discussed, in indirect searches the annihilation of Dark Matter particles in the halo happens in the non-relativistic regime and so the energy scale is in the order of m_χ. In direct searches we probe the non-relativistic recoil between nucleon and DM, with a energy scale in the order of KeV-MeV, depending on the Dark Matter mass. In these scenarios, the EFT paradigm is very solid. The situation might change when dealing with LHC, since the energy in play might be enough to see the whole dynamic and even produce the mediator particle. It is clear that if this is the case, the effective field theory fails completely. As we can see in equation (2.2.5), if the transferred momentum is smaller than the mass of the mediator, we can expand the propagator and find the relation between the cut-off mass scale and the mass of the mediator:

$$M_* = \frac{M_{med}}{\sqrt{g_q g_\chi}}\,, \tag{2.2.13}$$

where g_q and g_χ are the couplings of the mediator to quarks and Dark Matter. Comparing the transferred momentum p and the mediator mass M_{med}, we can recognise three regions:

- $p < M_{med}$, the approximation in equation (2.2.5) holds and the EFT is valid.

- $p \sim M_{med}$, the production cross section can have a resonant enhancement which is not described by the EFT.

- $p > M_{med}$, the expansion in equation (2.2.5) fails, the EFT is not reliable for a description of phenomena.

Another thing that needs to be checked when we are dealing with high energies is whether we violate the unitarity of the S-matrix. In particular, this request can also be used to constrain the allowed ratio between the mass of the mediator and the mass of Dark Matter for a fixed center mass energy s, in order to have a valid EFT description.

2.3 An alternative way: Simplified Models

In the previous section we have outlined the virtues and limitations of an effective field theory approach for the discovery of Dark Matter. In particular, EFT has gained popularity because it allows to focus on a small set of parameters and to have a model independent approach, a quality that is vital if the focus is to understand what Dark Matter is without having to solve the other problems of the Standard Model with a UV complete model. The EFT approach assumes that heavy particles are integrated out, leaving us with a contact interaction between partons (quarks or gluons) and the DM particle. As we mentioned previously, while this approach is perfectly fine for direct and indirect detection, it can fail at colliders that operate in the energy range of the LHC, since the momentum transfer involved might be high enough to resolve the contact interaction, i.e. is comparable to the cut-off scale, and the expansion in equation (2.2.5) is no longer valid. In other words, the particles responsible for the generation of the EFT operators might become relevant. The idea then is to use an alternative approach that is halfway between the EFT and complete model approaches, the simplified models [20]. The objective is to maintain a somewhat model independent approach, while at the same time incorporate the effects of the particles that were integrated out in the effective field theory approach, expanding the contact interaction and accounting for a mediator. In doing this we complicate a little bit the model, gaining more parameters but also more theoretical control. Simplified models allow us to focus on the kinematic while ignoring the underlying complete model that could stand behind.

We mentioned before that the most important signal we are looking for at colliders in Dark Matter searches is jet plus missing energy $\not{E}_T$, but simplified models have also the feature of allowing us to study signals with multi-jet+$\not{E}_T$. Indeed, the fact that we account for a mediator allow us to produce it on-shell (if we have enough energy) and therefore get a significant contribution to other processes.

Regarding the direct and indirect research, employing simplified models still allows us to constrain our models in a straightforward way with data coming from various experiments. In addition to that, simplified models can also give a correct description of the case with a light mediator, which is not possible in the EFT paradigm.

A good simplified model should satisfy the following criteria:

- it should be a consistent simplification of a complete model, in the sense that the complete model can reduce to it in a well defined limit,

- it should be complete enough to give an accurate description at the energy scale of LHC.

In order to automatically guarantee these requirements, we can use some general prescriptions, that are useful to keep in mind for any kind of simplified model:

- We want to minimally extend the Standard Model. We should add a viable particle candidate of Dark Matter, which has to be stable or stable at least in colliders timescale. We also add a mediator particle that connects the Standard Model to the Dark sector.

- The Lagrangian should respect all the Standard Model symmetries (Lorentz invariance, unbroken gauge symmetries) in addition to Dark Matter stability.

- In addition to these exact symmetries, the Standard Model has also other exact and approximate accidental global symmetries, such as for example the conservation of Baryon and Lepton number or the Custodial symmetry. We should build a model that does not violate these symmetries.

Simplified models can then be understood as the low energy limit of some new physics scenario in which heavier particles have been integrated out and we are left only with the lightest ones. By construction, they are characterized by a small amount of degrees of freedom, usually the masses of the new particles and the couplings. In the heavy mass limit of the mediator we can recover the EFT scenario.

The third prescription requires further analysis. In general, new physics will violate the accidental symmetries, in particular the flavour symmetry, and this will strongly constrain the parameter space of the model: the couplings will have to be small or the masses of new particles very heavy. To be more quantitative, the evidence for neutrino masses and the lower limits on proton lifetime require that the baryon and the lepton number should be conserved up to the GUT scale ($\sim 10^{16}$ GeV). Experiments on electron and neutron dipole moment require that the scale of flavour-conserving CP violation is beyond $\sim 10^7$ GeV, while the mass difference $K^0 - \bar{K}^0$ requires that strangeness violations $\Delta S = 2$ cannot appear at scales lower than $\sim 10^6$ GeV.

Because of the WIMP paradigm and other theoretical reasons, we think that new physics should appear at the TeV scale and if we insist on this point, then the new models we are building should be not too much generic and have a precise structure. In particular, we should ensure that the Baryon number, the Lepton number and CP violations are at least approximate symmetries. A slightly different argument can be done for flavour symmetry, that is not respected even in the Standard Model and therefore it looks pretentious to ask a new physics model to not violate it. On the other hand, we know experimentally that these violations are severely constrained at the TeV scale and so we should take into account this fact.

Minimal Flavour Violation

There is a systematic way to deal with restrictions on flavour changing neutral currents (FCNC) and CP violation and it is called Minimal Flavour Violation (MFV) [21]. The basic idea is that to ensure a small contribute to these violations, they should be governed by the Cabibbo-Kobayashi-Maskawa matrix. More precisely, we say that a Beyond Standard Model scenario respect MFV if the additional interactions are invariant under the global flavour group

$$G_q = U(3)_q \times U(3)_u \times U(3)_d \,, \tag{2.3.1}$$

or if they break it through the CKM matrix. The subscript q stand for the $SU(2)_{EW}$ doublets, while u and d for the three up and down singlets. In particular, CP violations has to be linked to the CKM phase.

Just for the sake of clarity, we will analyze two simple examples, implementing Minimal Flavour Violation.

As a first example, let us consider a simple model in which Dark Matter is represented by a scalar field ϕ and the mediator between the Standard Model and the dark sector is the Higgs field. This kind of models are called portal models. The interaction term between Higgs Dark Matter has to be

$$\mathcal{L} \supset \chi^2 |H|^2 \,. \tag{2.3.2}$$

The interaction between the mediator and the Standard Model quarks, following MFV, should either respect the global flavour group or break it through the Yukawa matrices. Since q is a doublet, while u and d are singlets, a combination like $\bar{q}u$ of left-handed and right-handed quarks breaks G_q and therefore we have to choose the second option. We then write the Lagrangian in the form

$$\mathcal{L} \supset -\sum_{ij} Y_{ij}^u \, \bar{q}_i \, H \, u_j + Y_{ij}^d \, \bar{q}_i \, \tilde{H} \, d_j + h.c. \,, \tag{2.3.3}$$

where i and j runs over the quark generations and $\tilde{H}_a = \epsilon_{ab} H_b$. This is nothing but the Standard Model Yukawa sector and after symmetry breaking and rotation to mass eigenstates, we are left with

$$\mathcal{L} \subset -\frac{h}{\sqrt{2}} \sum_i y_i^u \, \bar{u}_i \, u_i + y_i^d \, \bar{d}_i \, d_i \,. \tag{2.3.4}$$

In conclusion, if the portal to the dark sector is made out of a scalar field, its interaction with the SM quarks should be proportional to the Yukawa couplings.

Let us now consider a model in which the Dark Matter is a Dirac fermion χ and the mediator is a vector boson we call Z'. The coupling with Dark Matter is not constrained and it can be written as

$$\mathcal{L} \supset Z'_\mu \left(g_L^\chi \, \bar{\chi} \, \gamma^\mu \, P_L \, \chi + g_R^\chi \, \bar{\chi} \, \gamma^\mu \, P_R \, \chi \right), \tag{2.3.5}$$

where P_L and P_R are the chiral projectors.
This time, we can write bilinears of Standard Model quarks that do not break the flavour group and therefore MFV is implemented without employing the CKM matrix and we simply write

$$\mathcal{L} \supset Z'_\mu \sum_i g_L^q \left(\bar{u}_i \, \gamma^\mu \, P_L \, u_i + \bar{d}_i \, \gamma^\mu \, P_L \, d_i \right) + g_R^u \, \bar{u}_i \, \gamma^\mu \, P_R \, u_i + g_R^d \, \bar{d}_i \, \gamma^\mu \, P_R \, d_i \,. \tag{2.3.6}$$

Simplified Models classification

In order to discuss and study the various kind of models, we classify the Simplified Models in two categories, based on the kind of interaction that lead to the $2 \rightarrow 2$ annihilation process of Standard Model particles into Dark Matter particles or whether the mediators are charged or not. In each category then, we will use a nomenclature easy to recall, based on the spin and the gauge representation under $\mathrm{SU}(3)_c$ of both Dark Matter and the new mediator. It is also important to clarify which sector of the Standard Model is going to be coupled to the Dark sector.
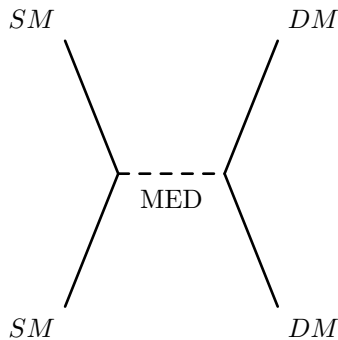

Figure 2.3.1: The characteristic annihilation process of a s-channel Simplified Model.
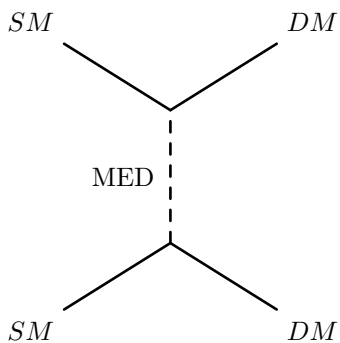
Figure 2.3.2: The characteristic annihilation process of a t-channel Simplified Model.

If the annihilation process of two Standard Model particles happens through the exchange of a mediator particle in the s-channel, then we are talking about an s-channel Simplified Model (see fig. 2.3.1). If on the other hand, the process is mediated through the t-channel, we call the model a t-channel Simplified Model (see fig. 2.3.2). This is the most important distinction since the phenomenology of s-channel and t-channel models is quite different. The first thing one can notice is the fact that in the s-channel case, it is possible to have a resonant process in the production of Dark Matter, whether in the t-channel this is not possible. Also, in order to ensure the stability of the Dark Matter particle, in a t-channel model it is mandatory to have a mediator with mass M higher than m_χ, so that the channel decay is closed kinematically. On the other hand, this is not compulsory in a s-channel model, since the elementary vertex always ensure that there are two Dark Matter particles interacting with the mediator and therefore the decay channel is automatically closed.

If we want to focus on LHC phenomenology then there are two possible interactions that we can build, with quarks or with gluons. It is important to specify which parton it is coupled to Dark Matter, since the phenomenology and the properties of the new particles change completely. In this work we will focus on t-channel models, focusing on the interaction with quarks and gluons, exploring all the possible viable patterns.

Chapter 3

Simplified t-channel models

We now want to look at different types of t-channel Dark Matter models, focusing in particular on those involving quarks interactions. The LHC has so far mostly explored s-channel models and therefore there is the need of exploring models with t-channel mediators more systematically.

In the following classification, we will always assume that Dark Matter is a singlet under all Standard Model gauge groups. In addition to that we will always consider the presence of only one particle of DM, without considering the possibility of a flavored case. Because of these choice, the mediator is compelled to carry color (either a triplet or an octet depending on whether the interaction is with quarks or gluons), electroweak charge and a generation index.

We perform the study of the simplified models by employing simulation tools such as MadGraph5 aMC@NLO event generator [22], the Mathematica [23] package FeynRules [24, 25] allowing us to implement the models and the Mathematica package FeynCalc [26, 27] to do analytical computation of amplitudes.

The notation we use in order to classify the models is easily explained. Each model is labeled with a string of characters in the form XN-Y0-Z. The first part gives information on the mediator, the second part on the Dark Matter particle and the last part on the Standard Model particle that is involved in the interaction. X and Y give the information about the spin of the particle (X,Y=S,F,V standing for scalar, fermion and vector respectively) while N gives information about the representation of the mediator under $SU(3)_c$ transformations. For the Dark Matter particle we stress our choice of a singlet candidate with a 0. Finally, Z can take values such as q, for quarks, and G for gluons.

mediator	DM	SM	
S3	F0	q	$(0\,t\,\frac{1}{2})$
F3	S0	q	$(\frac{1}{2}\,t\,0)$
F3	V0	q	
V3	F0	q	$(1\,t\,\frac{1}{2})$

Table 3.1: Classes of t-channel models we have studied. The notation (mediator spin / channel / DM spin) follows [19]. Note that the F3–V0–q model has not been covered in [19] as they restrict themselves to scalar and fermion DM.

3.1 Color triplet mediator

In this first section we focus on the interaction with quarks and because of the fact that Dark Matter is a singlet, the mediator must be a color triplet. If we restrict ourselves to dimension 4 operators, in the spirit of simplified models, there are four classes of models to study, see Tab. 3.1. We now proceed to build the models, analyzing their features and studying their phenomenology.

3.1.1 S3-F0-q model

The simplest model we can think of is one in which the Standard Model and Dark Matter interaction is mediated by a scalar particle. Dark Matter is a vector-like fermion (Dirac or Majorana) and since it cannot carry color, flavor or electric charge, the mediator has to do it, being a complex color triplet scalar field. We also invoke a $\mathbb{Z}_2$ discrete symmetry on the model, under which the new particles are odd. This is done in order to enforce the stability of the Dark Matter particle. The most general Lagrangian describing the interactions between DM and the left-handed and right-handed SM quarks is given by

$$\mathcal{L} = \sum_{i=1,2,3} g_i^L \left(\overline{Q}_L^{(i)} \eta_L^{(i)} \right) \chi + \left(g_i^{u,R} \bar{u}_R^{(i)} \eta_{u,R}^{(i)} + g_i^{d,R} \bar{d}_R^{(i)} \eta_{d,R}^{(i)} \right) \chi + h.c. \,, \qquad (3.1.1)$$

where χ is the Dark Matter field, $Q_L^{(i)} = (u_L, d_L)^{(i)}$ is the $SU(2)_{EW}$ doublet and $u_R^{(i)}$ and $d_R^{(i)}$ are the quarks singlet, with $i = 1, 2, 3$ being the flavor index. The mediators $\eta_L^{(i)} = (\eta_{u,L}, \eta_{d,L})^{(i)}$, $\eta_{u,R}^{(i)}$ and $\eta_{d,R}^{(i)}$ transform under the SM gauge groups as $(3, 2, -1/6)$, $(3, 1, 2/3)$ and $(3, 2, -1/3)$, respectively. They resemble the Minimal Supersymmetric Standard Model squarks and since several searches and constraints already exist related to them, it is possible to use the experimental data to put constraints on this model. In this framework, the Dark Matter particle is represented by the neutralino. In this scenario, the coupling g is fixed in terms of the $U(1)_Y$ gauge coupling as $g_u^{SUSY} =$

$4g'/(3\sqrt{2}) \approx 0.33$ for up-type quarks, and $g_d^{SUSY} = 2g'/(3\sqrt{2}) \approx 0.16$ for down-type quarks, respectively. In the spirit of simplified models, we will however keep g a free parameter.

The model we implemented in FeynRules is the most general possible, including different couplings to both left-handed and right-handed quarks and different masses for the mediators. In order to avoid Flavor Changing Neutral Currents however, the MFV hypothesis require us to use universal couplings and masses, $M_1 = M_2 = M_3 = M$ and $g_1 = g_2 = g_3 = g$. The parameter space of the model therefore consist of only 3 parameters $\{m_\chi, M, g\}$.
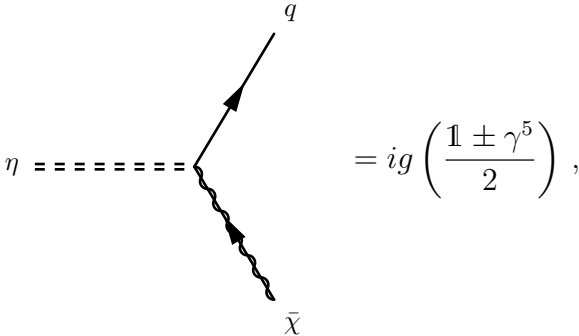
In order to ensure the stability of the Dark Matter particle we need $m_\chi < M$, so the decay channel is kinematically closed.

We also have to consider that, being charged under $SU(3)_c$, the mediator also couple to gluons and the interaction can be obtained from the kinetic term

$$\mathcal{L} \supset (D_\mu \eta)^\dagger (D^\mu \eta) - M^2 \eta^\dagger \eta \,, \tag{3.1.2}$$

where $D_\mu = \partial_\mu - i g_s t_F^a G_\mu^a$ is the covariant derivative.

The basic Feynman rule of this model is

$$= ig \left(\frac{\mathbb{1} \pm \gamma^5}{2} \right) , \tag{3.1.3}$$

where the plus sign is related to right-handed interactions, while the minus sign to left-handed interactions.

We can compute the decay width of the mediator, remembering that

$$d\Gamma = \frac{1}{2M} \frac{d^3 \vec{p}_1}{2E_1 (2\pi)^3} \frac{d^3 \vec{p}_2}{2E_2 (2\pi)^3} |\mathcal{M}|^2 (2\pi)^4 \delta^{(4)}(p - p_1 - p_2) \,, \tag{3.1.4}$$

where the center of mass frame in the decaying particle is assumed. M and p are the mass and the 4-momentum of the decaying particle, while p_1 and p_2 are the 4-momenta

of the produced particles. The decay width of the mediator can therefore be computed. The amplitude of the process can be obtained using the Feynman rule in eq. (3.1.3)

$$\mathcal{M} = g\, \bar{u}(p_2, m_q).P_R.v(p_1, m_\chi)\,, \tag{3.1.5}$$

where u and v are the spin states. The squared amplitude is then

$$|\mathcal{M}|^2 = g^2 \left(\bar{u}(p_2, m_q).P_R.v(p_1, m_\chi)\right)(\bar{v}(p_1, m_\chi).P_L.v(p_2, m_q))\,. \tag{3.1.6}$$

We now have to sum over the incoming and outgoing color index and take the average over the incoming one. Since color is conserved in the vertex and therefore the incoming mediator and the outgoing quark have the same color, we have to sum 3 times the same squared amplitude and then take the average dividing by 3, and so the color factor is 1. On the other hand we have to sum over the outgoing spin polarizations of the quark and of Dark Matter. We have

$$\sum_{spin} |\mathcal{M}|^2 = 2g^2 \left(p_1 \cdot p_2\right)\,. \tag{3.1.7}$$

In the center of mass frame the former expression gives

$$2g^2 \left(p_1 \cdot p_2\right) = g^2 \left(M^2 - m_\chi^2 - m_q^2\right)\,. \tag{3.1.8}$$

Performing the angular integration, one finally obtains the decay width

$$\Gamma(\eta \to \bar{\chi}q) = \frac{g^2 \lambda^{\frac{1}{2}}}{16\pi M^3} \left(M^2 - m_\chi^2 - m_q^2\right)\,, \tag{3.1.9}$$

where:
$$\lambda = M^4 + m_\chi^4 + m_q^4 - 2M^2 m_\chi^2 - 2M^2 m_q^2 - 2m_q^2 m_\chi^2 \tag{3.1.10}$$

is a factor coming from the phase space. This result has also been checked numerically against that of MadWidth. Another constraint to the model can generically come from requiring the width of the mediator to be at most a fraction (e.g. 30%) of its mass.
In the limit of heavy Dark Matter and mediator, the mass of the quark is negligible and the width can be approximated to

$$\Gamma(\eta \to \bar{\chi}q) \approx \frac{g^2 M}{16\pi} \left(1 - \frac{m_\chi^2}{M^2}\right)^2\,. \tag{3.1.11}$$
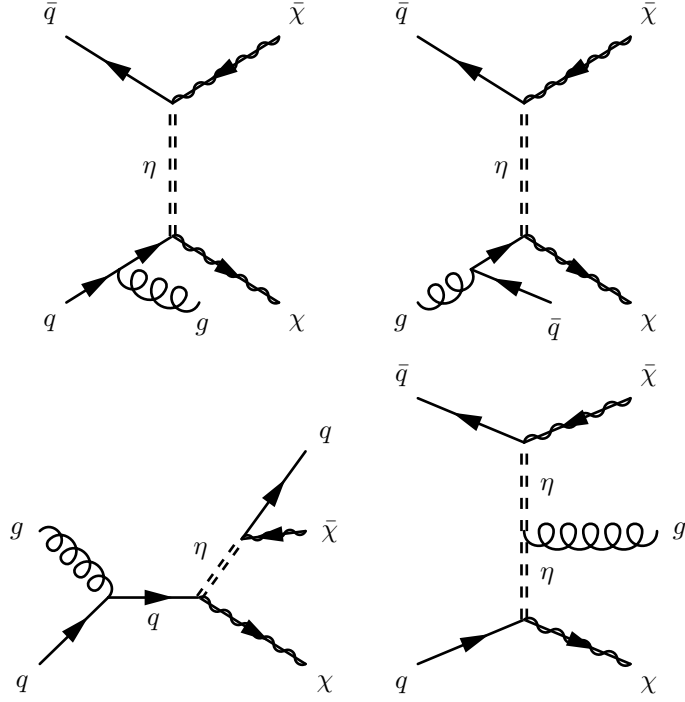
Figure 3.1.1: Some diagrams contributing to the 1-jet and missing energy signature. The first two are of the kind external leg bremsstrahlung, the third is single resonant production while the last one is internal bremsstrahlung.

We now focus on the LHC phenomenology of the model, that as already stated, is similar to the MSSM squark/neutralino production. In particular we should look at both 1-jet plus $\not{E}_T$ and 2-jet plus $\not{E}_T$ signatures.

Concerning the 1-jet signatures (see fig. 3.1.1) we have

$$q\,\bar{q} \to \chi\,\bar{\chi}\,g\,, \tag{3.1.12a}$$

$$q\,g \to \chi\,\bar{\chi}\,q\,, \tag{3.1.12b}$$

$$q\,g \to \chi\,\eta \to \chi\,\bar{\chi}\,q \tag{3.1.12c}$$

where the difference between the first two and the third process is that while in the first two the jet is produced through radiation from the initial state quarks or from the exchanged mediator, in the third we could produce an on-shell mediator that then decays, giving a resonant enhancement to the process.

51
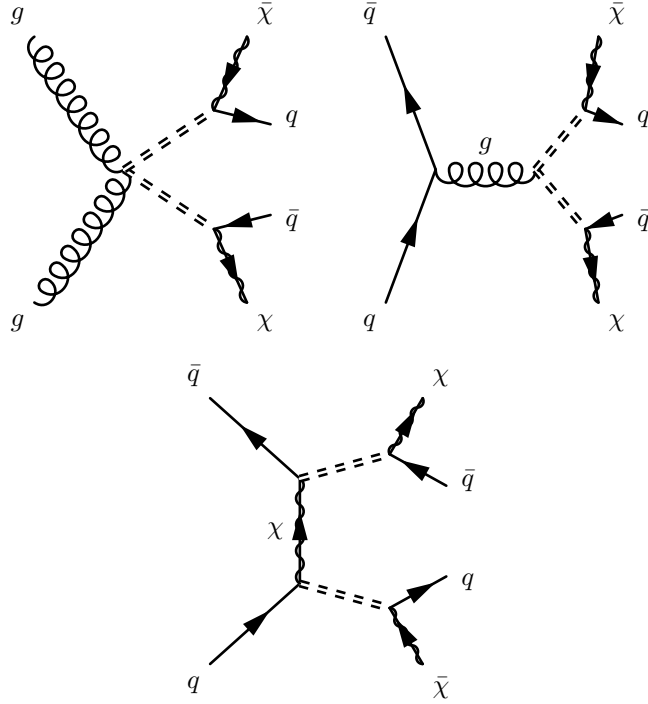
Figure 3.1.2: Some double resonant diagrams contributing to the 2-jet and missing energy signature.

On the other hand, for the 2-jet signal (see fig. 3.1.2) we have

$$g\,g \to \eta\,\eta^* \to \chi\,\bar{\chi}\,q\,\bar{q}, \qquad (3.1.13a)$$

$$q\,\bar{q} \to \eta\,\eta^* \to \chi\,\bar{\chi}\,q\,\bar{q}. \qquad (3.1.13b)$$

In both processes we can produce the mediator on-shell.

Apart from the fact that in the MSSM the coupling is fixed, while in the simplified model it is a free parameter, another key difference is that in the MSSM χ has to be a Majorana fermion while here we are free to choose freely between Dirac and Majorana.

From the LHC phenomenology perspective there is almost no difference between the model with a Majorana Dark Matter and the model with a Dirac Dark Matter (see for example fig. 3.1.3), but from a direct detection point of view is a whole different story. As we explained in section 1.2.3, when one computes DM-nucleon scattering there are two different contributions, a spin-independent one and a spin-dependent one. The spin independent constraints coming from experiments such as LUX 2013 are very strong and therefore they can severely restrict the parameter space of the model. However, while the

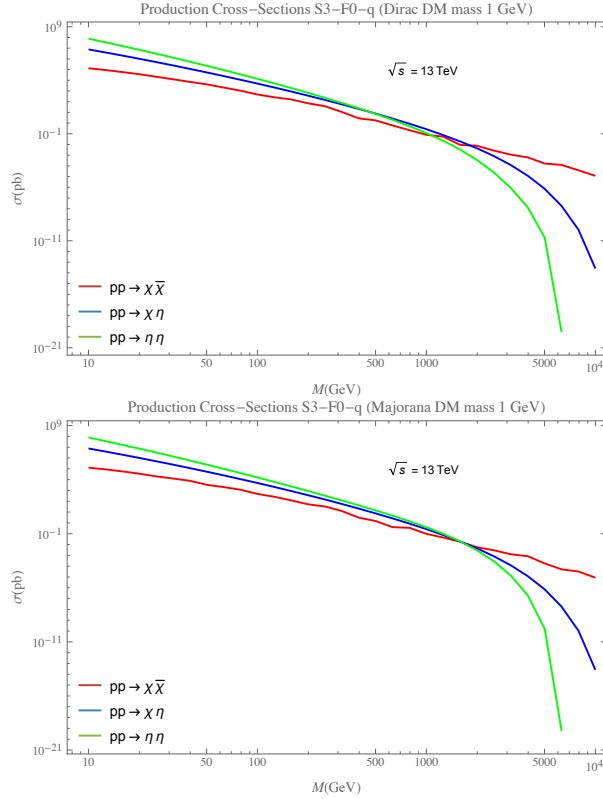Figure 3.1.3: These two plots show the behavior of the total cross section, in function of the mediator mass, for different processes simulated with MadGraph, assuming a collision of protons as in LHC. In the top panel we have the case of a Dirac Dark Matter, while in the bottom panel we have a Majorana DM, both with mass of 1 GeV. In both cases the coupling is $g = 1$ and we assumed interaction with both righ-handed and left-handed quarks. As previously mentioned, the phenomenology of the two model from LHC perspective is almost identical.

Dirac DM has a strong and dominant spin independent interaction with the nucleons, the SI scattering cross section of Majorana fermions vanishes at tree-level and therefore it is heavily suppressed. The dominant signal for Majorana DM is then the SD cross section. For this reason, the phenomenology of the two models is totally different from a direct detection perspective [28].

It is however important to notice that in the scenario of a Majorana fermion, we have some processes that are not allowed in the Dirac case. For example, since the Majorana particle is its own anti-particle, in the production process $q\bar{q} \to \chi\chi$ we also have the contribution coming from the exchange of the final states, being them identical. In addition to that there is a whole new production process of the mediator that is prohibited in the Dirac DM scenario, i.e. $qq \to \eta\eta$ (see fig. 3.1.4) and the counterpart with anti-quarks.
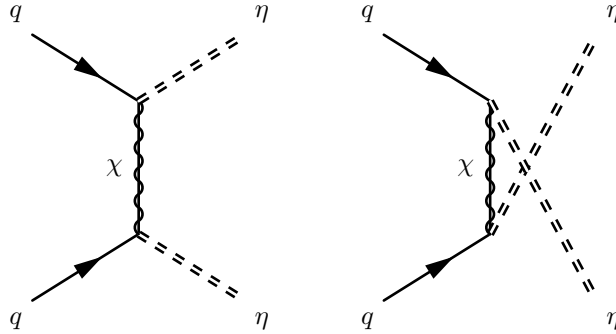
Figure 3.1.4: Feynman diagrams showing the production of two mediators through an exchange of a Majorana DM particle.

We can classify the possible signals we want to detect at LHC in three categories, depending on how many resonant mediator we have produced: no resonant mediator, one resonant mediator or two resonant mediator. In order to better understand the phenomenology of this model we produced plots (fig. 3.1.5) that can help us to better understand which of these signals is dominant in each region of the parameter space. Our plan is to study the model at Next-to-Leading Order, so that we can identify for each region on which processes it is better to compute the corrections, being the dominant ones. We assume that the Narrow Width Approximation [29] is valid and since each mediator has only one decay channel (each squark to the corresponding quark and Dark Matter particle), once it is produced it will certainly decay in the collider time scale within the detector. We chose three benchmark values of the DM mass and simulated the processes with MadGraph scanning the total cross sections in function of both the mass of the mediator and the coupling g. Let us now try to understand the plots. Suppose we fix the coupling at some value. For low mediator masses the 2 resonance process dominates because it has a significant contribution coming from the gluon annihilation (therefore the coupling of this process is g_s, the strong coupling of $SU(3)$). When the mass M increases, the phase space for this process shrinks until we reach the point in which it is not dominant anymore. If the fixed coupling is small, the transition line is with the blue region (the 1-resonance process, $\sigma \sim g^2$) since the no-resonance process is the most influenced by the value of the coupling ($\sigma \sim g^4$), otherwise it is with the red region. When we deal with heavy mediator the dominant process is always the no-resonance one, since it is the only one without it in the final state.

In summary, the 2-resonance process is the most sensitive to the mediator mass, while the 0-resonance is the least one. On the other hand, the 2-resonance process is the least influenced from the coupling g (there are some processes coming from the exchange of DM that contribute but they are less important) whereas the 0-resonance is the most one.
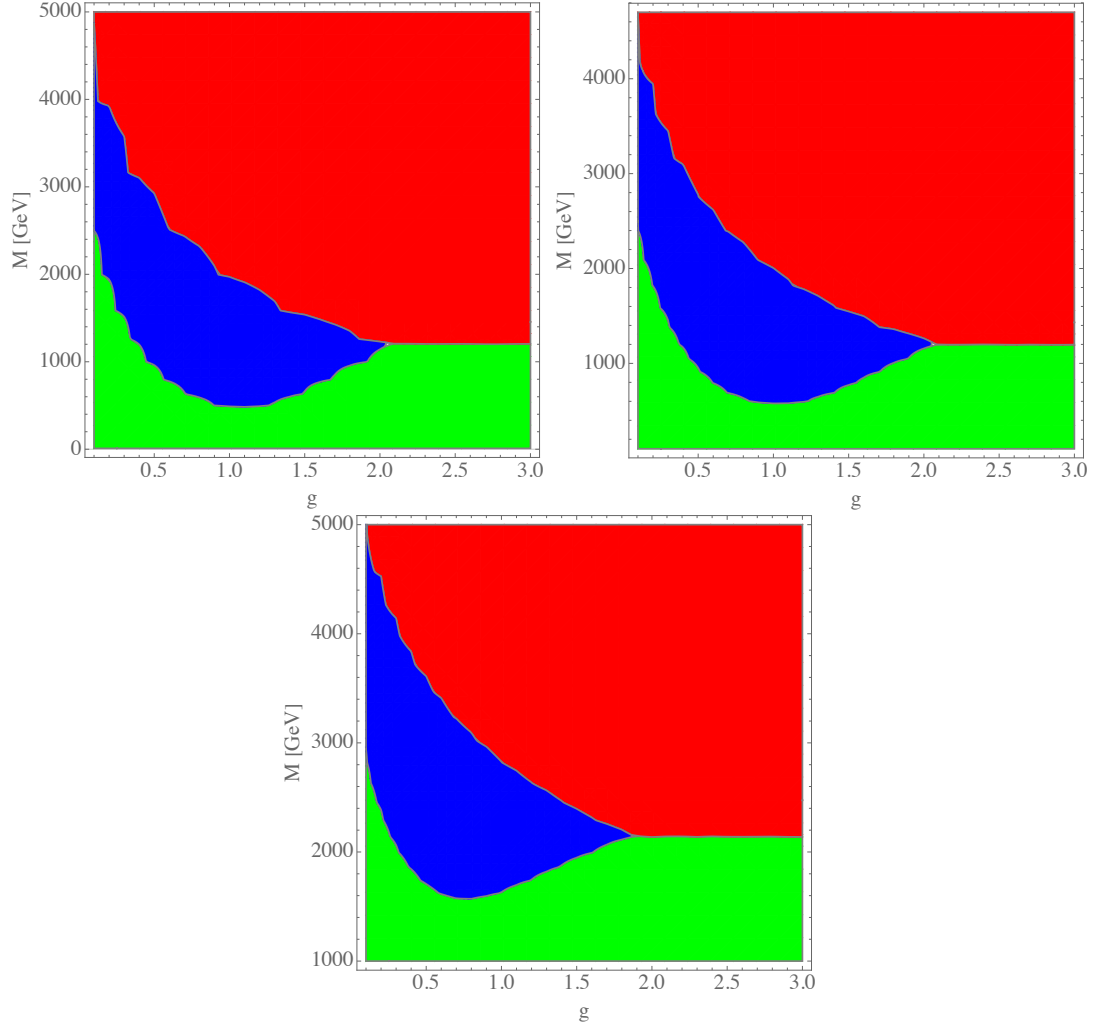
Figure 3.1.5: The plots show for each process the region of the parameter space in which is dominant, in the case of a 10 GeV (top left panel), 100 GeV (top right panel) and 1000 GeV (bottom panel) Dark Matter mass. The red corresponds to the no-resonance processes $(pp \to \chi\bar{\chi}j)$, the blue corresponds to the 1-resonance processes $(pp \to \chi\eta)$ while the green region is related to the 2-resonance processes $(pp \to \eta\eta)$. The simulation is done at the current LHC center of mass energy of 13 TeV. We can see that as the DM mass increase, the blue region widens.

55

3.1.2 F3-S0-q model

We will now consider a model in which the mediator is a vector-like fermion. By vector-like fermion we mean a fermion characterized by having the right-handed and the left-handed part transforming in the same way under $SU(2)$, so that we can directly write in the Lagrangian a Dirac mass term. A 2 to 2 scattering with a fermion mediator can only happen in the t-channel, so there are no models with this kind of particle in the s-channel simplified models. Since we are studying the interaction with quarks, Dark Matter can either be a scalar particle or a vector particle.

In this first section let us consider a scalar singlet DM χ coupled with a Yukawa interaction with a colored fermion η. The mediator is practically a 4-th generation quark. However, we have to use a vector-like quark, since a chiral perturbative 4-th generation is severely constrained by experiments and almost excluded. As before we invoke a $\mathbb{Z}_2$ symmetry under which the dark sector is odd, in order to ensure the stability of the Dark Matter particle. We will consider the following Lagrangian

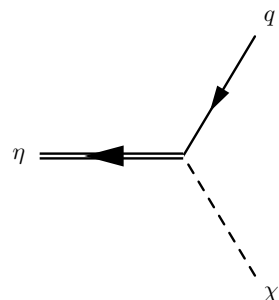$$\mathcal{L} \supset \frac{1}{2}\partial_\mu\chi\partial^\mu\chi - \frac{1}{2}m_\chi^2\chi^2 + \bar{\eta}(i\slashed{D} - M)\eta + y\chi\bar{\eta}q_R + h.c.\,, \qquad (3.1.14)$$

where q_R is a generic right-handed quark and therefore we can in principle have a different mediator for each Standard Model quark. Being charged under $SU(3)_c$, the mediator also couples to gluons, as can be seen by the presence of the covariant derivative. One can also choose to couple also the left-handed quarks in exactly the same way. Note that we can also add a portal Higgs term like $\chi^2 H^\dagger H$, which we assume to be small compared to the Yukawa interaction. The model implemented in FeynRules is the most general possible, including different couplings to both left-handed and right-handed quarks and different masses for the mediators. However, in order to avoid FCNCs the MFV hypothesis costrain us to use universal couplings and masses. The parameter space of the model therefore consists of 3 parameters $\{m_\chi, M, y\}$. As in the previous model, in order to ensure the stability of Dark Matter, we also require $m_\chi < M$, so that the decay channel is kinematically closed. The basic Feynman rule of the model is

$$= iy\left(\frac{\mathbb{1} \pm \gamma^5}{2}\right). \qquad (3.1.15)$$

We can now compute the decay width of the mediator. Denoting with p and M the 4-momentum and the mass of the mediator, while with p_1 and p_2 the 4-momenta of the produced particles, using eq. (3.1.15), we have the amplitude

$$\mathcal{M} = y\,\bar{u}(p_2, m_q).P_L.u(p, M)\,, \tag{3.1.16}$$

and the squared amplitude is then

$$|\mathcal{M}|^2 = y^2\,(\bar{u}(p_2, m_q).P_L.u(p, M))(\bar{u}(p, M).P_R.u(p_2, m_q))\,. \tag{3.1.17}$$

As in the previous case, summing on the color index of the outgoing quark and taking the average on the incoming particle gives a factor 1. On the other hand, in addition to summing on the outgoing spin polarizations this time we also have to average on the incoming ones. Therefore we have

$$\frac{1}{2}\sum_{spin}|\mathcal{M}|^2 = y^2(p \cdot p2) = \frac{1}{2}y^2\left(M^2 - m_\chi^2 + m_q^2\right)\,, \tag{3.1.18}$$

where we assumed the center of mass frame with the decaying particle at rest. Performing the angular integration, one finally obtains the decay width

$$\Gamma(\eta \to \chi q) = \frac{y^2\lambda^{\frac{1}{2}}}{32\pi M^3}\left(M^2 - m_\chi^2 + m_q^2\right)\,, \tag{3.1.19}$$

where λ is the factor coming from the phase space defined in eq. (3.1.10). This result has also been checked numerically against that of MadWidth. An important constraint to the model comes from the request that the width of the mediator particle is at most 30% of its mass.

In the limit of heavy Dark Matter and mediator masses, the mass of the quark is negligible and the width can be approximated to

$$\Gamma(\eta \to \chi q) \approx \frac{y^2 M}{32\pi}\left(1 - \frac{m_\chi^2}{M^2}\right)^2\,. \tag{3.1.20}$$

We now focus on the LHC phenomenology of the model, that is similar to the S3-F0-q model. Indeed, we have both 1-jet and 2-jet plus $\not{E}_T$ possible signals and so we can try to employ both in order to improve the discovery potential.

Concerning the 1-jet signatures (see fig. 3.1.6) we have both the external radiation and the internal radiation, in addition to the single resonance process.
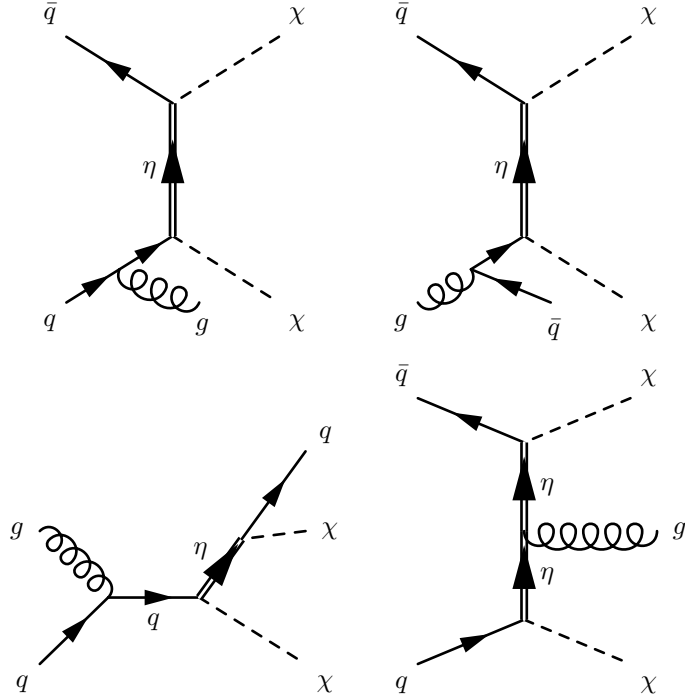
Figure 3.1.6: Some diagrams contributing to the 1-jet and missing energy signature. The first two are of the kind external radiation, the third is single resonant production while the last one is internal radiation.

The most important processes for this class of signatures are

$$q\,\bar{q} \to \chi\,\chi\,g\,, \tag{3.1.21a}$$

$$q\,g \to \chi\,\chi\,q\,, \tag{3.1.21b}$$

$$q\,g \to \chi\,\eta \to \chi\,\chi\,q\,, \tag{3.1.21c}$$

where the third process is characterized by the production of a resonance that gives an enhancement to the cross-section. Unlike the S3-F0 model with a Dirac Dark Matter, we have also to consider that there is no difference between a DM particle and the anti-particle, therefore we always have contribution of diagrams with final state exchange.
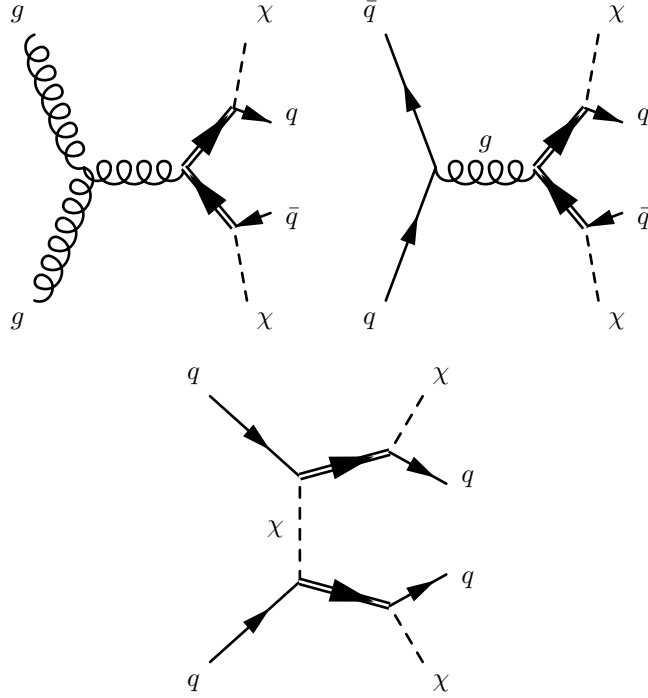
Figure 3.1.7: Some diagrams contributing to the 2-jet and missing energy signature.

Concerning the 2-jet plus missing energy signals (see fig. 3.1.7) we have

$$g\,g \to \eta\,\bar{\eta} \to \chi\,\chi\,q\,\bar{q}, \tag{3.1.22a}$$

$$q\,\bar{q} \to \eta\,\bar{\eta} \to \chi\,\chi\,q\,\bar{q}, \tag{3.1.22b}$$

$$q\,q \to \eta\,\eta \to \chi\,\chi\,q\,q. \tag{3.1.22c}$$

In all of these processes we can produce on-shell mediators and in this model we are also able to have a $q - q$ scattering, that is sensibly enhanced with respect to the $q - \bar{q}$ scattering because of the parton distribution function of the proton.

Beside the study of the LHC phenomenology, further analysis has been done for the other types of searches [30]. In particular, the relic density is dominated by different processes depending on the mass ratio $r = M/m_\chi$. If r is small, the annihilation cross section is dominated by internal bremsstrahlung in the quark-annihilation, while if r is big it is dominated by loop-induced annihilation into gluon pairs. The co-annihilation into quarks is very weak in the large r case and this can be also seen in the fig. 3.1.8 where the cross section for Dark Matter production steeply decreases in the limit of high mediator mass, because of a cancellation between the t-channel and u-channel diagrams.
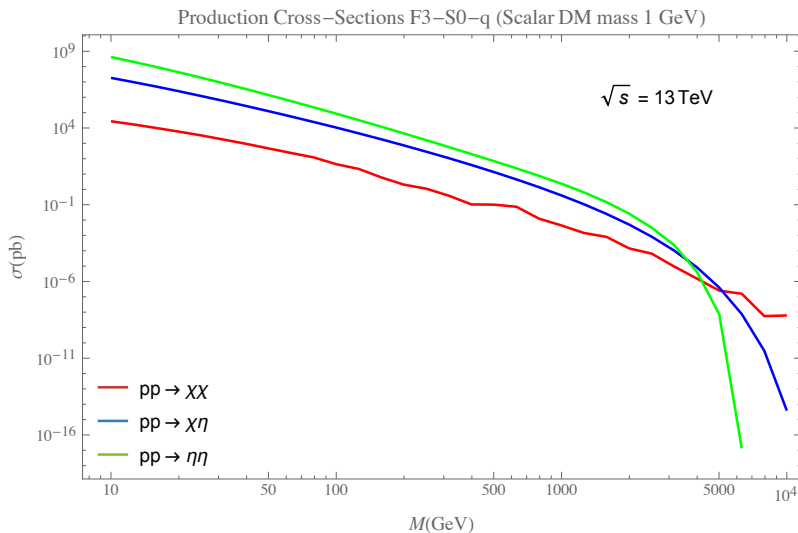
Figure 3.1.8: This plot show the behavior of the total cross section, in function of the mediator mass, for different processes simulated with MadGraph, assuming a collision of protons as in LHC. The coupling is set to $y = 1$ and we assumed interaction with both righ-handed and left-handed quarks.

If one uses the relic density in order to fix the Yukawa coupling y, then one can study the limits imposed by direct detection and find a lower limit on the Dark Matter mass. In particular the nucleons-DM interaction is influenced by both DM-quark scattering and loop induced DM-gluon scattering and the experiment LUX excludes a large part of the parameter space allowing only $m_\chi \gtrsim 200$ GeV. However, because of destructive interference between the DM-quark and the DM-gluon interaction for small r, we can evade the limits imposed by LUX in this scenario. This is a feature that is always to be checked when one deals with direct detection, since in particular cases, even if the DM-SM coupling is big we face cancellations that allows us to avoid the constraints. The most sensitive indirect detection bounds come from detection of γ-rays from dwarf galaxies and require $m_\chi \gtrsim 150$ GeV in the $r \gtrsim 1.4$ scenario.

As for the previous model, we have classified the possible signals at the LHC in three main categories, depending on how many resonant mediators are produced. We produced plots (fig. 3.1.9) that show in which area of the parameter space each of these processes is dominant, with the intention in future works of studying the model at NLO, so that we can identify for each region which process it is better to compute the corrections of. We assumed the validity of the Narrow Width Approximation and chose three benchmark values of Dark Matter mass, simulating the processes with MadGraph with a scan in both the coupling y and the mediator mass M. The same general analysis we have done for the S3-F0-q plots is also valid for these figures.
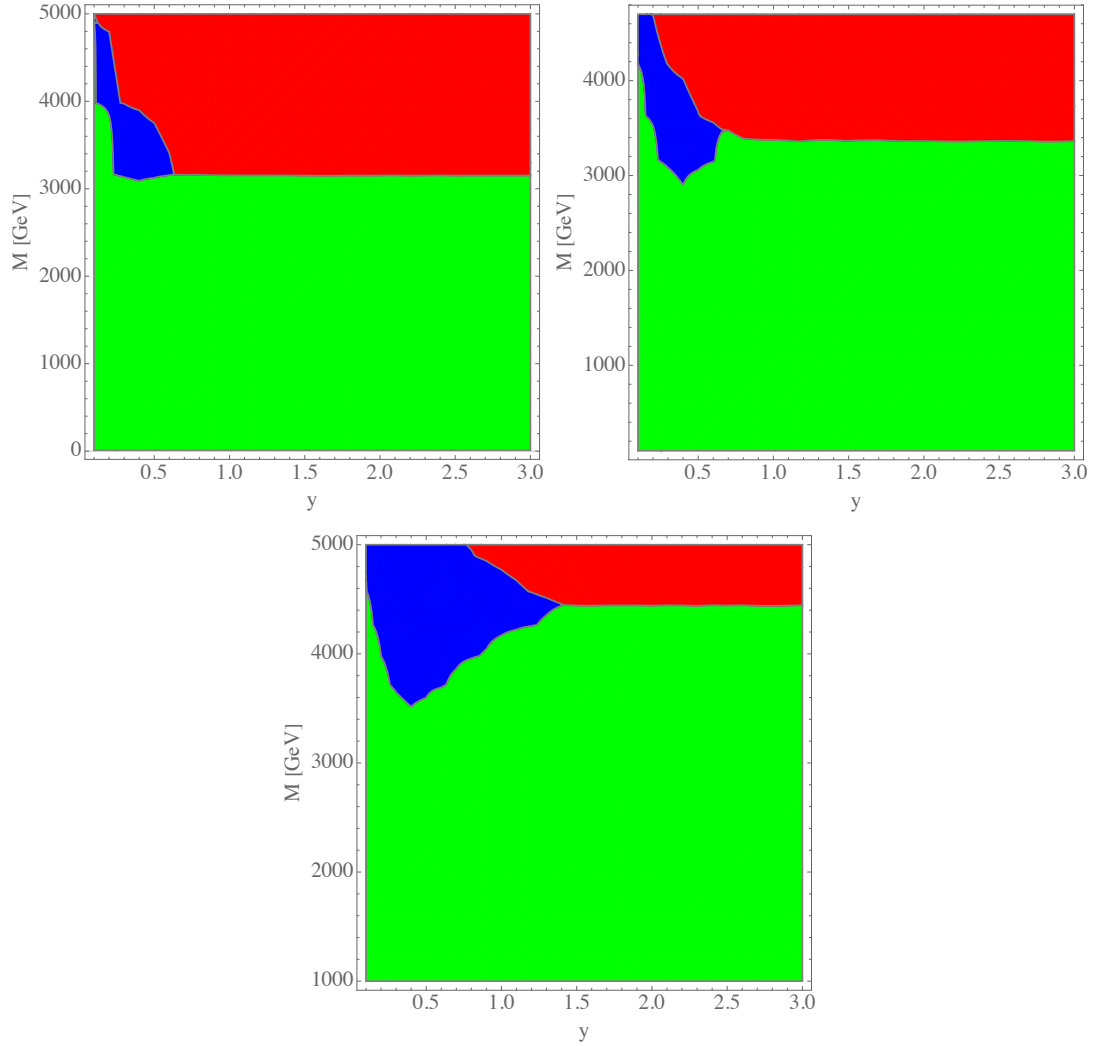
Figure 3.1.9: The plots show for each process the region of the parameter space in which is dominant, in the case of a 10 GeV (top left panel), 100 GeV (top right panel) and 1000 GeV (bottom panel) Dark Matter mass. The red corresponds to the no-resonance processes ($pp \rightarrow \chi\chi j$), the blue corresponds to the 1-resonance processes ($pp \rightarrow \chi\eta$) while the green region is related to the 2-resonance processes ($pp \rightarrow \eta\eta$). The simulation is done at the current LHC center of mass energy of 13 TeV. We can see that as the mass of the Dark Matter particle increase, the red region shrinks, while in particular the 2 resonance processes start to dominate in a wide portion of the analyzed parameter space.
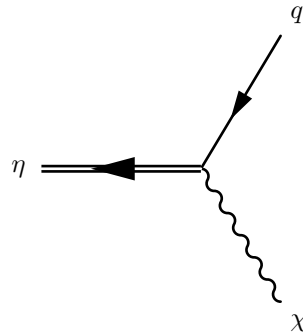
3.1.3 F3-V0-q model

As already mentioned, there is another possible model that features the presence of a vector-like fermion mediator, involving a real vector Dark Matter. Invoking the usual $\mathbb{Z}_2$ symmetry to enforce DM stability, we can write the Lagrangian

$$\mathcal{L} \supset -\frac{1}{4}\chi_{\mu\nu}\chi^{\mu\nu} + \frac{1}{2}m_\chi^2\chi_\mu\chi^\mu + g\,\bar{\eta}\,\gamma^\mu q_R\,\chi_\mu + h.c.\,, \qquad (3.1.23)$$

where $X_{\mu\nu}$ is the Dark Matter field strength and q_R is the generic right-handed quark. One can also study a model in which there is an interaction with left-handed doublets instead and the model we implemented in FeynRules is indeed very general and allows for both interactions, with different couplings for each quark and different masses for each mediator. However, if we want to avoid FCNCs under the MFV hypothesis, we have to use universal couplings and masses. The parameter space of the model is therefore made of the usual 3 parameters $\{m_\chi, M, g\}$. In order to kinematically close the decay channel of the Dark Matter particle, we require as usual that $M > m_\chi$. We could have also considered a complex vector DM but, while the real vector one has a suppressed spin independent DM-nucleon cross section, the complex one has not and therefore the parameter space is severely constrained by direct detection experiments, pushing the DM mass to several TeV or below 10 GeV [31].
The basic Feynman rule of the model is

$$= ig\gamma^\mu \left(\frac{\mathbb{1} \pm \gamma^5}{2}\right). \qquad (3.1.24)$$

We can now compute the width of the mediator. Denoting with p and M the 4-momentum and the mass of the mediator, while with p_1 and p_2 the 4-momenta of the outgoing particles, we can write the amplitude

$$\mathcal{M} = g\,\bar{u}(p_2, m_q).\gamma^\mu.P_R.u(p, M)\,\epsilon_\mu(p_2, m_\chi)\,. \qquad (3.1.25)$$

After squaring it, we have to sum on the color index of the outgoing quark and averaging on the incoming mediator particle. This operation gives a factor 1. Averaging over spin polarization and summing on the 3 vector polarizations, gives us

$$\frac{1}{2}\sum_{spin,pol}|\mathcal{M}|^2 = \frac{1}{2}\left(-\frac{2g^2p_1^2\,(p\cdot p_2)}{m_\chi^2} + \frac{4g^2\,(p\cdot p_1)\,(p_1\cdot p_2)}{m_\chi^2} + 4g^2\,(p\cdot p_2)\right) =$$

$$\frac{g^2\left(M^2\left(m_\chi^2 - 2m_q^2\right) + m_q^2 m_\chi^2 + m_q^4 - 2m_\chi^4 + M^4\right)}{2m_\chi^2} , \quad (3.1.26)$$

where we assumed the center of mass frame. Performing the angular integration one obtains the decay width of the mediator

$$\Gamma(\eta \to \chi q) = \frac{g^2\lambda^{\frac{1}{2}}\left(M^2\left(m_\chi^2 - 2m_q^2\right) + m_q^2 m_\chi^2 + m_q^4 - 2m_\chi^4 + M^4\right)}{32\pi M^3 m_\chi^2} , \quad (3.1.27)$$

where λ is the factor coming from the phase space defined in eq. (3.1.10). This result has also been checked numerically against that of MadWidth. If we consider the scenario of heavy Dark Matter and mediator, we have the approximate result

$$\Gamma(\eta \to \chi q) \approx \frac{g^2 M^3}{32\pi m_\chi^2}\left(1 - 3\frac{m_\chi^4}{M^4}\right) . \quad (3.1.28)$$

Before presenting some phenomenology of the model, we would like to show a mechanism that could generate this kind of simplified model. The idea is to add an additional $U_X(1)$ symmetry with the gauge boson being the vectorial Dark Matter acquiring mass through Higgs mechanism. We consider two quarks q_1 and q_2, respectively a SM-like quark and a vector-like quark. In particular we want to have a mixing between them in order to obtain 2 states that will be identified with the Standard Model quark and a new heavy quark. We assume that only the right-handed part of quarks is charged under the new $U_X(1)$ symmetry, with q_1 and q_2 having opposite charge. The gauge interaction is:

$$\mathcal{L}_q = \bar{q}_{1R}(i\slashed{\partial} + g_x\slashed{X})q_{1R} + \bar{q}_{2R}(i\slashed{\partial} - g_x\slashed{X})q_{2R} \quad (3.1.29)$$

where X_μ is the new gauge boson and g_x is the gauge coupling.
We can recast the interaction term in matrix form:

63

$$\begin{pmatrix} \bar{q}_{1R} & \bar{q}_{2R} \end{pmatrix} \begin{pmatrix} g_x \cancel{X} & 0 \\ 0 & -g_x \cancel{X} \end{pmatrix} \begin{pmatrix} q_{1R} \\ q_{2R} \end{pmatrix} \tag{3.1.30}$$

The idea is to find a way to have a mixing between q_1 and q_2 in order to cancel the diagonal term leaving an off diagonal interaction and therefore obtain a flavor changing neutral current [32]. This is why we chose opposite charges, since after an SO(2) transformation the trace is conserved and so if we want to cancel both the diagonal terms, we need the trace to be zero from the start.

Now we write the Yukawa interactions that generates the masses through Higgs mechanism. We introduce a scalar singlet Φ with charge 1 under $U_X(1)$, because we want to write a term mixing q_1 and q_2. We need also to give a charge 1 to the Higgs of the Standard Model, otherwise we cannot write the Yukawa term of the SM.

$$\mathcal{L}_{yuk} = -\lambda \bar{q}_{1R} \Phi q_{2L} - y \bar{q}_L \tilde{H} q_{1R} + h.c. \tag{3.1.31}$$

with q_L SU(2) doublet of the SM. After SSB, we have:

$$H \approx \frac{1}{\sqrt{2}}(h + v_1)$$
$$\Phi \approx \frac{1}{\sqrt{2}}(\phi + v_2) \tag{3.1.32}$$

with v_1 and v_2 vacuum expectation values of the two fields. The mass Lagrangian become (taking into account that being a vector-like quark we can write directly a mass term for q_2):

$$\mathcal{L}_M = -M \bar{q}_{2L} \, q_{2R} - \frac{\lambda v_2}{\sqrt{2}} \, \bar{q}_{2L} \, q_{1R} - \frac{y v_1}{\sqrt{2}} \, \bar{q}_{1L} \, q_{1R} + h.c. \tag{3.1.33}$$

In matrix form this can be written as:

$$\begin{pmatrix} \bar{q}_{1L} & \bar{q}_{2L} \end{pmatrix} \begin{pmatrix} \frac{y v_1}{\sqrt{2}} & 0 \\ \frac{\lambda v_2}{\sqrt{2}} & M \end{pmatrix} \begin{pmatrix} q_{1R} \\ q_{2R} \end{pmatrix} \tag{3.1.34}$$

If we define $x = \frac{\lambda v_2}{\sqrt{2}}$, then as in [33], we can define 2 SO(2) matrices V_L and V_R:

$$V_{L,R} = \begin{pmatrix} \cos\theta_{L,R} & \sin\theta_{L,R} \\ -\sin\theta_{L,R} & \cos\theta_{L,R} \end{pmatrix}, \tag{3.1.35}$$

so that:

$$\begin{pmatrix} q_1 \\ q_2 \end{pmatrix}_{L,R} = \begin{pmatrix} \cos\theta_{L,R} & \sin\theta_{L,R} \\ -\sin\theta_{L,R} & \cos\theta_{L,R} \end{pmatrix} \begin{pmatrix} q \\ q_H \end{pmatrix}_{L,R} \tag{3.1.36}$$

with q and q_H being the SM quark and the new heavy quark respectively. In doing so we can diagonalise the mass matrix:

$$\begin{pmatrix} \cos\theta_L & -\sin\theta_L \\ \sin\theta_L & \cos\theta_L \end{pmatrix} \begin{pmatrix} \frac{yv_1}{\sqrt{2}} & 0 \\ x & M \end{pmatrix} \begin{pmatrix} \cos\theta_R & \sin\theta_R \\ -\sin\theta_R & \cos\theta_R \end{pmatrix} = \begin{pmatrix} m_q & 0 \\ 0 & m_{q_H} \end{pmatrix}. \tag{3.1.37}$$

The relations between the input parameters and the masses and mixing angles are:

$$\frac{y^2 v_1^2}{2} = m_q^2 \left(1 + \frac{x^2}{M^2 - m_q^2} \right) \tag{3.1.38a}$$

$$m_{q_H}^2 = M^2 \left(1 + \frac{x^2}{M^2 - m_q^2} \right) \tag{3.1.38b}$$

$$\sin\theta_R = \frac{Mx}{\sqrt{(M^2 - m_q^2)^2 + M^2 x^2}} \tag{3.1.38c}$$

$$\sin\theta_L = \frac{m_q}{M} \sin\theta_R \tag{3.1.38d}$$

Following this rotation, we can see what happens to the new gauge interaction for the right-handed part:

$$\begin{pmatrix} \cos\theta_R & -\sin\theta_R \\ \sin\theta_R & \cos\theta_R \end{pmatrix} \begin{pmatrix} g_x X\!\!\!/ & 0 \\ 0 & -g_x X\!\!\!/ \end{pmatrix} \begin{pmatrix} \cos\theta_R & \sin\theta_R \\ -\sin\theta_R & \cos\theta_R \end{pmatrix} = \begin{pmatrix} c^2 - s^2 & 2sc \\ 2sc & s^2 - c^2 \end{pmatrix} g_x X\!\!\!/ , \tag{3.1.39}$$

where c and s stand for the cosine and the sine of the right-handed angle. We can see that if we rotate by an angle of $\frac{\pi}{4}$, we completely cancel the diagonal interaction and we get only flavor changing interaction.

The condition allows us to fix the M in function of x:

$$\sin \theta_R = \frac{\sqrt{2}}{2} = \frac{Mx}{\sqrt{(M^2 - m_q^2)^2 + M^2 x^2}} \,. \tag{3.1.40}$$

We can solve this equation by setting $z = \frac{M}{m_q}$ and $w = \frac{x}{m_q}$, in order to have dimensionless parameters, looking for solutions with $z > 1$. By squaring it, the equation becomes:

$$\frac{z^2 w^2}{(z^2 - 1)^2 + z^2 w^2} = \frac{1}{2} \,, \tag{3.1.41}$$

and the only solution satisfying $z > 1$ is:

$$z = \frac{1}{2}(\sqrt{w^2 + 4} + w) \,. \tag{3.1.42}$$

The mass of the new quark can be expressed in function of these parameters

$$m_{q_H}^2 = m_q^2 z^2 \left(1 + \frac{w^2}{z^2 - 1}\right) = m_q^2 F(w) \,, \tag{3.1.43}$$

with $F(w)$ being an increasing function in w, with $F(0) \to 1$. We can therefore see that the new quark has always a greater mass than the SM quark.

We can also give mass to the vector boson through the Higgs mechanism, bearing in mind that both H and Φ are charged under the new $U(1)_X$ symmetry. It is than easy to see that:

$$(D_\mu \Phi)^\dagger D^\mu \Phi + (D_\mu H)^\dagger D^\mu H \to \frac{1}{2} m_x^2 X_\mu X^\mu \tag{3.1.44}$$

with $m_x = g_x \sqrt{v_1^2 + v_2^2}$.
We are then left with the Lagrangian:

$$\mathcal{L} = g_x \, \bar{q}_R \gamma^\mu q_{HR} X_\mu + h.c. - \frac{1}{4} X_{\mu\nu} X^{\mu\nu} + \frac{1}{2} m_x^2 X_\mu X^\mu \,. \tag{3.1.45}$$

It is also important to notice that this rotation does not affect at all the interaction to gluons of the two quarks, since it is proportional to the identity in SO(2). Also we end up with 3 degrees of freedom for this model, namely g_x, v_2 and λ or if we prefer m_q, m_{q_H} and g_x. This is exactly the Lagrangian of the F3-V0-q simplified model we are studying.
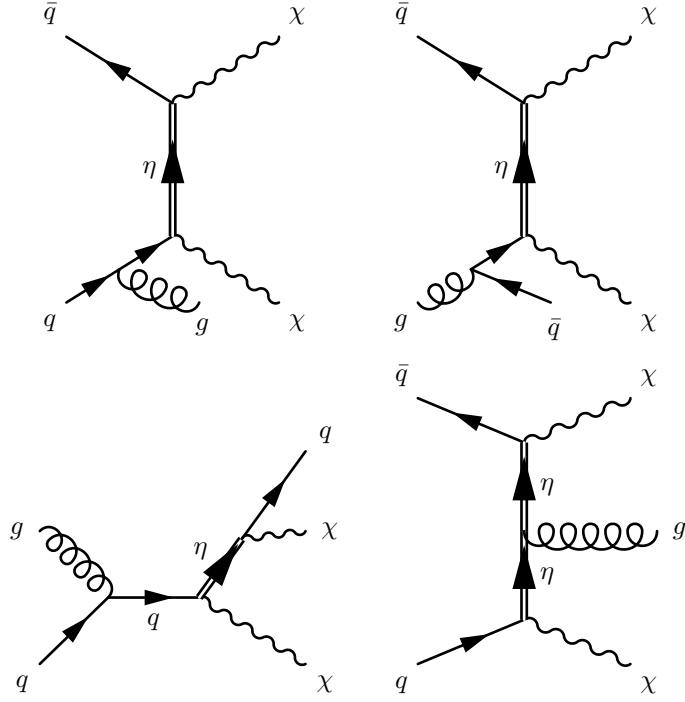
Figure 3.1.10: Some diagrams contributing to the 1-jet and missing energy signature. The first two are of the kind external radiation, the third is single resonant production while the last one is internal radiation.

Let us now focus on the phenomenology of the model. As in the previous model we have both 1-jet and 2-jet plus $\not{E}_T$ signatures at the LHC. The most important processes for the 1-jet are

$$q\,\bar{q} \to \chi\,\chi\,g\,, \tag{3.1.46a}$$

$$q\,g \to \chi\,\chi\,q\,, \tag{3.1.46b}$$

$$q\,g \to \chi\,\eta \to \chi\,\chi\,q\,, \tag{3.1.46c}$$

where the first two processes involve internal and external radiation and the third one is a resonant process (see fig. 3.1.10). Notice also that since the vector Dark Matter is real, there is no difference between a particle and an anti-particle, so we always have contributions from diagrams in which the final state are exchanged.
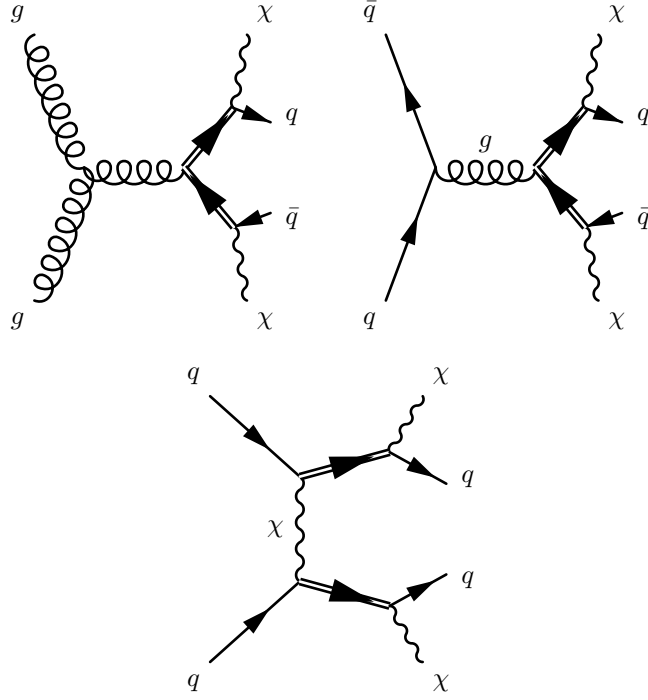
Figure 3.1.11: Some diagrams contributing to the 2-jet and missing energy signature.

Concerning the 2-jet we have the double resonance processes (see fig. 3.1.11)

$$g\,g \to \eta\,\bar{\eta} \to \chi\,\chi\,q\,\bar{q}\,, \tag{3.1.47a}$$

$$q\,\bar{q} \to \eta\,\bar{\eta} \to \chi\,\chi\,q\,\bar{q}\,, \tag{3.1.47b}$$

$$q\,q \to \eta\,\eta \to \chi\,\chi\,q\,q\,. \tag{3.1.47c}$$

As in the F3-S0-q model, we can exploit the presence of the $q - q$ scattering process and his enhancement because of the parton distribution function of the proton.

The annihilation cross section for a pair of DM particles into Standard Model particles is not suppressed and this leads to small couplings if one wants to satisfy the relic density restriction. This model is also characterized by a very large and dominant cross section for the production of the colored mediator, as can be seen in fig. 3.1.12.

This feature can also be seen in the region plots we produced to classify the possible signals at LHC. We considered three kind of signatures, depending on how many resonant mediators are being produced. As in the previous models we looked for the regions in the parameter space in which each set of processes is dominant, with the future

68
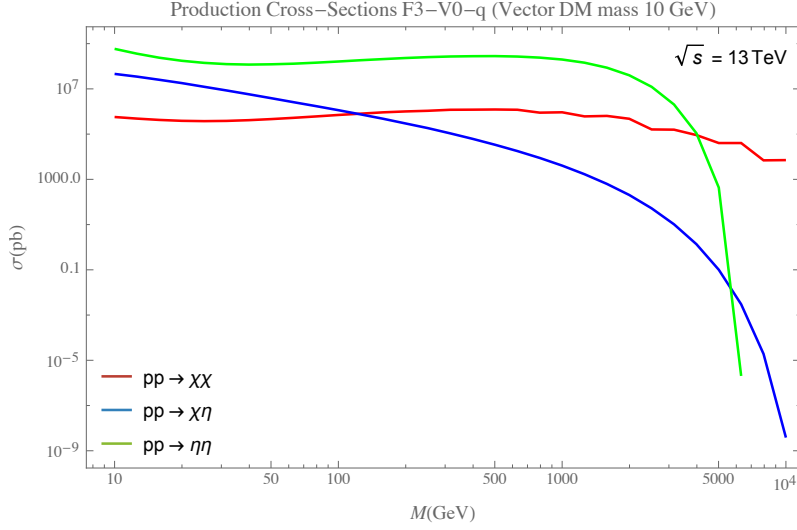
Figure 3.1.12: This plot show the behavior of the total cross section, in function of the mediator mass, for different processes simulated with MadGraph, assuming a collision of protons as in LHC. The coupling is set to $g = 1$ and we assumed interaction with both righ-handed and left-handed quarks.

intention of studying the model at NLO and identify which process is better to compute the corrections of (see fig. 3.1.13). We assumed the validity of the Narrow Width Approximation, so that the mediator always decays within the detector in a DM particle and in a quark with probability 1, and we did this for three benchmark values of the Dark Matter mass. We simulated the processes with MadGraph scanning both in the coupling g and the mediator mass M. In the plots we can clearly see that the parameter space of the model is almost completely dominated by the double resonant process when the Dark Matter mass is low. As the mass increase, the red region is the more influenced by that because of the phase space suppression. Therefore, in the region where the coupling is small and the mediator mass is high (this leads to a phase space suppression of the double resonant cross section) the one resonant process starts to dominate more and more. This explains why in the third plot we see the emergence of the blue region. We should also consider the possibility that in a complete model, the double resonant contribution coming from the t-channel exchange of a DM particle ($pp \to \eta\eta \propto M^2/m_\chi^2$ at the matrix element level) is cut off by the Higgs sector responsible for giving the mass to the vector Dark Matter. This analysis is treated in more detail in [31].
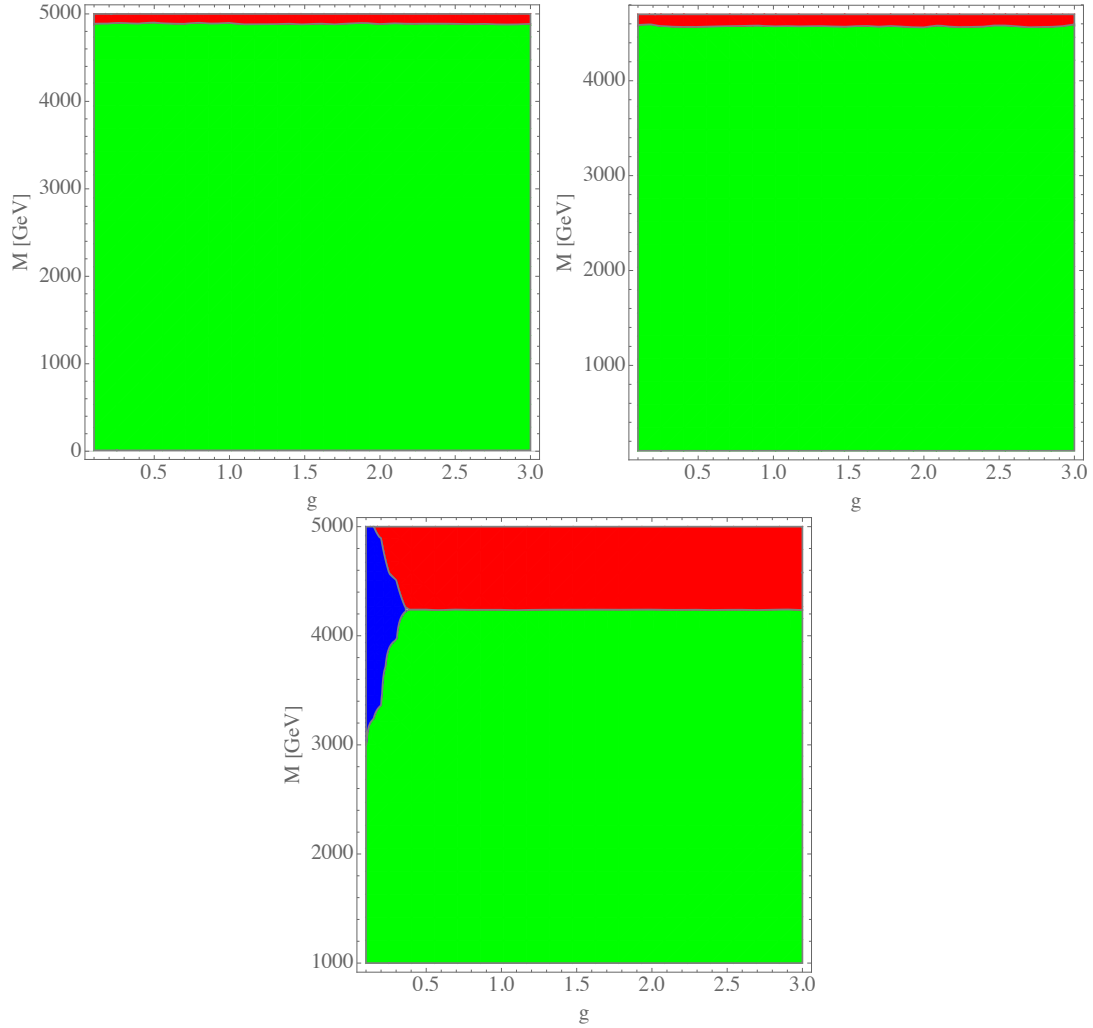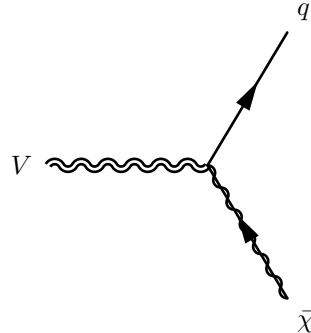
Figure 3.1.13: The plots show for each process the region of the parameter space in which is dominant, in the case of a 10 GeV (top left panel), 100 GeV (top right panel) and 1000 GeV (bottom panel) Dark Matter mass. The red corresponds to the no-resonance processes ($pp \to \chi\chi j$), the blue corresponds to the 1-resonance processes ($pp \to \chi\eta$) while the green region is related to the 2-resonance processes ($pp \to \eta\eta$). The simulation is done at the current LHC center of mass energy of 13 TeV. We can clearly see in the plot that as far as the Dark Matter is light, the parameter space is dominated by the 2 resonance process.

3.1.4 V3-F0-q model

The last t-channel simplified model involving quarks that we will consider is character-ized by the presence of a colored vector triplet V^μ coupled to a fermion Dark Matter (either Dirac or Majorana). As in the previous models, we can decide whether to couple right-handed quarks with a SU(2) singlet mediator or couple the SU(2) doublet with a doublet mediator. The model we implemented in FeynRules and that we used to produce simulations in MadGraph is the most general possible, involving both couplings and the possibility to switch off one by one the interactions we are not interested in. We also invoke the $\mathbb{Z}_2$ under which the dark sector is odd, in order to ensure the Dark Matter stability. For the sake of simplicity, let us consider the Lagrangian involving the interaction with left-handed quarks

$$\mathcal{L} \supset g\,\bar{q}_L\,\gamma_\mu\,\chi\,V^\mu + h.c. \tag{3.1.48}$$

where it is understood that we have a similar term for each quark. To avoid the presence of FCNCs, the MFV requires all the three generation couplings to be equal and all the vector mediators to have the same mass M. We are then left with a three dimensional parameter space $\{m_\chi, M, g\}$. To ensure the DM particle stability we also require $M > m_\chi$, so that the decay channel is kinematically closed. The Feynman rule of the model is

$$= ig\gamma^\mu\left(\frac{\mathbb{1}\pm\gamma^5}{2}\right). \tag{3.1.49}$$

We can now compute the decay width of the mediator. Denoting with p and M the momentum and the mass of the mediator, while with p_1 and p_2 the masses of the outgoing particles, we can write the amplitude

$$\mathcal{M} = g\,\bar{u}(p_1, m_q).\gamma^\mu.P_L.v(p_2, m_\chi)\,\epsilon_\mu(p, M)\,. \tag{3.1.50}$$

After squaring it, the sum over the outgoing color index and the average over the incoming

gives a factor 1. Then, we average over the 3 incoming vector polarizations and the outgoing spin polarizations to obtain

$$\frac{1}{3} \sum_{spin,pol} |\mathcal{M}|^2 = \frac{1}{3} \left(4g^2 \left(\frac{(p \cdot p_1)(p \cdot p_2)}{M^2} - p_1 \cdot p_2 \right) + 6g^2 (p_1 \cdot p_2) \right) =$$
$$\frac{2}{3} g^2 \left(-\frac{(m_\chi^2 - m_q^2)^2}{2M^2} - \frac{m_q^2}{2} - \frac{m_\chi^2}{2} + M^2 \right) , \quad (3.1.51)$$

where we chose the center of mass frame to do the explicit calculation. Performing the angular integration, we obtain the decay width

$$\Gamma(V \to q\bar{\chi}) = \frac{g^2 \lambda^{\frac{1}{2}}}{24\pi M^3} \left(-\frac{(m_\chi^2 - m_q^2)^2}{2M^2} - \frac{m_q^2}{2} - \frac{m_\chi^2}{2} + M^2 \right) , \quad (3.1.52)$$

where λ is the phase space factor defined in eq. (3.1.10). This result has been checked numerically against that of MadWidth. In the heavy mediator and DM scenario, the width can be approximated to

$$\Gamma(V \to q\bar{\chi}) \approx \frac{g^2 M}{24\pi} \left(1 - \frac{m_\chi^2}{M^2} \right)^{\frac{3}{2}} . \quad (3.1.53)$$

Before studying the phenomenology of the model, let us focus on the interaction between the mediator and gluons. As explained in [34], the Lagrangian is not straightforward to write. The most general interaction we can write is

$$\mathcal{L} \supset -\frac{1}{2} V_{\mu\nu}^\dagger V^{\mu\nu} - ig_s(1-k) V^{\dagger\mu} t_F^a V^\nu G_{\mu\nu a} , \quad (3.1.54)$$

where $V_{\mu\nu} = D_\mu V_\nu - D_\nu V_\mu$, the covariant derivative $D_\mu = \partial_\mu - ig_s t_F^a A_\mu^a$ and $G_{\mu\nu a}$ is the gluon field strength. There are two terms that we can write and they are SU(3) gauge invariant by themselves, so the coupling constant of the second is not fixed. In any model, in which the colored vectors are fundamental objects, they will be gauge bosons of an extended gauge group (for example in [35] they emerge from an SU(5) gauge group and are called Leptoquarks) and the coupling would be fixed by gauge invariance with $k = 0$. This kind of choice will also insure that cross sections have a unitary behavior. On the other hand, the mediator can be a low energy manifestation of a more fundamental theory, maybe even a composite state. In this scenario there are no constraints on the coupling of the second term and a so-called anomalous chromomagnetic moment can
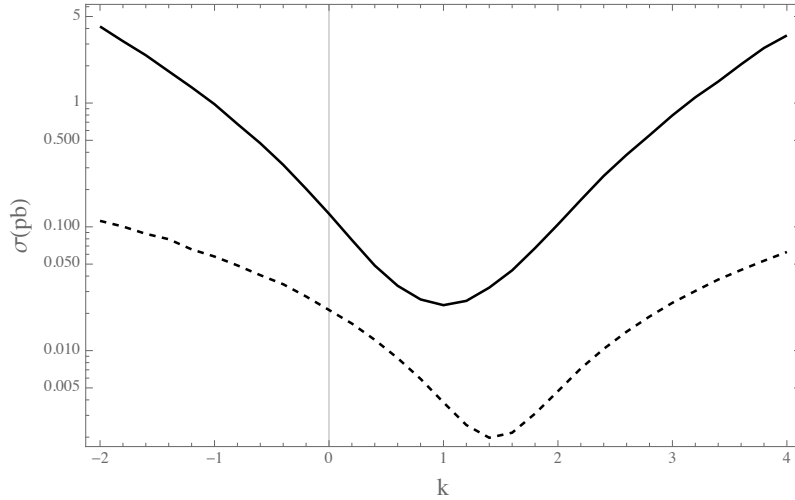
Figure 3.1.14: This plot shows the production cross section of a pair of 1 TeV mediators at the LHC in function of k, simulated with MadGraph. The dashed line corresponds to $q\bar{q}$ annihilation, while the solid curve corresponds to gg annihilation.

appear, characterized by $k \neq 0$. In the case of $k = 1$ we are in the special scenario called Minimal Coupling. The model implemented in FeynRules takes into account this fact, allowing to decide the value of the parameter k (see the fig. 3.1.14).

Let us now show that, if one assumes that the mediator comes from a $SU(5)$ Grand Unified Theory, the model one end up with is the one with $k = 0$. $SU(5)$ is the smallest Lie Group that contains the gauge group of the Standard Model without introducing any new fermion. The dimension of the group is 24 and therefore we have 24 gauge fields that are organised like

$$24 \rightarrow (3, 2) \oplus (\bar{3}, 2) \oplus (8, 1) \oplus (1, 3) \oplus (1, 1) , \qquad (3.1.55)$$

where the numbers denote $SU(3)$ and $SU(2)$ respectively. We retrieve the photon, the 3 weak boson and the gluons, but we also get a color triplet and $SU(2)$ doublet and its anti-particle that is precisely the leptoquark. Let us now build the generators of the group, that are 5×5 traceless matrices. The idea is to choose them in such a way that the subgroup $SU(3)$ operates on the first three rows while the sub-group $SU(2)$ on the

last two. The first 12 generators are then

$$L^a = \begin{pmatrix} \frac{\lambda^a}{2} & 0 \\ 0 & 0 \end{pmatrix} \qquad a = 1, ..., 8 \tag{3.1.56a}$$

$$L^i = \begin{pmatrix} 0 & 0 \\ 0 & \frac{\sigma^i}{2} \end{pmatrix} \qquad i = 1, ..., 3 \tag{3.1.56b}$$

$$L^{12} = \frac{1}{\sqrt{30}} diag(-2, -2, -2, 3, 3) \,, \tag{3.1.56c}$$

where the last one corresponds to the hypercharge. We are left with 12 matrices, that we can write in the following form

$$L = \frac{1}{2} \begin{pmatrix} 0 & M \\ M^\dagger & 0 \end{pmatrix} \,, \tag{3.1.57}$$

where M is a 3×2 matrix without any constraint since the trace of L is always zero and it is hermitean by definition and the factor $1/2$ is due to normalization reasons. So we can choose the last 12 matrices by putting 1 and i alternatively in each of the 6 spot of the M matrix. The Yang-Mills Lagrangian is

$$\mathcal{L}_{YM} = -\frac{1}{2} tr[V^{\mu\nu} V_{\mu\nu}] \,, \tag{3.1.58}$$

where $V_{\mu\nu} = \partial_\mu V_\nu - \partial_\nu V_\mu - ig_5(V_\mu V_\nu - V_\nu V_\mu)$ and $V_\mu = L^i V_\mu^i$ is the 5×5 matrix

$$V_\mu = \begin{pmatrix} \mathbf{G}_\mu & X_\mu/\sqrt{2} \; Y_\mu/\sqrt{2} \\ \hline X_\mu^\dagger/\sqrt{2} & \mathbf{W}_\mu/\sqrt{2} \\ Y_\mu^\dagger/\sqrt{2} & \end{pmatrix} + \frac{1}{\sqrt{30}} B_\mu \begin{pmatrix} -2I & 0 \\ \hline 0 & 3I \end{pmatrix} \tag{3.1.59}$$

where X and Y are triplets that together form the $SU(2)$ doublet. If we keep only the gluon field and the leptoquark field X, we can compute explicitly the field strength $V_{\mu\nu}$. The computation is very tedious, but in the end one can find exactly

$$-\frac{1}{2} tr[V^{\mu\nu} V_{\mu\nu}] \rightarrow -\frac{1}{2} X_{\mu\nu}^\dagger X_{\mu\nu} - ig_5 X^{\mu\dagger} G_{\mu\nu} X^\nu \,, \tag{3.1.60}$$
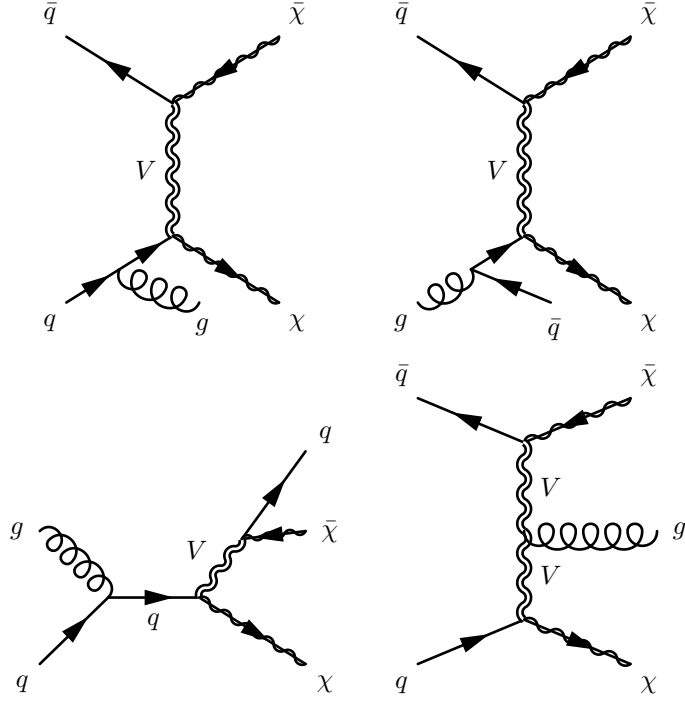
Figure 3.1.15: Some diagrams contributing to the 1-jet and missing energy signature. The first two are of the kind external leg bremsstrahlung, the third is single resonant production while the last one is internal bremsstrahlung.

that is precisely the mediator-gluon interaction of the V3-F0-q Lagrangian with $k = 0$.

We focus now on the phenomenology of the model, which is very similar to the S3-F0-q model one. In particular we have both the 1-jet and the 2-jet plus $\not{E}_T$ signatures. Concerning the 1-jet signatures (see fig. 3.1.15) we have

$$q\,\bar{q} \to \chi\,\bar{\chi}\,g\,, \tag{3.1.61a}$$

$$q\,g \to \chi\,\bar{\chi}\,q\,, \tag{3.1.61b}$$

$$q\,g \to \chi\,V \to \chi\,\bar{\chi}\,q\,, \tag{3.1.61c}$$

where in the last process we have a resonant enhancement to the signal because of the production of an on-shell mediator.
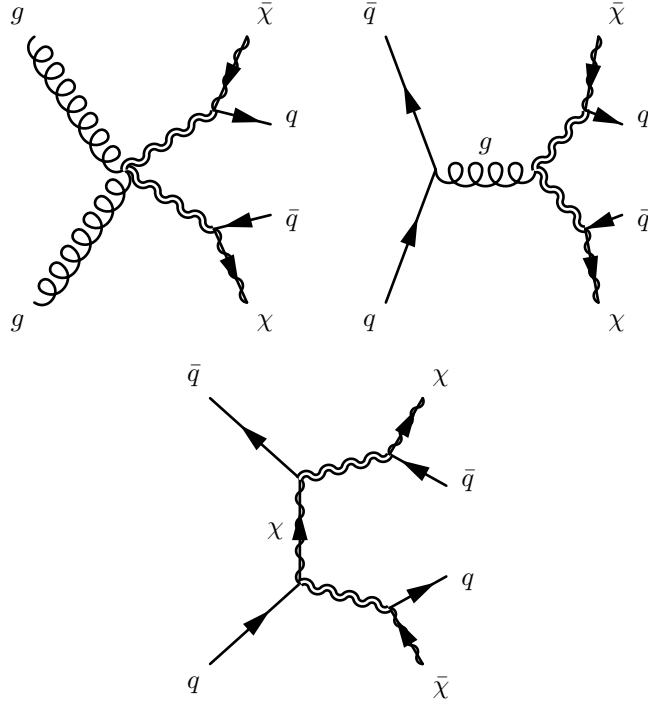
Figure 3.1.16: Some double resonant diagrams contributing to the 2-jet and missing energy signature.

For the 2-jet signal (see fig. 3.1.16) we have the usual

$$g\,g \to V\,V^* \to \chi\,\bar{\chi}\,q\,\bar{q}\,, \tag{3.1.62a}$$

$$q\,\bar{q} \to V\,V^* \to \chi\,\bar{\chi}\,q\,\bar{q}\,, \tag{3.1.62b}$$

where we produce on-shell mediators in both processes.

This model has not been studied much in the literature, in particular from the LHC phenomenology perspective, but we plan to do it in future works. It is possible, however, to translate some leptoquarks studies in order to use them to put constraints on the parameter space, since at least in the gluon-mediator sector the interaction is exactly the same. Also for this model we produced with MadGraph a plot showing a mass scan in the mediator mass, for three different processes, considering both a Dirac and a Majorana DM (see fig. 3.1.17). The LHC phenomenology is almost identical, but we know and already explained in the S3-F0-q paragraph that from a direct detection perspective there is a huge difference, since a Majorana DM has a suppresses spin independent cross section, while the Dirac has not.
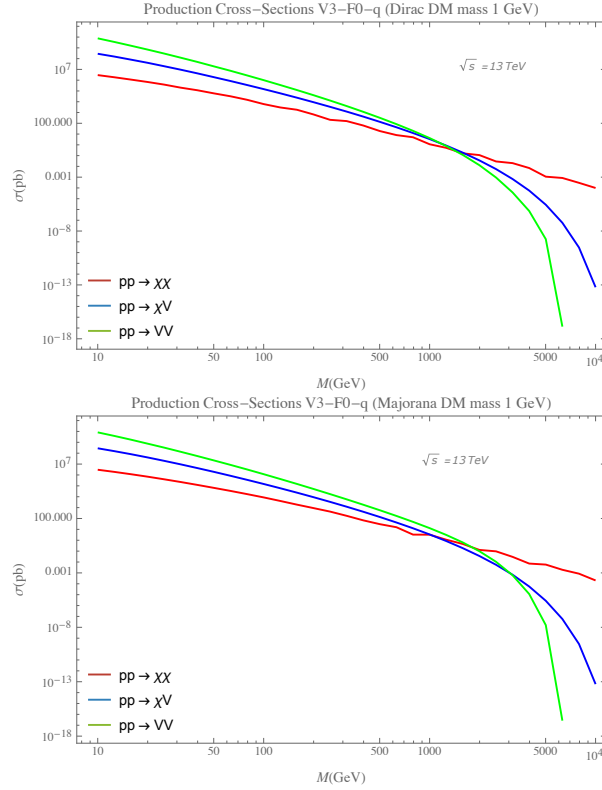
Figure 3.1.17: These two plots show the behavior of the total cross section, in function of the mediator mass, for different processes simulated with MadGraph, assuming a collision of protons as in LHC. In the top panel we have the case of a Dirac Dark Matter, while in the bottom panel we have a Majorana DM, both with mass of 1 GeV. In both cases the coupling is $g = 1$ and we assumed interaction with both righ-handed and left-handed quarks.

Following the same pattern of the other models we also classified the possible LHC signals into three main categories, depending on whether we have a 0-resonance process, a single resonance or a double resonance. We produced plots in order to understand which process dominate in each of the parameter space area, with the intention of studying it at NLO in future works. As in the previous cases we assumed the Narrow Width Approximation, i.e. the mediator decays with probability one within the detector, and we did it for three benchmark values of the Dark Matter mass. We computed the cross section with MadGraph, scanning in both the mediator mass M and the coupling g, assuming interaction with both left-handed and right handed quarks. The plots are very similar to the S3-F0-q ones, confirming once again the similarity between the two, at least from a phenomenological perspective see fig. 3.1.18.
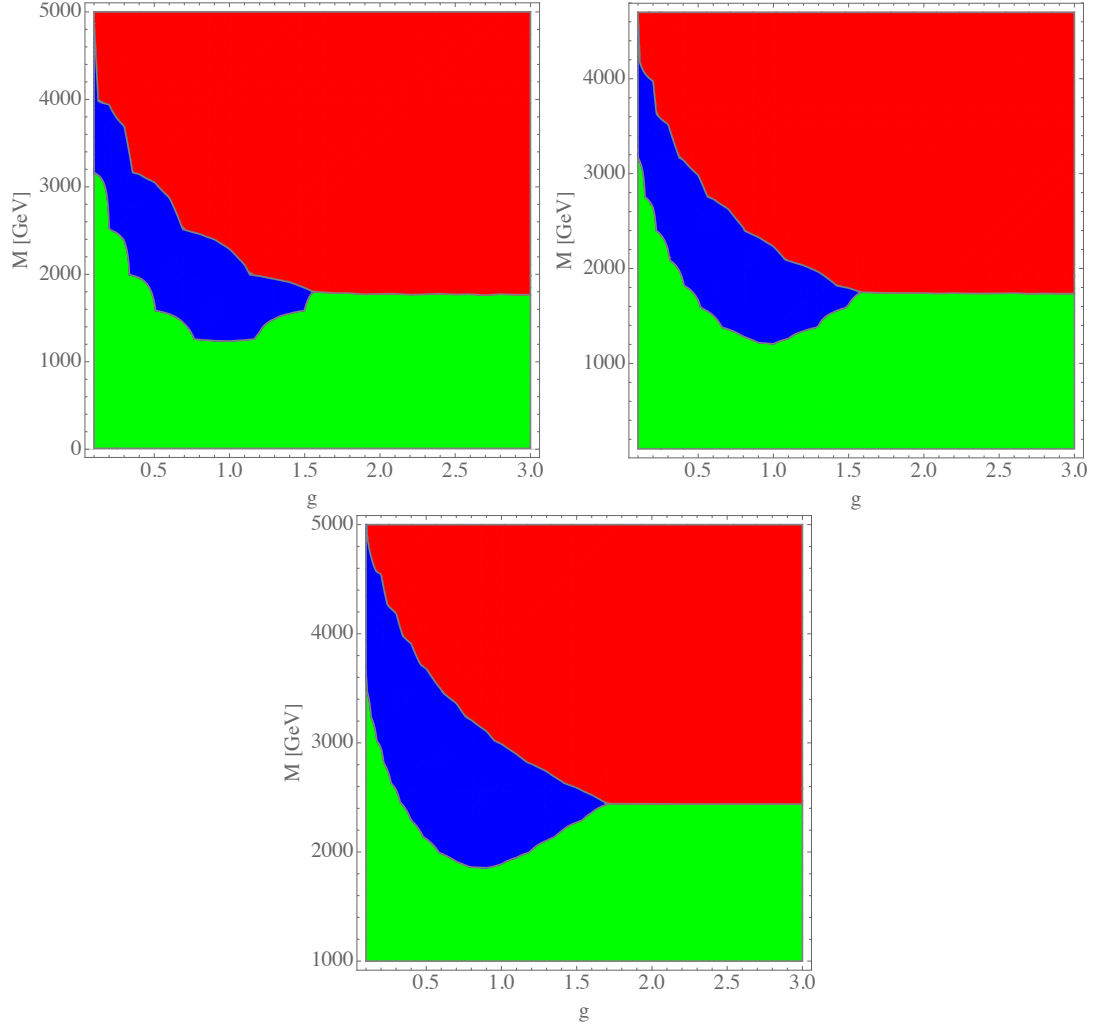
Figure 3.1.18: The plots show for each process the region of the parameter space in which is dominant, in the case of a 10 GeV (top left panel), 100 GeV (top right panel) and 1000 GeV (bottom panel) Dark Matter mass. The red corresponds to the no-resonance processes ($pp \to \chi\bar\chi j$), the blue corresponds to the 1-resonance processes ($pp \to \chi\eta$) while the green region is related to the 2-resonance processes ($pp \to \eta\eta$). The simulation is done at the current LHC center of mass energy of 13 TeV. We can see that as the DM mass increase, the blue region widens. These plots are very similar to the S3-F0-q ones.

3.2 Color octet mediator

The are other t-channel simplified models that are worth of being studied and they involve an interaction term with gluons instead of quarks. Since the Dark Matter particle cannot be colored, the mediator needs to be a color octet. In this section we will list all the possible models that we can build with some comments, but we leave their analyses to future works. One common feature of these models, apart from the notable exception of the last one, is the fact that we need to build non-renormalizable Lagrangian terms. For this reason they can be thought of as loop-induced interactions and they need to be treated carefully, leading to a non trivial phenomenology.

The first model we can build is the S8-S0-G model, with a scalar octet mediator and a scalar DM. The corresponding Lagrangian, enforcing the usual $\mathbb{Z}_2$ symmetry, is

$$\mathcal{L} \supset \frac{c}{\Lambda^2}(D^\mu G^a_{\mu\nu})(D^\nu \eta^a)\chi + \frac{c'}{\Lambda^2}G^{\mu\nu c}\left(\eta^a T^c_{a,b} G^b_{\mu\nu}\right)\chi. \tag{3.2.1}$$

An interesting feature of this model is the fact that the 3-vertex interaction coming from the first Lagrangian term gives a zero contribution everytime the gluon is on-shell, therefore we cannot use this vertex to compute the usual SM-SM scattering into DM-DM. Also we have to consider that every diagram with two vertices has a $1/\Lambda^4$ suppression. For this reason it is important to carefully understand which diagram is dominant at leading order. In addition to these t-channel terms, we have also to deal with other operators, that can influence the phenomenology contributing to the same signals, namely

$$\mathcal{L} \supset \lambda_1 \eta^a \eta^a \chi^2 + \frac{\lambda_2}{\Lambda^2}G^a_{\mu\nu}G^{\mu\nu a}\chi^2 + \frac{\lambda_3}{\Lambda^2}G^a_{\mu\nu}G^{\mu\nu a}\eta^b\eta^b, \tag{3.2.2}$$

where the first one has the interesting feature of being a dimension 4 operator. While the second and the third terms can contribute to production of Dark Matter and double resonance signal at tree level, the first one cannot influence the collider phenomenology at tree level, since it does not involve Standard Model particles. However, it is possible to insert this operator in a loop diagram (see fig. 3.2.1). The interesting aspect of this model is then to understand if and in which region of the parameter space the loop diagrams are dominating over the higher order operators. The two contributions are both suppressed, but for different reasons: one has a loop suppression, the other is suppressed because of the new physics scale Λ. Therefore there can be a non trivial phenomenology behind this model.

The second model we can think of is the F8-F0-G, featuring a fermion octet mediator, gluino like, and a fermion DM.
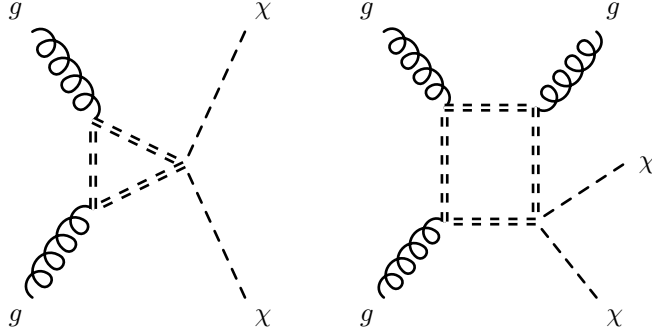
Figure 3.2.1: Feynman diagrams showing how the 4-vertex interaction between the mediator and Dark Matter can contribute to the phenomenology of the model at one loop. On the left a contribution to the DM production, on the right a contribution to 1-jet plus missing energy signal.

The Lagrangian of the model is

$$\mathcal{L} \supset \frac{c}{\Lambda} G^a_{\mu\nu} \left(\bar{\eta}^a \sigma^{\mu\nu} \chi \right) + h.c. \tag{3.2.3}$$

This operator resembles a SUSY operator and therefore there are already studies of this kind of mediator in the literature, but not in the context of a simplified model with a DM particle. In particular, limits from QCD productions tells us that for DM masses below 100 GeV we need mediators heavier than 1150 TeV.

The third model we can build involve again a scalar octet mediator coupled to a real vector Dark Matter, the S8-V0-G model. The Lagrangian of this model is

$$\mathcal{L} \supset \frac{c}{\Lambda} G^a_{\mu\nu} \left(D^\nu \eta^a \right) \chi^\mu + \frac{c'}{\Lambda} G^a_{\mu\nu} \left(\partial^\nu \chi^\mu \right) \eta^a \,. \tag{3.2.4}$$

Also in this model we can add a 4-vertex interaction between the mediator and the Dark Matter particle, thanks to the dimension 4 operator

$$\mathcal{L} \supset \lambda \eta^a \eta^a \chi^\mu \chi_\mu \,. \tag{3.2.5}$$

We can then make the same argument we expressed for the S8-S0-G model, since this operator can contribute to loop diagrams that can in principle be more important than the higher dimension operators. However, in this model we are dealing with dimension 5 operators instead of 6 and this might change a bit the situation.

The fourth model involve a vector octet mediator and a scalar DM particle, the V8-S0-G model. The Lagrangian is
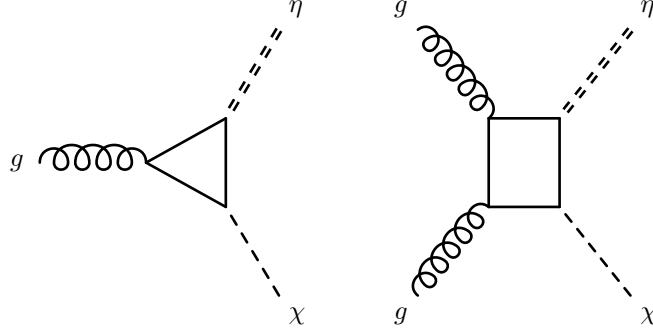
Figure 3.2.2: Feynman diagrams showing how a loop can induce the interactions of higher order. The plain line represent some heavy particle that can be integrated out from the theory.

$$\mathcal{L} \supset \frac{c}{\Lambda} G^a_{\mu\nu} \left(D^\nu V^{\mu a} \right) \chi + \frac{c'}{\Lambda} G^a_{\mu\nu} \left(\partial^\nu \chi \right) V^{\mu a} \,. \tag{3.2.6}$$

Even in this case, we can build a dimension 4 operator

$$\mathcal{L} \supset \lambda V^{\mu a} V_{\mu a} \chi^2 \,, \tag{3.2.7}$$

giving the interesting situation mentioned before.

Finally, the V8-V0-G model that features a vector octet mediator and a real vector Dark Matter, with Lagrangian

$$\mathcal{L} \supset c \, G^a_{\mu\nu} \chi^\mu V^{\nu a} \,, \tag{3.2.8}$$

where this model differs from the others, because it does not features non-renormalizable Lagrangian terms. This model is therefore very peculiar, characterized by a different phenomenology from the other models of this class.

We want to stress once more that the most important difference between these models and the models with color triplet mediators is the fact that we have to deal with higher dimension operators. We can think of them as being produced by a more fundamental loop interaction, in which the particles running through the loop are heavy and have been integrated out from the theory (see fig. 3.2.2). The scale of new physics Λ which appear in the coupling of the operator is indeed related to the mass of this new particle and it is therefore a highly suppressing factor. For this reason the phenomenology of these models will be quite different from the previously studied ones. The zero resonance and the one resonance process will be strongly suppressed by the insertion of these kind of

81
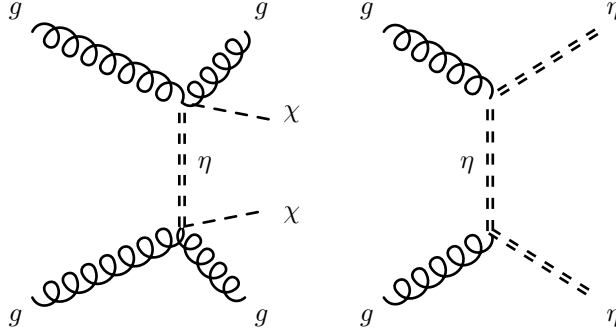
Figure 3.2.3: Feynman diagrams of the production of a 2 jet and missing energy signal without resonances (on the left) and with two resonance (on the right) in the S8-S0-G model.

operators, but they will not affect the double resonance, that features QCD vertices and is therefore proportional only to the strong coupling g_s. These kind of processes produce two jets plus missing energy signals, through the decay of each mediator into a gluon and a DM particle with the insertion of the loop-induced operator. Notwithstanding, if there is only one viable decay channel, the branching ratio will be one and will not depend on the small coupling. Therefore the double resonance would be the only kind of signal not affected by the Λ suppression, dominating over the other two.

As an example, let us consider the S8-S0-G model. If we want to produce a couple of Dark Matter particles in a collider as LHC with no resonances we have to consider the process $gg \to gg\chi\chi$ mediated by the exchange of the octet mediator (see fig. 3.2.3). This is the only way to have at tree level a t-channel scattering, since the 3-vertex with only one gluon is zero whenever the gluon is on-shell. Each vertex of this diagram carries a factor $1/\Lambda^2$ and therefore the amplitude is proportional to $1/\Lambda^4$ and the cross section to $1/\Lambda^8$. If the integrated out particle is beyond the reach of the LHC, one can assume that Λ is at least $\gtrsim 10$ TeV. This means that the cross section related to this diagram is suppressed by an extremely small factor. On the other hand, the same signal coming from the second diagram in fig. 3.2.3 involves only QCD vertices and the first diagram is therefore negligible in comparison. Even the signals coming from loop diagrams as in fig. 3.2.1 are obviously subleading and therefore in first approximation, the phenomenology of the model is dominated by the double resonance signal.

Conclusion and outlook

In this work we presented the Dark Matter problem, focusing in particular on the particle physics perspective. At first we outlined the possible detection methods and we gave a brief analysis of the Dark Matter candidates that has been considered in recent years. We qualitatively and quantitatively discussed the problem of the relic density, i.e. the content of Dark Matter in the Universe. We discussed the possibility of detecting it through indirect detection, measuring excesses of photons or other Standard Model particles coming from the Universe, and through direct detection, with experiments that aim at measuring the recoil of atoms that scatter with an incoming Dark Matter particle. In the end, we focused on the collider searches and the possibility to find Dark Matter through missing energy signals. In fact, since Dark Matter cannot be detected directly (it does not have nor weak, strong and electromagnetic interaction) we need to look for processes in which the transverse momentum is not conserved, because we missed the other particle or particles. We then discussed some of the leading candidate, explaining why the WIMP (Weakly Interacting Massive Particle) has become the leading paradigm and therefore the one we employed during the rest of the work.

Having in mind the problem we are dealing with and the current status of it, we discussed the possible theoretical frameworks we can use in order to produce theoretical models to test with detection experiments, focusing in particular on collider phenomenology. We discussed why, despite their appeal, the complete models are not the best way to face this issue, having a parameter space too rich that can lead to difficulties in understanding the phenomenology. The preference of dealing with a small number of model parameters lead us to study two different frameworks: the effective field theory and the simplified model approach. The EFT allows us to keep a small number of parameters and a model independent approach, a vital virtue if one wants to understand what Dark Matter is without finding a complete UV theory. While it is very effective in dealing with direct and indirect detection because of the low energies involved, it can suffer from an important limitation in collider searches. The energy at LHC can be enough to resolve the contact interaction and even to produce a resonant new particle, which the EFT framework fails to describe. For this reason we presented an intermediate approach, using simplified models. While maintaining some model independence, we can incorporate the effect

of the integrated out particle accounting for a mediator in the interaction between the Standard Model and Dark Matter. While we complicate a bit the models, we gain more theoretical control, yet we continue to ignore the underlying complete model that could stand behind.

We outlined the main criteria one has to employ in order to build a simplified model and then we classified the models depending on the kinematic channel involved in the interaction and the Standard Model particle participating to it. Since the s-channel models had already been deeply studied in the literature, we decided to focus on the t-channel ones, concentrating in particular in the interaction with quarks. We discussed them systematically both from a theoretical and phenomenological point of view. We also implemented them in FeynRules, in order to study their behavior in LHC simulations with the software MadGraph. All the models produced have been validated comparing numerical MadGraph results with analytical computation for different processes. In particular, for each model, we discussed the possible signals at LHC and we produced plots, showing which of these would be dominant in each region of the parameter space. These plots in particular would be helpful for NLO improvements, since we know now which processes are important in each region, so we can compute the corrections of them. In the end, we also briefly presented some simplified models involving interactions with gluons, showing their Lagrangian and discussing some of their different features.

In future works, we want to account for the relic density of Dark Matter in the universe, using this constraint to find the viable parameter space regions of the models. We also plan to complete the study of the collider phenomenology of these models at NLO, using data from the LHC Run 2 at 13 TeV to put additional constraints to the parameter space. We would also like to extend the analysis to the study of the simplified models involving gluons.

Appendix A

Validation of the FeynRules models

A.1   S3-F0-q Model

In this model we have a fermionic Dark Matter χ and a scalar mediator η interacting with quarks. The mediator η has to be colored and charged, so it's a complex scalar field with color index. The mediator is similar to the squarks. In principle we couple the mediator with both right-handed and left-handed quarks. We'll consider both the case in which dm is Dirac and Majorana.

$$\mathcal{L} \supset (D_\mu \eta)^\dagger (D^\mu \eta) + c_R \eta \bar{q}_R \chi + c_L \eta \bar{q}_L \chi + h.c.$$

$$ic \left(\frac{\mathbb{1} \pm \gamma^5}{2} \right)$$
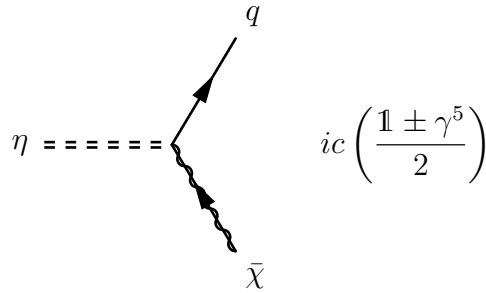
Decay width:

$$\Gamma(\eta \to \bar{\chi}q) = \frac{c^2 \lambda^{\frac{1}{2}}}{16\pi M^3} \left(M^2 - m_\chi^2 - m_q^2 \right)$$

where:

$$\lambda = M^4 + m_\chi^4 + m_q^4 - 2M^2 m_\chi^2 - 2M^2 m_q^2 - 2m_q^2 m_\chi^2$$

is a factor coming from the phase space.

$q\ \bar{q} \to \chi\ \bar{\chi}$ cross section

There is only 1 diagram at leading order, the scattering through t-channel. I consider the quarks massless and compute only the amplitude related to right-handed quarks.
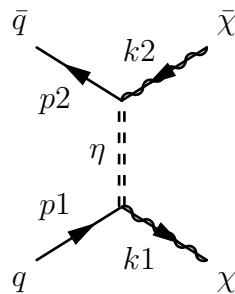
$$\frac{1}{9}\sum_{color}\frac{1}{4}\sum_{polar}|\mathcal{M}| = \frac{c^4\left(\frac{m_\chi^2}{2} - \frac{t}{2}\right)^2}{3\left(t - M^2\right)^2}$$

Agreement of the analytical result with the MadGraph implementation of the model:

```
Phase space point:

--------------------------------------------------------------------------------
n       E               px              py              pz              m
1   0.5000000E+03   0.0000000E+00   0.0000000E+00   0.5000000E+03   0.0000000E+00
2   0.5000000E+03   0.0000000E+00   0.0000000E+00  -0.5000000E+03   0.0000000E+00
3   0.5000000E+03  -0.1592168E+03   0.2071512E+03   0.4261906E+03   0.1000000E+02
4   0.5000000E+03   0.1592168E+03  -0.2071512E+03  -0.4261906E+03   0.1000000E+02
--------------------------------------------------------------------------------
Matrix element =    3.9379373486051568E-004  GeV^            0
My Analytical Result =    3.9379373486051551E-004  GeV^            0
```

$q\,g \to \chi\,\eta$ cross section

There are 2 diagrams at leading order, the scattering through an s-channel quark and the scattering through a t-channel squark.
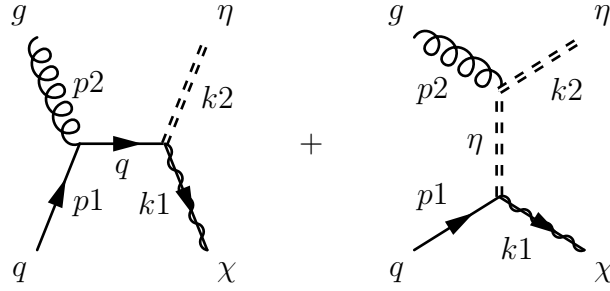
$$\frac{1}{24}\sum_{color}\frac{1}{4}\sum_{polar}|\mathcal{M}| = \frac{c^2 g^2 \left(-2m_\chi^2 M^2 \left(m_\chi^2 + t\right) + M^4 \left(3m_\chi^2 - u\right) + t \left(m_\chi^2(t + 2u) - tu\right)\right)}{12s \left(M^2 - t\right)^2}$$

Agreement of the analytical result with the MadGraph implementation of the model:

```
Phase space point:

-----------------------------------------------------------------------------
n       E              px              py              pz              m
1   0.1010000E+04   0.0000000E+00   0.0000000E+00   0.1010000E+04   0.0000000E+00
2   0.1010000E+04   0.0000000E+00   0.0000000E+00  -0.1010000E+04   0.0000000E+00
3   0.7625000E+03  -0.2428333E+03   0.3159416E+03   0.6500148E+03   0.1000000E+02
4   0.1257500E+04   0.2428333E+03  -0.3159416E+03  -0.6500148E+03   0.1000000E+04
-----------------------------------------------------------------------------
Matrix element =      6.0554414806177438E-002  GeV^              0
My Analytical Result =      6.0554414806177376E-002  GeV^              0
```

$q\,\bar{q} \to \eta\,\eta^*$ cross section

There are 2 diagrams at leading order, the scattering through an s-channel gluon and the scattering through a t-channel DM particle.
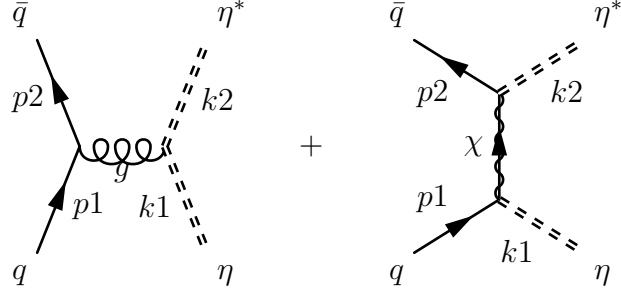
$$\frac{1}{9}\sum_{color}\frac{1}{4}\sum_{polar}|\mathcal{M}| = \frac{(tu - M^4)\left(9c^4s^2 - 16c^2g^2s\left(m_\chi^2 - t\right) + 16g^4\left(m_\chi^2 - t\right)^2\right)}{36s^2\left(m_\chi^2 - t\right)^2}$$

Agreement of the analytical result with the MadGraph implementation of the model:

```
Phase space point:

-------------------------------------------------------------------------
n       E              px              py              pz              m
1    0.2000000E+04   0.0000000E+00   0.0000000E+00   0.2000000E+04   0.0000000E+00
2    0.2000000E+04   0.0000000E+00   0.0000000E+00  -0.2000000E+04   0.0000000E+00
3    0.2000000E+04  -0.5516534E+03   0.7177363E+03   0.1476663E+04   0.1000000E+04
4    0.2000000E+04   0.5516534E+03  -0.7177363E+03  -0.1476663E+04   0.1000000E+04
-------------------------------------------------------------------------
Matrix element =    2.2963529979597550       GeV^            0
My Analytical Result =    2.2963529979597563       GeV^            0
```

$g\ g \to \eta\ \eta^*$ cross section

There are 4 diagrams at leading order, the 4 vertex interaction between 2 gluons and 2 mediator particle, the scattering through an s-channel gluon, the scattering through a t-channel and through the u-channel mediator particle.
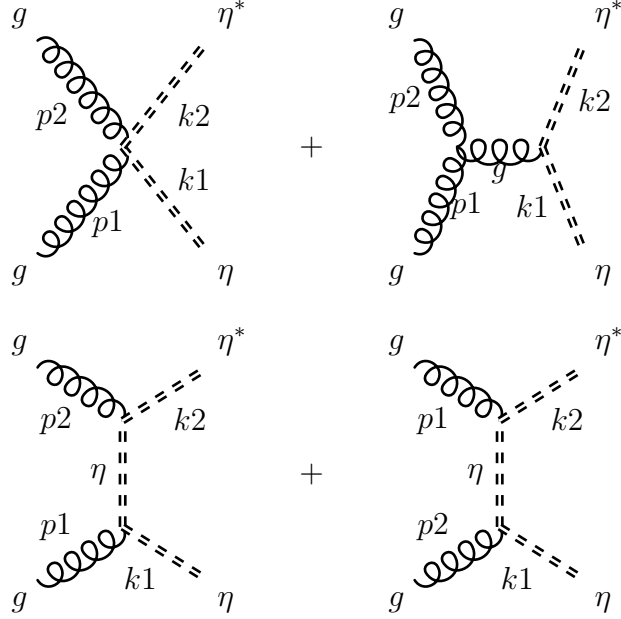
$$\frac{1}{64}\sum_{color}\frac{1}{4}\sum_{polar}|\mathcal{M}| = \frac{g^4}{48s^2\left(M^2-t\right)^2\left(M^2-u\right)^2}\left(5M^8 + M^4\left(t^2+u^2\right)\right.$$

$$\left. - 4M^6(t+u) + t^2u^2\right)\left(9\left(2M^4 - 2M^2(t+u) + t^2+u^2\right) - s^2\right)$$

Agreement of the analytical result with the MadGraph implementation of the model:

```
Phase space point:

-------------------------------------------------------------------------------
n      E               px              py              pz              m
1   0.2000000E+04   0.0000000E+00   0.0000000E+00   0.2000000E+04   0.0000000E+00
2   0.2000000E+04   0.0000000E+00   0.0000000E+00  -0.2000000E+04   0.0000000E+00
3   0.2000000E+04  -0.5516534E+03   0.7177363E+03   0.1476663E+04   0.1000000E+04
4   0.2000000E+04   0.5516534E+03  -0.7177363E+03  -0.1476663E+04   0.1000000E+04
-------------------------------------------------------------------------------
Matrix element =   0.13862765552219608      GeV^            0
My Analytical Result =   0.13862765552219589      GeV^            0
```

$q\ \bar{q} \rightarrow \chi_M\ \bar{\chi}_M$ cross section (Majorana DM)

There are 2 diagrams at leading order, the scattering through t-channel and u-channel.
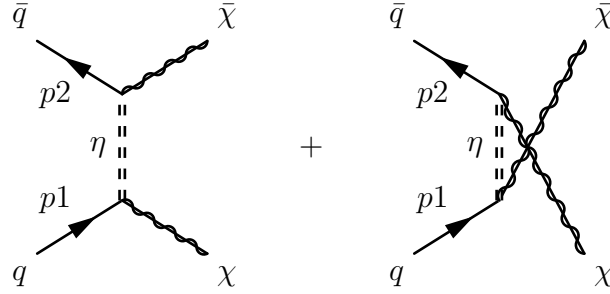
$$\frac{1}{9}\sum_{color}\frac{1}{4}\sum_{polar}|\mathcal{M}| = \frac{1}{24}c^4\left(-\frac{2sm_\chi^2}{(M^2-t)(M^2-u)} + \frac{(m_\chi^2-t)^2}{(M^2-t)^2} + \frac{(m_\chi^2-u)^2}{(M^2-u)^2}\right)$$

Agreement of the analytical result with the MadGraph implementation of the model:

```
Phase space point:

-------------------------------------------------------------------------
n       E               px              py              pz              m
1   0.2000000E+06   0.0000000E+00   0.0000000E+00   0.2000000E+06   0.0000000E+00
2   0.2000000E+06   0.0000000E+00   0.0000000E+00  -0.2000000E+06   0.0000000E+00
3   0.2000000E+06  -0.5516534E+05   0.7177363E+05   0.1476663E+06   0.1000000E+06
4   0.2000000E+06   0.5516534E+05  -0.7177363E+05  -0.1476663E+06   0.1000000E+06
-------------------------------------------------------------------------
Matrix element =    0.10660893348345203       GeV^            0
My Analytical Result =    0.10660893348345198       GeV^            0
```

$q\ q \rightarrow \eta\ \eta$ cross section (Majorana DM)

There are 2 diagrams at leading order, the scattering through a t-channel and the scattering through a a-channel DM Majorana particle.
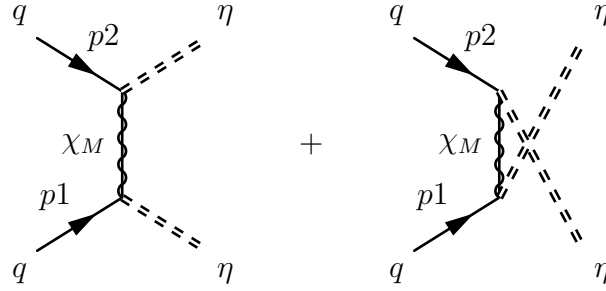
$$\frac{1}{9}\sum_{color}\frac{1}{4}\sum_{polar}|\mathcal{M}| = \frac{c^4 s m_\chi^2\left(-8m_\chi^2(t+u)+8m_\chi^4+3t^2+2tu+3u^2\right)}{24\left(m_\chi^2-t\right)^2\left(m_\chi^2-u\right)^2}$$

Agreement of the analytical result with the MadGraph implementation of the model:

```
Phase space point:

-------------------------------------------------------------------------------
n      E              px             py             pz             m
1   0.2000000E+04  0.0000000E+00  0.0000000E+00  0.2000000E+04  0.0000000E+00
2   0.2000000E+04  0.0000000E+00  0.0000000E+00 -0.2000000E+04  0.0000000E+00
3   0.2000000E+04 -0.5516534E+03  0.7177363E+03  0.1476663E+04  0.1000000E+04
4   0.2000000E+04  0.5516534E+03 -0.7177363E+03 -0.1476663E+04  0.1000000E+04
-------------------------------------------------------------------------------
Matrix element =    5.3258791381600751E-004  GeV^              0
My Analytical Result =    5.3258791381600784E-004  GeV^              0
```

91

A.2 F3-S0-q Model

In this model we have a real scalar Dark Matter χ and a fermionic mediator η interacting with quarks. The mediator η has to be colored and charged. In principle we couple the mediator with both right-handed and left-handed quarks. The mediator of this model is like a 4-th generation quark.

$$\mathcal{L} \supset \bar{\eta}(i\not{D} - M)\eta + c_R \chi \bar{\eta} q_R + c_L \chi \bar{\eta} q_L + h.c.$$

$$ic\left(\frac{\mathbb{1} \pm \gamma^5}{2}\right)$$

Decay width:

$$\Gamma(\eta \to q\chi) = \frac{c^2 \lambda^{\frac{1}{2}}}{32\pi M^3}\left(M^2 + m_q^2 - m_\chi^2\right)$$

$q\,\bar{q} \to \chi\,\chi$ cross section

There are 2 diagram at leading order, the scattering through t-channel and u-channel. I consider the quarks massless and compute only the amplitude related to right-handed quarks.
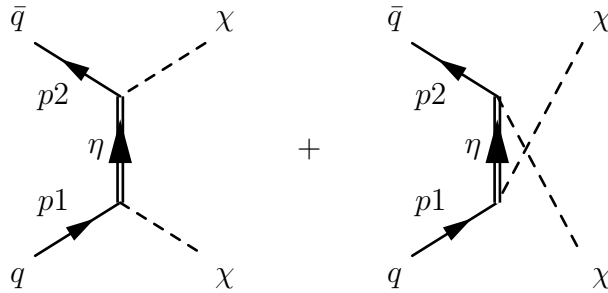
$$\frac{1}{9} \sum_{color} \frac{1}{4} \sum_{polar} |\mathcal{M}| = \frac{c^4 (t-u)^2 \left(tu - m_\chi^4\right)}{24 \left(M^2 - t\right)^2 \left(M^2 - u\right)^2}$$

Agreement of the analytical result with the MadGraph implementation of the model:

```
Phase space point:

----------------------------------------------------------------------
n      E              px              py              pz              m
1   0.5000000E+03   0.0000000E+00   0.0000000E+00   0.5000000E+03   0.0000000E+00
2   0.5000000E+03   0.0000000E+00   0.0000000E+00  -0.5000000E+03   0.0000000E+00
3   0.5000000E+03  -0.1592168E+03   0.2071512E+03   0.4261906E+03   0.1000000E+02
4   0.5000000E+03   0.1592168E+03  -0.2071512E+03  -0.4261906E+03   0.1000000E+02
----------------------------------------------------------------------
Matrix element =    4.8317660208522416E-004  GeV^              0
My Analytical Result =    4.8317660208522330E-004  GeV^              0
```

$q\, g \rightarrow \chi\, \eta$ **cross section**

There are 2 diagrams at leading order, the scattering through an s-channel quark and the scattering through a t-channel mediator.
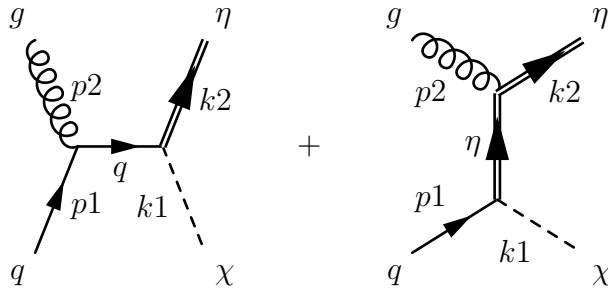
$$\frac{1}{24} \sum_{color} \frac{1}{4} \sum_{polar} |\mathcal{M}| = \frac{c^2 g^2 \left(-2m_\chi^2 M^4 + M^2 \left(-2um_\chi^2 + 3m_\chi^4 + u(2t+u)\right) - t\left(m_\chi^4 + u^2\right)\right)}{12s \left(M^2 - t\right)^2}$$

93

Agreement of the analytical result with the MadGraph implementation of the model:

```
Phase space point:

 -------------------------------------------------------------------------
 n       E              px              py              pz              m
 1   0.1010000E+04   0.0000000E+00   0.0000000E+00   0.1010000E+04   0.0000000E+00
 2   0.1010000E+04   0.0000000E+00   0.0000000E+00  -0.1010000E+04   0.0000000E+00
 3   0.7625000E+03  -0.2428333E+03   0.3159416E+03   0.6500148E+03   0.1000000E+02
 4   0.1257500E+04   0.2428333E+03  -0.3159416E+03  -0.6500148E+03   0.1000000E+04
 -------------------------------------------------------------------------
 Matrix element =    0.22774089706258885        GeV^                   0
 My Analytical Result =    0.22774089706258885        GeV^                   0
```

$q\, q \to \eta\, \eta$ cross section

There are 2 diagrams at leading order, the scattering through a t-channel and the scattering through a a-channel DM particle.
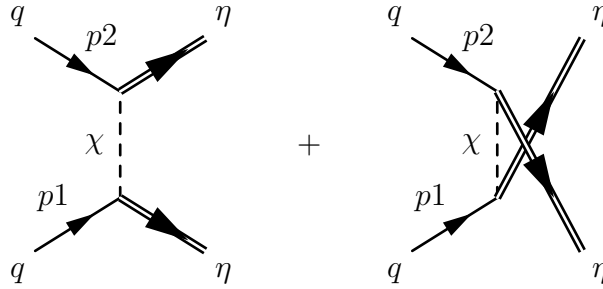
$$\frac{1}{9}\sum_{color}\frac{1}{4}\sum_{polar}|\mathcal{M}| = \frac{c^4}{24\left(m_\chi^2 - t\right)^2\left(m_\chi^2 - u\right)^2}\left(M^4\left(-4m_\chi^2(t+u) + 4m_\chi^4 + 3t^2 - 2tu + 3u^2\right)\right.$$
$$\left. -6M^2\left(m_\chi^4(t+u) - 4tum_\chi^2 + tu(t+u)\right) + m_\chi^4\left(3t^2 + 2tu + 3u^2\right) - 8tum_\chi^2(t+u) + 8t^2u^2\right)$$

Agreement of the analytical result with the MadGraph implementation of the model:

```
Phase space point:

---------------------------------------------------------------------------
n        E            px            py             pz            m
1   0.2000000E+04  0.0000000E+00  0.0000000E+00   0.2000000E+04  0.0000000E+00
2   0.2000000E+04  0.0000000E+00  0.0000000E+00  -0.2000000E+04  0.0000000E+00
3   0.2000000E+04 -0.5516534E+03  0.7177363E+03   0.1476663E+04  0.1000000E+04
4   0.2000000E+04  0.5516534E+03 -0.7177363E+03  -0.1476663E+04  0.1000000E+04
---------------------------------------------------------------------------
Matrix element =   0.68067633713716535       GeV^            0
My Analytical Result =   0.68067633713716535       GeV^            0
```
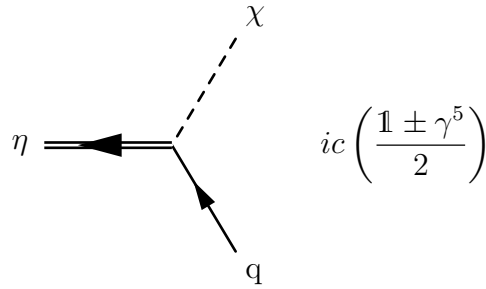
$q\,\bar{q} \to \eta\,\bar{\eta}$ cross section

There are 2 diagrams at leading order, the scattering through an s-channel gluon and the scattering through a t-channel DM particle.
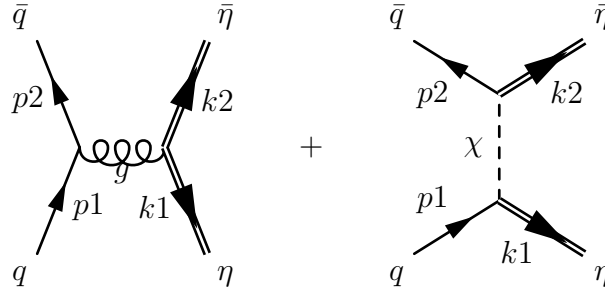
$$\frac{1}{9}\sum_{color}\frac{1}{4}\sum_{polar}|\mathcal{M}| = \frac{1}{36s^2\left(m_\chi^2 - t\right)^2}\left(9c^4s^2\left(M^2 - t\right)^2 - 16c^2g^2s\left(m_\chi^2 - t\right)\left(3M^4 - M^2(3t+u)+t^2\right)+\right.$$

$$\left. 16g^4\left(m_\chi^2 - t\right)^2\left(6M^4 - 4M^2(t+u)+t^2+u^2\right)\right)$$

Agreement of the analytical result with the MadGraph implementation of the model:

```
Phase space point:

--------------------------------------------------------------------------
n       E               px              py              pz              m
1   0.2000000E+04   0.0000000E+00   0.0000000E+00   0.2000000E+04   0.0000000E+00
2   0.2000000E+04   0.0000000E+00   0.0000000E+00  -0.2000000E+04   0.0000000E+00
3   0.2000000E+04  -0.5516534E+03   0.7177363E+03   0.1476663E+04   0.1000000E+04
4   0.2000000E+04   0.5516534E+03  -0.7177363E+03  -0.1476663E+04   0.1000000E+04
--------------------------------------------------------------------------
Matrix element =      1.0289823967555369        GeV^              0
My Analytical Result =      1.0289823967555372        GeV^              0
```

$g\ g \to \eta\ \bar{\eta}$ cross section

There are 3 diagrams at leading order, the scattering through an s-channel gluon, the scattering through a t-channel and through the u-channel mediator particle.

$$\frac{1}{64}\sum_{color}\frac{1}{4}\sum_{polar}|\mathcal{M}| = \frac{g^4\left(7M^4 - 7M^2(t+u) + 4t^2 - tu + 4u^2\right)}{24s^2\left(M^2 - t\right)^2\left(M^2 - u\right)^2}(-6M^8 + M^4\left(3t^2 + 14tu + 3u^2\right) -$$
$$M^2\left(t^3 + 7t^2u + 7tu^2 + u^3\right) + tu\left(t^2 + u^2\right))$$

Agreement of the analytical result with the MadGraph implementation of the model:

```
Phase space point:

--------------------------------------------------------------------------------
n       E               px              py              pz              m
1    0.2000000E+04   0.0000000E+00   0.0000000E+00   0.2000000E+04   0.0000000E+00
2    0.2000000E+04   0.0000000E+00   0.0000000E+00  -0.2000000E+04   0.0000000E+00
3    0.2000000E+04  -0.5516534E+03   0.7177363E+03   0.1476663E+04   0.1000000E+04
4    0.2000000E+04   0.5516534E+03  -0.7177363E+03  -0.1476663E+04   0.1000000E+04
--------------------------------------------------------------------------------
Matrix element =     2.1370983838751267       GeV^            0
My Analytical Result =    2.1370983838751245       GeV^            0
```

A.3   F3-V0-q Model

In this model we have a vector scalar Dark Matter χ and a fermionic mediator η interacting with quarks. The mediator η has to be colored and charged. In principle we couple the mediator with both right-handed and left-handed quarks. The mediator of this model is like a 4th generation quark.

$$\mathcal{L} \supset \bar{\eta}(i\not{D} - M)\eta + c_R \chi_\mu \bar{\eta}\gamma^\mu q_R + c_L \chi_\mu \bar{\eta}\gamma^\mu q_L + h.c.$$

$$ic\gamma^\mu \left(\frac{\mathbb{1} \pm \gamma^5}{2} \right)$$

Decay width:

$$\Gamma(\eta \to q\chi) = \frac{c^2 \lambda^{\frac{1}{2}} \left(M^2 \left(m_\chi^2 - 2m_q^2 \right) + m_q^2 m_\chi^2 + m_q^4 - 2m_\chi^4 + M^4 \right)}{32\pi m_\chi^2 M^3}$$

$q\ \bar{q} \to \chi\ \chi$ cross section

There are 2 diagram at leading order, the scattering through t-channel and u-channel. I consider the quarks massless and compute only the amplitude related to right-handed quarks.
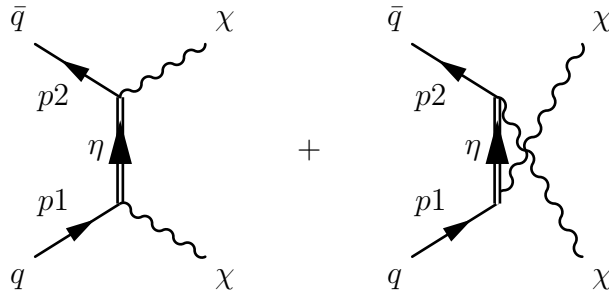
$$\frac{1}{9}\sum_{color}\frac{1}{4}\sum_{polar}|\mathcal{M}| = \frac{c^4}{24m_\chi^4\left(M^2-t\right)^2\left(M^2-u\right)^2}(M^4(m_\chi^4\left(7t^2-6tu+7u^2\right)-$$

$$16m_\chi^6(t+u)-4m_\chi^2(t-u)^2(t+u)+24m_\chi^8+tu(t-u)^2)-8m_\chi^4M^2(t+u)\left(-2m_\chi^2(t+u)+3m_\chi^4+tu\right)$$

$$-4m_\chi^4\left(m_\chi^4\left(t^2-8tu+u^2\right)+4tum_\chi^2(t+u)-tu\left(t^2+u^2\right)\right))$$

Agreement of the analytical result with the MadGraph implementation of the model:

```
Phase space point:

--------------------------------------------------------------------------
n       E            px              py              pz              m
1   0.5000000E+03  0.0000000E+00   0.0000000E+00   0.5000000E+03   0.0000000E+00
2   0.5000000E+03  0.0000000E+00   0.0000000E+00  -0.5000000E+03   0.0000000E+00
3   0.5000000E+03 -0.1592168E+03   0.2071512E+03   0.4261906E+03   0.1000000E+02
4   0.5000000E+03  0.1592168E+03  -0.2071512E+03  -0.4261906E+03   0.1000000E+02
--------------------------------------------------------------------------
Matrix element =     48600.805526734359      GeV^              0
My Analytical Result =     48600.805526734286      GeV^              0
```
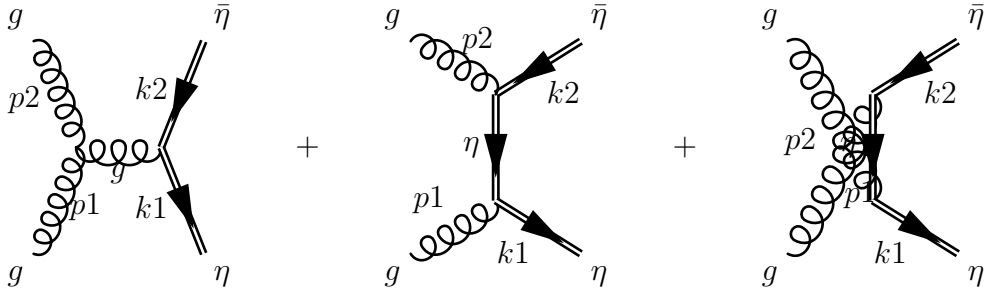
$q\,g \to \chi\,\eta$ cross section

There are 2 diagrams at leading order, the scattering through an s-channel quark and the scattering through a t-channel mediator.
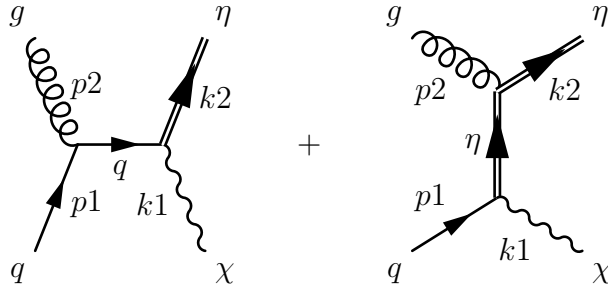
$$\frac{1}{24}\sum_{color}\frac{1}{4}\sum_{polar}|\mathcal{M}| = \frac{c^2 g^2}{12 s m_\chi^2 \left(M^2 - t\right)^2}(2m_\chi^2 M^6 + M^2(2m_\chi^2 \left(6t^2 + 6tu + u^2\right) -$$
$$m_\chi^4(9t + 4u) + 6m_\chi^6 - tu^2) + M^4 \left(-6m_\chi^2(2t + u) + 3m_\chi^4 + u(2t + u)\right) -$$
$$2tm_\chi^2 \left(-2tm_\chi^2 + m_\chi^4 + 2t^2 + 2tu + u^2\right))$$

Agreement of the analytical result with the MadGraph implementation of the model:

```
Phase space point:

-------------------------------------------------------------------------
n       E              px              py              pz              m
1   0.1010000E+04   0.0000000E+00   0.0000000E+00   0.1010000E+04   0.0000000E+00
2   0.1010000E+04   0.0000000E+00   0.0000000E+00  -0.1010000E+04   0.0000000E+00
3   0.7625000E+03  -0.2428333E+03   0.3159416E+03   0.6500148E+03   0.1000000E+02
4   0.1257500E+04   0.2428333E+03  -0.3159416E+03  -0.6500148E+03   0.1000000E+04
-------------------------------------------------------------------------
Matrix element =     2278.3604051802622      GeV^             0
My Analytical Result =    2278.3604051802604      GeV^             0
```
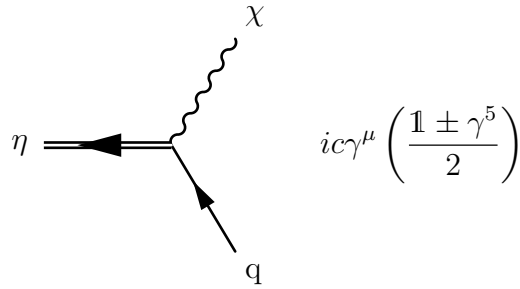
$q\,q \rightarrow \eta\,\eta$ cross section

There are 2 diagrams at leading order, the scattering through a t-channel and the scattering through a a-channel DM particle.
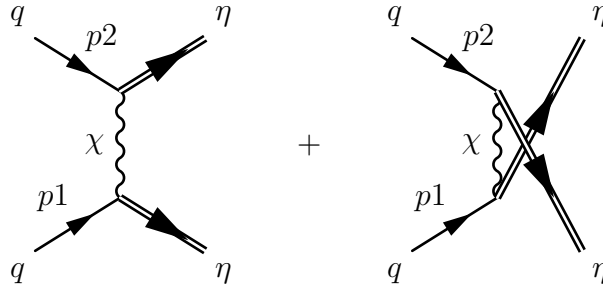
$$\frac{1}{9}\sum_{color}\frac{1}{4}\sum_{polar}|\mathcal{M}| = \frac{c^4}{24m_\chi^4\left(m_\chi^2 - t\right)^2\left(m_\chi^2 - u\right)^2}$$
$$\left(M^4\left(m_\chi^4\left(179s^2 + 68su + 4u^2\right) + 160sm_\chi^6 - 4m_\chi^2\left(3t^3 + 7t^2u + 7tu^2 + 3u^3\right) + 8t^2u^2\right) - \right.$$
$$8sm_\chi^4 M_\eta^2\left(16sm_\chi^2 + 9s^2 + 8su + 4u^2\right) - $$
$$2M^6(m_\chi^4(83s + 4u) - 4m_\chi^2\left(3t^2 + 5tu + 3u^2\right) + 3tu(t + u)) + $$
$$M^8\left(-4m_\chi^2(t + u) + 4m_\chi^4 + 3t^2 - 2tu + 3u^2\right) - $$
$$\left.4sm_\chi^4\left(-8s^2m_\chi^2 + 8m_\chi^4(t + u) - s\left(3s^2 + 4su + 4u^2\right)\right)\right)$$

Agreement of the analytical result with the MadGraph implementation of the model:

```
Phase space point:
```

```
--------------------------------------------------------------------------
n       E              px              py              pz              m
1   0.2000000E+04  0.0000000E+00   0.0000000E+00   0.2000000E+04   0.0000000E+00
2   0.2000000E+04  0.0000000E+00   0.0000000E+00  -0.2000000E+04   0.0000000E+00
3   0.2000000E+04 -0.5516534E+03   0.7177363E+03   0.1476663E+04   0.1000000E+04
4   0.2000000E+04  0.5516534E+03  -0.7177363E+03  -0.1476663E+04   0.1000000E+04
--------------------------------------------------------------------------
Matrix element =    68138902.982058331      GeV^              0
My Analytical Result =    68138902.982058257      GeV^              0
```

$q\,\bar{q} \to \eta\,\bar{\eta}$ cross section

There are 2 diagrams at leading order, the scattering through an s-channel gluon and the scattering through a t-channel DM particle.
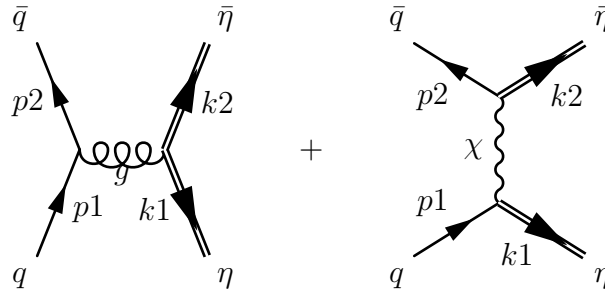
$$\frac{1}{9}\sum_{color}\frac{1}{4}\sum_{polar}|\mathcal{M}| = \frac{1}{36s^2m_\chi^4\left(m_\chi^2-t\right)^2}$$
$$\left(9c^4s^2\left(M^4\left(4sm_\chi^2+4m_\chi^4+t^2\right)-8um_\chi^4M^2+4u^2m_\chi^4+M^8-2tM^6\right)-\right.$$
$$16c^2g^2sm_\chi^2\left(m_\chi^2-t\right)\left(M^2\left(t^2-2m_\chi^2(t+3u)\right)+M^4\left(6m_\chi^2-3t-u\right)+2u^2m_\chi^2+3M^6\right)+$$
$$\left.16g^4m_\chi^4\left(m_\chi^2-t\right)^2\left(6M^4-4M^2(t+u)+t^2+u^2\right)\right)$$

Agreement of the analytical result with the MadGraph implementation of the model:

```
Phase space point:

-----------------------------------------------------------------------
n       E              px              py              pz              m
1   0.2000000E+04  0.0000000E+00  0.0000000E+00  0.2000000E+04  0.0000000E+00
2   0.2000000E+04  0.0000000E+00  0.0000000E+00 -0.2000000E+04  0.0000000E+00
3   0.2000000E+04 -0.5516534E+03  0.7177363E+03  0.1476663E+04  0.1000000E+04
4   0.2000000E+04  0.5516534E+03 -0.7177363E+03 -0.1476663E+04  0.1000000E+04
-----------------------------------------------------------------------
Matrix element =     91753874.555083826      GeV^              0
My Analytical Result =    91753874.555083677      GeV^              0
```

$g\,g \to \eta\,\bar{\eta}$ cross section

There are 3 diagrams at leading order, the scattering through an s-channel gluon, the scattering through a t-channel and through the u-channel mediator particle.

$$\frac{1}{64}\sum_{color}\frac{1}{4}\sum_{polar}|\mathcal{M}| = \frac{g^4\left(7M^4 - 7M^2(t+u) + 4t^2 - tu + 4u^2\right)}{24s^2\left(M^2 - t\right)^2\left(M^2 - u\right)^2}\left(-6M^8 + M^4\left(3t^2 + 14tu + 3u^2\right) - \right.$$

$$\left. M^2\left(t^3 + 7t^2u + 7tu^2 + u^3\right) + tu\left(t^2 + u^2\right)\right)$$

Agreement of the analytical result with the MadGraph implementation of the model:

```
Phase space point:

-------------------------------------------------------------------------
n        E              px              py              pz              m
1   0.2000000E+04  0.0000000E+00   0.0000000E+00   0.2000000E+04   0.0000000E+00
2   0.2000000E+04  0.0000000E+00   0.0000000E+00  -0.2000000E+04   0.0000000E+00
3   0.2000000E+04 -0.5516534E+03   0.7177363E+03   0.1476663E+04   0.1000000E+04
4   0.2000000E+04  0.5516534E+03  -0.7177363E+03  -0.1476663E+04   0.1000000E+04
-------------------------------------------------------------------------
Matrix element =    2.1370983838751267       GeV^              0
My Analytical Result =    2.1370983838751245       GeV^              0
```

A.4 V3-F0-q Model

In this model we have a fermionic Dark Matter χ and a complex vector mediator V interacting with quarks. The mediator η has to be colored, and charged. In principle we couple the mediator with both right-handed and left-handed quarks. The mediator of this model is like a Leptoquark of the SU(5) GUT.

$$\mathcal{L} \supset -\frac{1}{2}V_{\mu\nu}^\dagger V^{\mu\nu} - ig(1-k)V^{\dagger\mu}t_F^a V^\nu G_{\mu\nu a} + c_R V_\mu \bar{q}_R \gamma^\mu \chi + c_L V_\mu \bar{q}_L \gamma^\mu \chi + h.c.$$

With $V^{\mu\nu} = D_\mu V_\nu - D_\nu V_\mu$, the covariant derivative being $D_\mu = \partial_\mu - igt_F^a A_\mu^a$ and $G_{\mu\nu a}$ the gluon field strenght. k represent the anomalous chromomagnetic coupling. If $k = 0$ we are in the case "Yang-Mills", i.e. the Vector field is a gauge field that gain mass through a Simmetry Breaking mechanism. If $k = 1$ we are in the case of Minimal Coupling. We'll consider both these scenarios.
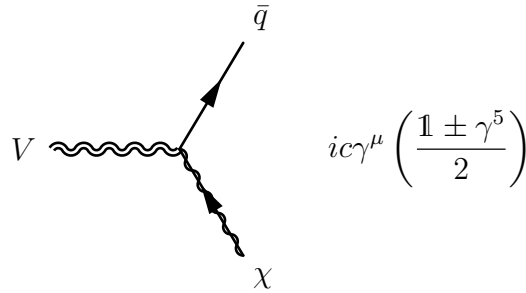
Decay width:

$$\Gamma(V \to q\bar{\chi}) = \frac{c^2 \lambda^{\frac{1}{2}}}{24\pi M^3}\left(M^2 - \frac{m_q^2}{2} - \frac{m_\chi^2}{2} - \frac{1}{2M^2}\left(m_q^2 - m_\chi^2\right)^2\right)$$

$q\,\bar{q} \to \chi\,\bar{\chi}$ cross section

There is only 1 diagram at leading order, the scattering through t-channel. I consider the quarks massless and compute only the amplitude related to right-handed quarks.
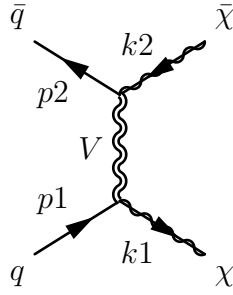
$$\frac{1}{9}\sum_{color}\frac{1}{4}\sum_{polar}|\mathcal{M}| = \frac{c^4\left(4sm_\chi^4 M^2 + 4M^4\left(m_\chi^2 - u\right)^2 + m_\chi^4\left(m_\chi^2 - t\right)^2\right)}{12M^4\left(M^2 - t\right)^2}$$

Agreement of the analytical result with the MadGraph implementation of the model:

```
Phase space point:

--------------------------------------------------------------------------------
n       E               px              py              pz              m
1   0.5000000E+03  0.0000000E+00   0.0000000E+00   0.5000000E+03   0.0000000E+00
2   0.5000000E+03  0.0000000E+00   0.0000000E+00  -0.5000000E+03   0.0000000E+00
3   0.5000000E+03 -0.1592168E+03   0.2071512E+03   0.4261906E+03   0.1000000E+02
4   0.5000000E+03  0.1592168E+03  -0.2071512E+03  -0.4261906E+03   0.1000000E+02
--------------------------------------------------------------------------------
Matrix element =   0.24803098873266002      GeV^            0
My Analytical Result =   0.24803098873266000      GeV^            0
```
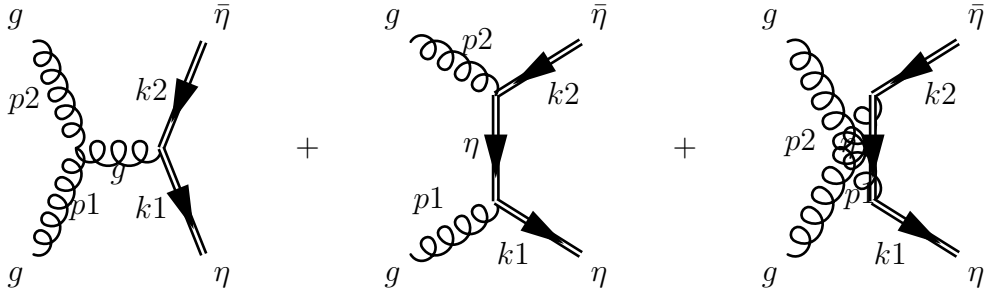
$q\,g \to \chi\,V$ cross section

There are 2 diagrams at leading order, the scattering through an s-channel quark and the scattering through a t-channel mediator.

105

Yang-Mills case:

$$\frac{1}{24}\sum_{color}\frac{1}{4}\sum_{polar}|\mathcal{M}| = \frac{c^2g^2}{12s\,(M^3-tM)^{\,2}}(2M^2(m_\chi^2\left(t^2+6tu+6u^2\right)-3m_\chi^4(t+2u)+m_\chi^6-$$
$$u\left(t^2+2tu+2u^2\right))+M^4\left(-m_\chi^2(4t+9u)+3m_\chi^4+4u^2\right)+M^6\left(6m_\chi^2-2u\right)+tm_\chi^2\left(m_\chi^2(t+2u)-tu\right))$$

Agreement of the analytical result with the MadGraph implementation of the model:

```
Phase space point:

--------------------------------------------------------------------------
n        E              px             py             pz             m
1    0.1010000E+04   0.0000000E+00   0.0000000E+00   0.1010000E+04   0.0000000E+00
2    0.1010000E+04   0.0000000E+00   0.0000000E+00  -0.1010000E+04   0.0000000E+00
3    0.7625000E+03  -0.2428333E+03   0.3159416E+03   0.6500148E+03   0.1000000E+02
4    0.1257500E+04   0.2428333E+03  -0.3159416E+03  -0.6500148E+03   0.1000000E+04
--------------------------------------------------------------------------
Matrix element =    2.8024730629307655        GeV^              0
My Analytical Result =    2.8024730629307628        GeV^              0
```

Minimal Coupling case:

$$\frac{1}{24}\sum_{color}\frac{1}{4}\sum_{polar}|\mathcal{M}| = \frac{c^2g^2}{48sM^4\,(M^2-t)^{\,2}}(M^4(m_\chi^2\left(-8s^2+s(6u-13t)+8\left(t^2+6tu+6u^2\right)\right)-$$
$$m_\chi^4(s+24(t+2u))+8m_\chi^6+2\left(4s^2u+s\left(t^2+3tu-2u^2\right)-4u\left(t^2+2tu+2u^2\right)\right))+$$
$$M^2\left(m_\chi^4\left(8s^2-6st+4t(t+2u)\right)+m_\chi^2\left(-8s^3-8s^2u+st(7t+6u)-4t^2u\right)-st\left(t^2+2tu+2u^2\right)\right)+$$
$$M^6\left(m_\chi^2(7s-4(4t+9u))+12m_\chi^4-s(t+4u)+16u^2\right)+8M^8\left(3m_\chi^2-u\right)+st^2m_\chi^2\left(m_\chi^2-t\right))$$

Agreement of the analytical result with the MadGraph implementation of the model:

```
Phase space point:

--------------------------------------------------------------------------
n        E              px             py             pz             m
1    0.1010000E+04   0.0000000E+00   0.0000000E+00   0.1010000E+04   0.0000000E+00
```
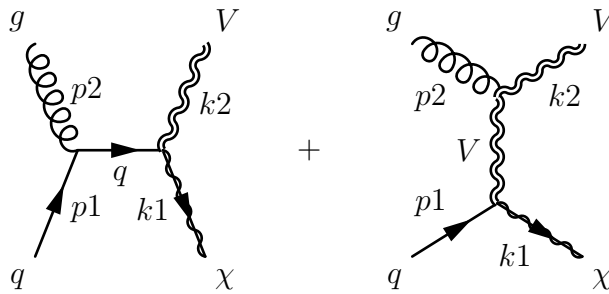
```
2   0.1010000E+04   0.0000000E+00   0.0000000E+00  -0.1010000E+04   0.0000000E+00
3   0.7625000E+03  -0.2428333E+03   0.3159416E+03   0.6500148E+03   0.1000000E+02
4   0.1257500E+04   0.2428333E+03  -0.3159416E+03  -0.6500148E+03   0.1000000E+04
--------------------------------------------------------------------------
Matrix element =   0.61900380168922153       GeV^              0
My Analytical Result =   0.61900380168922087       GeV^              0
```

$q\ \bar{q} \to V\ V^*$ cross section

There are 2 diagrams at leading order, the scattering through an s-channel gluon and
the scattering through a t-channel DM particle.
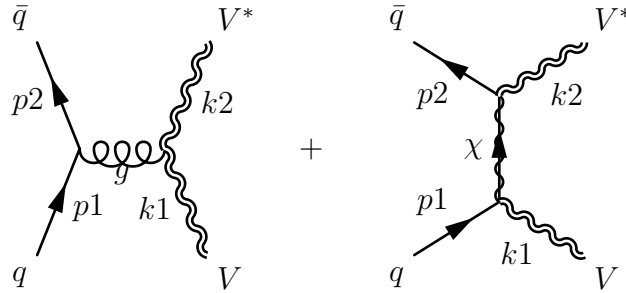
Yang-Mills case:

$$
\frac{1}{9}\sum_{color}\frac{1}{4}\sum_{polar}|\mathcal{M}| = \frac{1}{36 s^2 M^4 \left(m_\chi^2 - t\right)^2}\left(-9 c^4 s^2 \left(4 M^8 + 4 t^2 M^2(t+u) - t M^4 (7t+4u) - t^3 u\right)+\right.
$$
$$
8 c^2 g^2 s \left(m_\chi^2 - t\right)\left(4 M^8 + 2 t M^2\left(2 s^2 + 2 s t + t^2\right) + M^6(8 s - 6 t) - 5 s t M^4 - s t^2(s+t)\right) -
$$
$$
4 g^4 \left(m_\chi^2 - t\right)^2 (12 M^8 + M^4 \left(17 s^2 + 20 s u + 12 u^2\right) - 2 s M^2\left(2 s^2 + 3 s u + 2 u^2\right) -
$$
$$
4 M^6 (s + 6 u) + s^2 u(s+u)))
$$

Agreement of the analytical result with the MadGraph implementation of the model:

```
Phase space point:

--------------------------------------------------------------------------
```

```
n        E              px             py             pz              m
1    0.2000000E+04  0.0000000E+00  0.0000000E+00  0.2000000E+04  0.0000000E+00
2    0.2000000E+04  0.0000000E+00  0.0000000E+00 -0.2000000E+04  0.0000000E+00
3    0.2000000E+04 -0.5516534E+03  0.7177363E+03  0.1476663E+04  0.1000000E+04
4    0.2000000E+04  0.5516534E+03 -0.7177363E+03 -0.1476663E+04  0.1000000E+04
----------------------------------------------------------------------
Matrix element =    23.738073361946711      GeV^              0
My Analytical Result =    23.738073361946718      GeV^              0
```

Minimal Coupling case:

$$\frac{1}{9}\sum_{color}\frac{1}{4}\sum_{polar}|\mathcal{M}| = \frac{1}{36s^2M^4\left(m_\chi^2 - t\right)^2}(-9c^4s^2\left(4M^8 + 4t^2M^2(t + u) - tM^4(7t + 4u) - t^3u\right) +$$

$$8c^2g^2s\left(m_\chi^2 - t\right)\left(4M^8 + 2tM^2\left(2s^2 + s(3t + u) + t^2\right) + M^6(4s - 6t) - 4stM^4 - st^2(s + t + u)\right) -$$

$$4g^4\left(m_\chi^2 - t\right)^2(12M_V^8 + M^4\left(17s^2 + s(t + 21u) + 12u^2\right) - sM^2\left(4s^2 + 6su - 3(t + u)^2 + 4u^2\right) -$$

$$8M^6(2s + 3u) + su(s - t)(s + t + u)))$$

Agreement of the analytical result with the MadGraph implementation of the model:

```
Phase space point:

----------------------------------------------------------------------
n        E              px             py             pz              m
1    0.2000000E+04  0.0000000E+00  0.0000000E+00  0.2000000E+04  0.0000000E+00
2    0.2000000E+04  0.0000000E+00  0.0000000E+00 -0.2000000E+04  0.0000000E+00
3    0.2000000E+04 -0.5516534E+03  0.7177363E+03  0.1476663E+04  0.1000000E+04
4    0.2000000E+04  0.5516534E+03 -0.7177363E+03 -0.1476663E+04  0.1000000E+04
----------------------------------------------------------------------
Matrix element =    24.443435951651487      GeV^              0
My Analytical Result =    24.443435951651491      GeV^              0
```

$g\ g \to V\ V^*$ **cross section**

There are 4 diagrams at leading order, the 4 vertex interaction between 2 gluons and 2 mediator particle, the scattering through an s-channel gluon, the scattering through a t-channel and through the u-channel mediator particle.
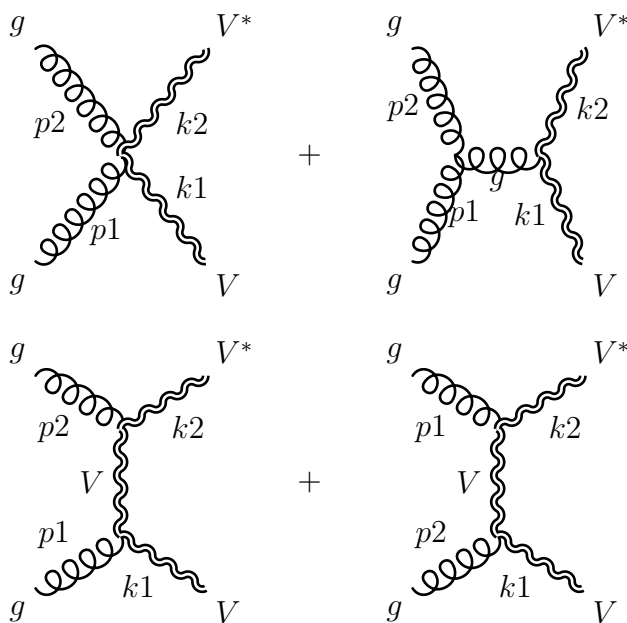
Yang-Mills case:

$$\frac{1}{64}\sum_{color}\frac{1}{4}\sum_{polar}|\mathcal{M}| = \frac{g^4}{24s^2\,(M^2-t)^2\,(M^2-u)^2}\big(3M^8+M^4\left(7s^2+6su+18u^2\right)-4M^2(s^3+2s^2u+$$

$$3su^2+3u^3)-12uM^6+2s^4+4s^3u+7s^2u^2+6su^3+3u^4\big)\left(7M^4-7M^2(t+u)+4t^2-tu+4u^2\right)$$

Agreement of the analytical result with the MadGraph implementation of the model:

```
Phase space point:

--------------------------------------------------------------------------
n      E              px             py             pz             m
1   0.2000000E+04  0.0000000E+00  0.0000000E+00  0.2000000E+04  0.0000000E+00
2   0.2000000E+04  0.0000000E+00  0.0000000E+00 -0.2000000E+04  0.0000000E+00
```

```
3   0.2000000E+04 -0.5516534E+03  0.7177363E+03  0.1476663E+04  0.1000000E+04
4   0.2000000E+04  0.5516534E+03 -0.7177363E+03 -0.1476663E+04  0.1000000E+04
------------------------------------------------------------------------
Matrix element =    33.221081987480673      GeV^           0
My Analytical Result =    33.221081987480652      GeV^           0
```

Minimal Coupling case:

$$\frac{1}{64}\sum_{color}\frac{1}{4}\sum_{polar}|\mathcal{M}| = \frac{g^4}{1536s^2M^4\left(M^2-t\right)^2\left(M^2-u\right)^2}(1344M^{16}+2M^{12}(1417s^2+1344su+$$

$$96\left(4t^2+27tu+74u^2\right)s)-s^2tuM^2\left(2s\left(81t^2+134tu+81u^2\right)+229t^3+593t^2u+593tu^2+229u^3\right)-$$

$$2M^{10}\left(1324s^3+s^2(1515t+3307u)+1344su(t+3u)+192u\left(8t^2+19tu+43u^2\right)\right)+$$

$$M^8(896s^4+8s^3(411t+635u)+s^2\left(1447t^2+6160tu+8167u^2\right)+384su\left(4t^2+13tu+25u^2\right)+$$

$$192u^2\left(24t^2+22tu+59u^2\right))-M^6(896s^4(t+u)+s^3\left(2054t^2+3372tu+3846u^2\right)+$$

$$s^2\left(-359t^3+5115t^2u+5691tu^2+4825u^3\right)+384su^2\left(8t^2+5tu+15u^2\right)+192u^3\left(16t^2+3tu+23u^2\right))+$$

$$2M^4(64s^4\left(4t^2-tu+4u^2\right)+s^3\left(131t^3+955t^2u+315tu^2+643u^3\right)+$$

$$s^2\left(-97t^4+835t^3u+1747t^2u^2+611tu^3+799u^4\right)+192su^3\left(4t^2-tu+4u^2\right)+96u^4\left(4t^2-tu+4u^2\right))-$$

$$1344M^{14}(t+5u)+s^2t^2u^2\left(28s(t+u)+47t^2+68tu+47u^2\right))$$

Agreement of the analytical result with the MadGraph implementation of the model:

```
Phase space point:

------------------------------------------------------------------------
n      E            px            py            pz            m
1   0.2000000E+04  0.0000000E+00  0.0000000E+00  0.2000000E+04  0.0000000E+00
2   0.2000000E+04  0.0000000E+00  0.0000000E+00 -0.2000000E+04  0.0000000E+00
3   0.2000000E+04 -0.5516534E+03  0.7177363E+03  0.1476663E+04  0.1000000E+04
4   0.2000000E+04  0.5516534E+03 -0.7177363E+03 -0.1476663E+04  0.1000000E+04
------------------------------------------------------------------------
Matrix element =    8.5715676248823822      GeV^           0
My Analytical Result =    8.5715676248823680      GeV^           0
```

$q \bar{q} \to \chi_M \bar{\chi}_M$ **cross section (Majorana DM)**

There are 2 diagrams at leading order, the scattering through t-channel and u-channel.
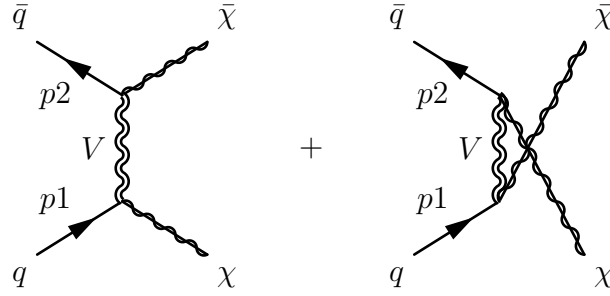
$$\frac{1}{9} \sum_{color} \frac{1}{4} \sum_{polar} |\mathcal{M}| = \frac{c^4}{24 M_V^4 \left(M^2 - t\right)^2 \left(M^2 - u\right)^2} (4M^8 \left(-2m_\chi^4 + t^2 + u^2\right) +$$

$2m_\chi^2 M^2 \left(m_\chi^4 \left(3t^2 - 2tu + 3u^2\right) + m_\chi^2 \left(-2t^3 + t^2 u + tu^2 - 2u^3\right) + m_\chi^6(t + u) - 2tu \left(t^2 + u^2\right)\right) +$
$4M^6 \left(m_\chi^2 \left(t^2 - 4tu + u^2\right) + 2m_\chi^4(t + u) + 2m_\chi^6 - 2 \left(t^3 + u^3\right)\right) + M^4 (m_\chi^4 \left(5t^2 - 16tu + 5u^2\right) -$
$4m_\chi^2 \left(t^3 - 3t^2 u - 3tu^2 + u^3\right) - 8m_\chi^6(t+u) - 2m_\chi^8 + 4 \left(t^4 + u^4\right)) + m_\chi^8 \left(t^2 - 4tu + u^2\right) + 2t^2 u^2 m_\chi^4)$

Agreement of the analytical result with the MadGraph implementation of the model:

```
Phase space point:
```

```
---------------------------------------------------------------------------
n       E              px              py              pz              m
1   0.2000000E+06  0.0000000E+00  0.0000000E+00  0.2000000E+06  0.0000000E+00
2   0.2000000E+06  0.0000000E+00  0.0000000E+00 -0.2000000E+06  0.0000000E+00
3   0.2000000E+06 -0.5516534E+05  0.7177363E+05  0.1476663E+06  0.1000000E+06
4   0.2000000E+06  0.5516534E+05 -0.7177363E+05 -0.1476663E+06  0.1000000E+06
---------------------------------------------------------------------------
Matrix element =     10660026.873484505      GeV^            0
My Analytical Result =    10660026.873484492      GeV^            0
```
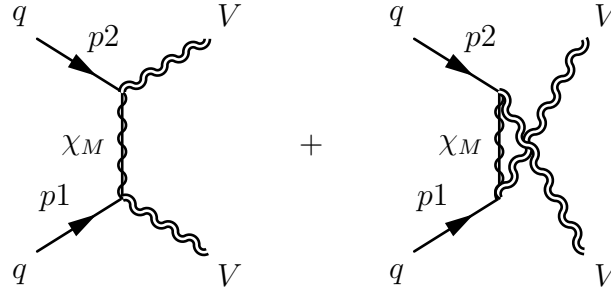
$q \; q \to V \; V$ cross section (Majorana DM)

There are 2 diagrams at leading order, the scattering through a t-channel and the scattering through a a-channel DM Majorana particle.

$$\frac{1}{9}\sum_{color}\frac{1}{4}\sum_{polar}|\mathcal{M}| = -\frac{c^4 m_\chi^2}{24M^4\left(m_\chi^2 - t\right)^2\left(m_\chi^2 - u\right)^2}(4M^2(m_\chi^4\left(3s^2 + 6su + 4u^2\right)+8tum_\chi^2(t+u)-$$

$$tu\left(3t^2 + 2tu + 3u^2\right)) - 4M^4\left(m_\chi^4(9s + 8u) + 6m_\chi^2(t+u)^2 - 3\left(t^3 + t^2u + tu^2 + u^3\right)\right) +$$

$$4M^6\left(8m_\chi^2(t+u) + 4m_\chi^4 - 3t^2 - 2tu - 3u^2\right) - sm_\chi^4\left(3s^2 + 4su + 4u^2\right) - 8tum_\chi^2(t+u)^2 + 8t^2u^2(t+u))$$

Agreement of the analytical result with the MadGraph implementation of the model:

```
Phase space point:

    -----------------------------------------------------------------------------
    n       E              px              py              pz              m
    1   0.2000000E+04  0.0000000E+00  0.0000000E+00  0.2000000E+04  0.0000000E+00
    2   0.2000000E+04  0.0000000E+00  0.0000000E+00 -0.2000000E+04  0.0000000E+00
    3   0.2000000E+04 -0.5516534E+03  0.7177363E+03  0.1476663E+04  0.1000000E+04
    4   0.2000000E+04  0.5516534E+03 -0.7177363E+03 -0.1476663E+04  0.1000000E+04
    -----------------------------------------------------------------------------
    Matrix element =    3.7819064956393422E-002  GeV^            0
    My Analytical Result =    3.7819064956393422E-002  GeV^            0
```

112

Ringraziamenti

Vorrei concludere questo lavoro ringraziando tutte le persone che mi hanno aiutato, in un modo o nell'altro, durante il percorso di studi e nella preparazione della tesi.

Prima di tutto voglio ringraziare il Prof. Roberto Soldati e il Prof. Fabio Maltoni per avermi guidato nello studio di questo argomento e avermi aiutato a diventare uno studente migliore.

Inoltre voglio ringraziare tutte le persone che mi hanno sostenuto e dato consigli durante la mia permanenza in Belgio, con menzione particolare per Ambresh che si è trattenuto a volte fino a tardi in ufficio solo per aiutarmi a risolvere dei problemi. Un grazie anche a Kentarou, per l'aiuto e la disponibilità dimostrata.

Il grazie più importante va ai miei compagni di studio, con la quale ho condiviso prima la triennale e poi la magistrale, tra risate e momenti di isteria collettiva. Ringrazio Luca, incredibile fonte di conoscenza, Matteo, la miglior persona che conosca con cui condividere il disagio, e Onofrio per le interminabili discussioni su tutto lo scibile umano. Ringrazio Mauri per esserci rimasto vicino anche quando ha cambiato Università e Riccardo, compagno di studi e insostituibile Chef in terra straniera. A voi tutti, il mio grazie più sentito.

Un grazie anche a Deborah, alla quale questo lavoro è dedicato, per essermi stata accanto in ogni momento. Abbiamo condiviso difficoltá e successi insieme, non so come avrei fatto senza di te.

Infine voglio ringraziare i miei genitori, senza i quali nulla di ciò che ho realizzato sarebbe stato possibile.

Bibliography

[1] Gianfranco Bertone and Dan Hooper. A History of Dark Matter. *Submitted to: Rev. Mod. Phys.*, 2016.

[2] M. Schwarzschild. *AJ*, 59:273, 1954.

[3] D. H. Rogstad and G. S. Shostak. *Astrophys. J.*, 176:315, 1972.

[4] M. Whittle. *Graduate extragalactic astronomy, lecture notes*, 2016.

[5] Michael Klasen, Martin Pohl, and Gunter Sigl. Indirect and direct search for dark matter. *Prog. Part. Nucl. Phys.*, 85:1–32, 2015.

[6] F. Aharonian et al. H.E.S.S. observations of the Galactic Center region and their possible dark matter interpretation. *Phys. Rev. Lett.*, 97:221102, 2006. [Erratum: Phys. Rev. Lett.97,249901(2006)].

[7] Pierre Jean et al. Early SPI / INTEGRAL measurements of 511 keV line emission from the 4th quadrant of the Galaxy. *Astron. Astrophys.*, 407:L55, 2003.

[8] Francesca Calore, Ilias Cholis, and Christoph Weniger. Background Model Systematics for the Fermi GeV Excess. *JCAP*, 1503:038, 2015.

[9] J. L. Feng et al. Planning the Future of U.S. Particle Physics (Snowmass 2013): Chapter 4: Cosmic Frontier. In *Proceedings, Community Summer Study 2013: Snowmass on the Mississippi (CSS2013): Minneapolis, MN, USA, July 29-August 6, 2013*, 2014.

[10] E. Aprile et al. Limits on spin-dependent wimp-nucleon cross sections from 225 live days of xenon100 data. *Phys. Rev. Lett.*, 111:021301, Jul 2013.

[11] Giorgio Busoni. *Dark Matter Indirect Detection and Collider Search: the Good and the Bad*. PhD thesis, SISSA, Trieste, 2015.

[12] K. A. Olive et al. Review of Particle Physics. *Chin. Phys.*, C38:090001, 2014.

[13] Jonathan L. Feng. Dark Matter Candidates from Particle Physics and Methods of Detection. *Ann. Rev. Astron. Astrophys.*, 48:495–545, 2010.

[14] Takehiko Asaka and Mikhail Shaposhnikov. The nuMSM, dark matter and baryon asymmetry of the universe. *Phys. Lett.*, B620:17–26, 2005.

[15] Jalal Abdallah et al. Simplified Models for Dark Matter Searches at the LHC. *Phys. Dark Univ.*, 9-10:8–23, 2015.

[16] Nima Arkani-Hamed, Gordon L. Kane, Jesse Thaler, and Lian-Tao Wang. Supersymmetry and the LHC inverse problem. *JHEP*, 08:070, 2006.

[17] Ben Gripaios. Lectures on Effective Field Theory. 2015.

[18] A. V. Manohar. Effective field theories. *Lect. Notes Phys.*, 479:311–362, 1997.

[19] Andrea De Simone and Thomas Jacques. Simplified models vs. effective field theory approaches in dark matter searches. *Eur. Phys. J.*, C76(7):367, 2016.

[20] Jalal Abdallah et al. Simplified Models for Dark Matter and Missing Energy Searches at the LHC. 2014.

[21] G. D'Ambrosio, G. F. Giudice, G. Isidori, and A. Strumia. Minimal flavor violation: An Effective field theory approach. *Nucl. Phys.*, B645:155–187, 2002.

[22] J. Alwall, R. Frederix, S. Frixione, V. Hirschi, F. Maltoni, O. Mattelaer, H. S. Shao, T. Stelzer, P. Torrielli, and M. Zaro. The automated computation of tree-level and next-to-leading order differential cross sections, and their matching to parton shower simulations. *JHEP*, 07:079, 2014.

[23] Wolfram Research, Inc. Mathematica 11.0.

[24] Adam Alloul, Neil D. Christensen, Cline Degrande, Claude Duhr, and Benjamin Fuks. FeynRules 2.0 - A complete toolbox for tree-level phenomenology. *Comput. Phys. Commun.*, 185:2250–2300, 2014.

[25] Celine Degrande. Automatic evaluation of UV and R2 terms for beyond the Standard Model Lagrangians: a proof-of-principle. *Comput. Phys. Commun.*, 197:239–262, 2015.

[26] Vladyslav Shtabovenko, Rolf Mertig, and Frederik Orellana. New Developments in FeynCalc 9.0. *Comput. Phys. Commun.*, 207:432–444, 2016.

[27] R. Mertig, M. Bhm, and A. Denner. Feyn calc - computer-algebraic calculation of feynman amplitudes. *Computer Physics Communications*, 64(3):345 – 359, 1991.

[28] Ashok Goyal and Mukesh Kumar. Fermionic Dark Matter in a simple *t*-channel model. *JCAP*, 1611(11):001, 2016.

[29] D. Berdine, N. Kauer, and D. Rainwater. Breakdown of the Narrow Width Approximation for New Physics. *Phys. Rev. Lett.*, 99:111601, 2007.

[30] Federica Giacchino, Alejandro Ibarra, Laura Lopez Honorez, Michel H. G. Tytgat, and Sebastian Wild. Signatures from Scalar Dark Matter with a Vector-like Quark Mediator. *JCAP*, 1602(02):002, 2016.

[31] Spencer Chang, Ralph Edezhath, Jeffrey Hutchinson, and Markus Luty. Effective WIMPs. *Phys. Rev.*, D89(1):015011, 2014.

[32] Chuan-Ren Chen, Yu-Kuang Chu, and Ho-Chin Tsai. An Elusive Vector Dark Matter. *Phys. Lett.*, B741:205–209, 2015.

[33] Giacomo Cacciapaglia, Aldo Deandrea, Daisuke Harada, and Yasuhiro Okada. Bounds and Decays of New Heavy Vector-like Top Partners. *JHEP*, 11:159, 2010.

[34] Thomas G. Rizzo. Searches for scalar and vector leptoquarks at future hadron colliders. *eConf*, C960625:NEW151, 1996. [,953(1996)].

[35] Howard Georgi and S. L. Glashow. Unity of all elementary-particle forces. *Phys. Rev. Lett.*, 32:438–441, Feb 1974.

[36] T. Plehn. *Dark Matter from a Particle Theorist's Perspective, lecture notes*, 2016.